LIBRARY OF THE UNIVERSITY OF ADELAIDE
17.4.70

OXIDATION-REDUCTION REACTIONS IN SOLUTION

by

Keith James ELLIS, B.Sc. (Hons.) (Adelaide)

A Thesis submitted to the University of Adelaide in partial fulfilment of the requirements for the degree of Doctor of Philosophy.

Department of Physical and Inorganic Chemistry,
The University of Adelaide.

February, 1969

This thesis contains no material previously submitted for a degree or diploma in any University, and, to the best of my knowledge and belief, contains no material previously published or written by another person, except where due reference is made in the text.

K.J. Ellis
1969

Acknowledgements

I wish to thank very sincerely my supervisor, Dr. G.S. Laurence, for the continued guidance, help and encouragement he has given to me during these years. The helpful discussions with other staff members has also been gratefully appreciated.

I acknowledge with thanks the receipt of a Commonwealth Postgraduate Award from the Commonwealth Government and a University Research Grant from the University of Adelaide.

My thanks go to Mrs. D. Hewish for the typing of the text, and Miss J. Zdysiewicz for the preparation of the diagrams.

I wish to express my gratitude to my parents for the opportunities they have given me, and particularly for their moral support and encouragement during my years at the University.

Summary

This thesis is concerned with thermal and photochemical oxidations by Fe(III) species in aqueous solution.

In part 1, the photochemically induced electron transfer in the ferric thiocyanate complex ion ($FeNCS^{2+}$) is discussed. When irradiated with light of wavelength corresponding to its charge transfer absorption, the primary process is given by

$$FeNCS^{2+} \xrightarrow{h\nu} (Fe^{2+}....NCS^{\bullet})$$

The complete mechanism for the overall process is described in terms of reaction of the radical species with Fe^{2+}, Fe(III) species, and water.

$$FeNCS^{2+} \xrightarrow{\phi_1} Fe^{2+} + SCN^{\bullet}$$

$$SCN^{\bullet} + SCN^{-} \longrightarrow (SCN)_2^{-}$$

$$Fe^{2+} + (SCN)_2^{-} \xrightarrow{k_1} FeNCS^{2+} + SCN^{-}$$

$$FeNCS^{2+} + (SCN)_2^{-} \xrightarrow{k_2} Fe^{2+} + (SCN)_2 + SCN^{-}$$

$$FeOH^{2+} + (SCN)_2^{-} \xrightarrow{k_3} Fe^{2+} + (SCN)_2 + OH^{-}$$

$$Fe^{3+} + (SCN)_2^{-} \xrightarrow{k_4} Fe^{2+} + (SCN)_2$$

$$(SCN)_2^{-} + H_3O^{+} \xrightarrow{k_5} X$$

At 25°C, values of ϕ_1 at wavelengths of 3660 Å, 4358 Å and 5461 Å are determined as are the relative values of the rate constants

k_1, k_2, k_3, k_4 and k_5.

It is shown that a thiocyanate radical species does exist in solution following the irradiation, by observing the induced polymerisation of vinyl monomers and by the effect of scavengers added to the reaction solutions.

It is also shown that the radical can be produced by the action of chloride free radicals on thiocyanate ion.

$$FeCl^{2+} \xrightarrow{h\nu} Fe^{2+} + Cl^{\bullet}$$

$$Cl^{\bullet} + SCN^{-} \longrightarrow Cl^{-} + SCN^{\bullet}$$

In Part 2 of the thesis, the detection of transient intermediates in two thermal oxidation-reduction reactions (Fe^{3+}/I^{-} and Fe^{3+}/Ascorbic acid) is considered using a stopped-flow technique.

In the reduction of ferric ion by ascorbic acid, evidence is found for the formation of a ferric ascorbate complex,

$$Fe^{3+} + H_2A \longrightarrow FeHA^{2+} + H^{+}$$

and estimates are made of the formation constant and extinction coefficient of the d-d absorption spectrum of the complex. The kinetics of the formation of the complex appear to indicate a two step process.

In the case of the oxidation of iodide ion by ferric ion, no

intermediate was detected, and it is probable that the oxidation-reduction reaction proceeds by the initial formation of an ion pair

i.e. $$Fe^{3+} + I^- \longrightarrow (Fe^{3+}....I^-)$$

$$(Fe^{3+}....I^-) + I^- \longrightarrow \text{products.}$$

The kinetics of the oxidation-reduction reactions were studied using the stopped-flow apparatus. Although it is shown that the reaction is initially first order in ferric ion and second order in iodide ion, and that ferrous ion has a retarding effect, the overall mechanism is not completely understood.

Table of Contents

Page

PART 1

The Photolysis of $FeNCS^{2+}$ Complex Ion in Aqueous Solution

Chapter 1: Introduction

1.1 Spectra of Transition Metal Ions and Their Complexes in Solution 1

1.2 Types of Photochemical Reactions in Inorganic Systems 6

1.3 Mechanism of Product Formation in Photo-Redox Reactions 12

1.4 Photochemistry of Labile Ferric Complexes in Solution 15

Chapter 2: Experimental 22

2.1 Materials 22

2.2 Analyses 24

2.3 Apparatus 32

2.4 Procedure for Photolysis Experiments 34

2.5 Actinometry and Quantum Yield Calculations 36

2.6 Errors 39

Chapter 3: Results 41

3.1 Stoichiometry of the Reaction 41

3.2 Light Intensity Dependence 43

3.3 Dependence of $\phi_{Fe^{2+}}$ on Ferrous Concentration 43

Page

3.4 Dependence of $\phi_{Fe^{2+}}$ on Acid Concentration 46

3.5 Dependence of $\phi_{Fe^{2+}}$ on $FeNCS^{2+}$ Concentration 46

3.6 Dependence of $\phi_{Fe^{2+}}$ on Fe^{3+} Concentration 49

3.7 Wavelength Dependence 50

3.8 Temperature Dependence 51

Chapter 4: Discussion 52

4.1 The Primary Photochemical Act 52

4.2 The Nature of the Thiocyanate Radical Species 53

4.3 The Reaction Scheme 55

4.4 Stoichiometry 55

4.5 Reaction of the Radical with Species Other Than Fe^{II} and Fe^{III} Complexes 57

4.6 Light Intensity Dependence 59

4.7 Effect of Ferrous Ion 63

4.8 Effect of $FeOH^{2+}$ and $FeNCS^{2+}$ 63

4.9 Calculation of Relative Rate Constants 64

4.10 Ferric Dependence 66

4.11 Comparisons with Other Work 67

4.12 Wavelength Dependence 69

4.13 Temperature Dependence 70

Page

Chapter 5: Qualitative Experiments 72

5.1 Effect of Radical Scavengers 72

5.2 Initiation of Polymerisation 75

5.3 Low Temperature Irradiation 77

5.4 Effect of Nitrous Oxide 78

5.5 The $FeCl^{2+}/FeNCS^{2+}$ Reaction 78

5.6 Production of the $SCN^{\bullet}$ Radical by Oxidising Agents 80

PART 2

Thermal Oxidation-Reduction Reactions 82

Chapter 1: Introduction 82

Chapter 2: The Oxidation of Ascorbic Acid by Ferric Ion in Aqueous Solution 91

2.1 Introduction 91

2.2 Experimental 94

2.3 Results 105

2.4 Discussion 111

2.5 Proposed Mechanism of Intermediate Formation 119

2.6 The Overall Reaction 125

Chapter 3: The Oxidation of Iodide Ion by Ferric Ion in Aqueous Solution 128

3.1 Introduction 128

3.2 Experimental 131

Page

3.3 Results and Discussion 138

3.4 Conclusion 151

Appendices

I Derivation of Rate Expressions 153

II Derivation of Rate Expressions 156

III Experimental Results for Fe^{3+}/Ascorbic acid Reaction 158

References 162

PART 1

THE PHOTOLYSIS OF $FeNCS^{2+}$ COMPLEX ION IN AQUEOUS SOLUTION

LIBRARY OF THE UNIVERSITY OF ADELAIDE

CHAPTER 1

Introduction

1.1 Spectra of Transition Metal Ions and Their Complexes in Solution

Solvated transition metal ions and their complexes in solution usually exhibit two series of absorption bands, the most obvious difference being in the magnitude of their extinction coefficients.

1.1.a d-d Spectra

In general the fairly weak (ε = 1-10) bands in the visible or near U.V. region of the spectrum are due to transitions between the various d orbitals of the central metal ion. These can be treated theoretically using the Crystal Field or Ligand Field theories.[1,2] Since the d orbitals are symmetric with respect to complete inversion through the centre, then by the La Porte rule,[3] which requires that transitions are allowed only between states of opposite parity, any d-d transitions are forbidden. However, these transitions can become weakly allowed under the influence of ligands since the symmetry is somewhat disturbed and there is some mixing of the d and p orbitals of the metal ion. A d-p transition being allowed, the normally forbidden transition will occur with a low intensity which can be roughly related to the extent of mixing of the d and p orbitals.

1.1.b Charge Transfer Spectra

The more intense spectra ($\varepsilon \doteq 10^4$), which are often found nearer to the U.V. region than those due to d-d transitions are usually "charge transfer" (C.T.) spectra. It is obvious from the high intensity that these must be "La Porte allowed". i.e. they involve transitions between states of opposite parity. This type of spectrum is not unique to ionic species in solution, but occurs in the gas and solid phases as well as in organic systems.[4] In the general case we may consider that in the transition responsible for the optical absorption, an electron from one molecule or ion (the donor, D) is transferred completely to another molecule or ion (the acceptor, A).

Mulliken[4] was the first to discuss these spectra in quantum mechanical terms, although others[5,6] had earlier recognised the existence of charge transfer phenomena. He considered that in organic charge transfer complexes the bonding in the complexes is due to resonance between a no-bond ground state (DA) and a polar excited state (D^+A^-), giving rise to a stabilised ground state having a wave function

$$\psi_0 = \psi(DA) + \lambda\psi(D^+A^-)$$

and an excited charge transfer state

$$\psi_1 = \psi(D^+A^-) - \mu\psi(DA)$$

where λ and μ are constants which are usually small compared with unity.

Murrel[7] has extended the molecular orbital treatment of charge transfer systems and considered the energies and intensities of charge transfer bands, while Orgel[8] has applied the theory to inorganic systems and Dainton[9] has discussed it in relation to electron transfer reactions.

The wavelength of the absorption maximum is found empirically to be dependent on both the ionisation potential (Is) of the donor, and the electron affinity (Ea) of the acceptor. The energy required for the transition is given by[7]

$$h\nu = Is - Ea - C$$

where C is the difference between the energies of formation of the ground and excited states.

For a series of complexes of the same central metal ion with different ligands, it is found that the absorption maxima are shifted characteristically with the ligand, because of the differing electron affinities of the ligand. For example, compare Figures 1 and 2, which show that the absorption peak of the chloride complex is always at shorter wavelengths than the bromide, which in turn is at lower wavelengths than the iodide complex.

Similarly, although the closed shell metal ions show no charge transfer absorption in aqueous solution down to the limits of

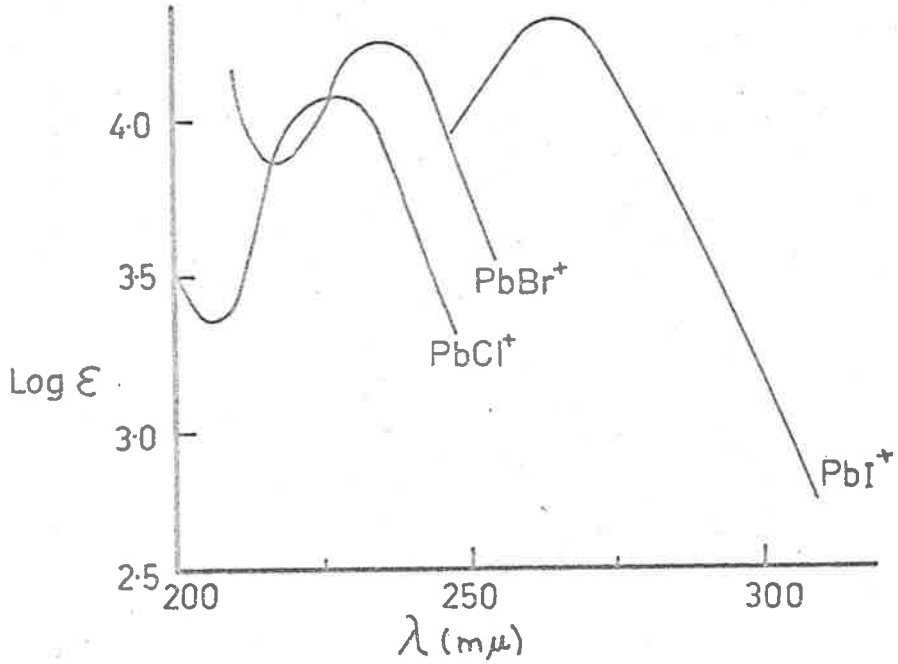

FIG. 1. Spectra of PbX^+ Complexes ($X = Cl^-, Br^-, I^-$).
(From Ref. 8 pg. 431).

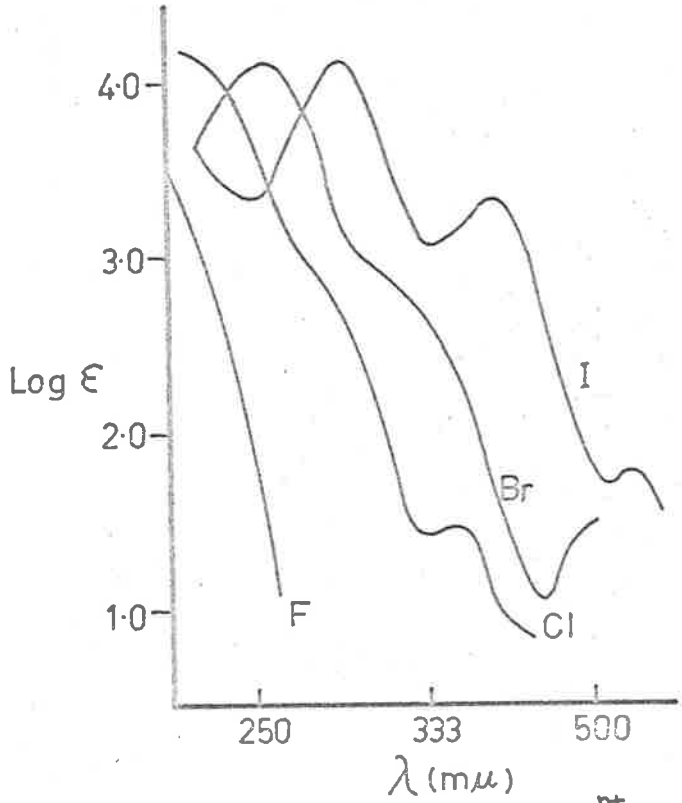

FIG. 2. Spectra of $[Co(NH_3)_5X]^{n+}$; X = F, Cl, Br, I.
(From Ref. 1, pg. 100)

observation, the hydrated transition metal ions do show strong absorption in the U.V. region which may be assigned to either charge transfer to solvent (C.T.T.S.) or charge transfer from solvent to cation, depending on the oxidation potential of the cation and solvent. This transition was usually written in the Fe^{2+} system[6] as giving rise to H atoms,

$$Fe^{2+}(H_2O) \xrightarrow{h\nu} Fe^{3+} + OH^- + H$$

but more recent work[10,11] has shown the transition to be due to the reaction

$$Fe^{2+} \xrightarrow{h\nu} Fe^{3+} + e'_{aq}$$

Dainton[12] had shown earlier that a plot of the energy corresponding to the long wavelength edge of the charge transfer band of bivalent transition metal ions versus the redox potential of the M^{2+}/M^{3+} system is a straight line of slope 23 kcal/volt, showing that the minimum energy for the charge transfer process corresponds closely to the energy required for the reaction

$$M^{2+}_{aq} \longrightarrow M^{3+}_{aq} + e'$$

1.1.c Comparison of Effects of Light Absorption by Different Spectral Bands

It is apparent that light absorption in a d-d band leads to a redistribution of the charge around the metal ion such that the

electron density along some coordination directions increases, and in some other directions decreases, while charge transfer absorption results in a redistribution of charge between the central metal ion and its ligands so as to tend to change the oxidation numbers of metal and ligands. Absorption in a d-d band will therefore be expected to lead to excited states which will give rise to substitution type reactions, while charge transfer absorption should result in redox type reactions.

Although this correlation does hold in many cases, it is also true that there is a great deal of experimental data[13,14] which is apparently anomalous. Balzani, Moggi and Carassiti[15] suggest that this may be due to the excited state reached in the primary transition undergoing a radiationless deactivation (e.g. between states of different multiplicity) to give a different excited state which then undergoes reaction. In view of this situation, it can be seen that much more work remains to be done on the photochemistry of transition metal ions and their complexes in solution, before the processes involved are completely understood. Despite the uncertainty as to the nature of the excited states involved in these reactions, it is of interest to discuss briefly the various types of photo-reactions which are known to occur in transition metal complexes, and to point out the wide variety of processes which have been proposed to explain the observed experimental results.

1.2 Types of Photochemical Reactions in Inorganic Systems

1.2.a Photosubstitution and Related Reactions

(1) Photo-substitution.

This type of reaction is of the form

$$[ML_n]^{z+} + X \overset{h\nu}{\rightleftharpoons} [ML_{n-1}X]^{z+} + L$$

e.g. $$[Fe(CN)_6]^{3-} + N_3^- \overset{h\nu}{\rightleftharpoons} [Fe(CN)_5N_3]^{3-} + CN^- \qquad \text{ref. 16}$$

In general, there are two possible mechanisms for this type of reaction, according to whether the rate determining step is the dissociation of the ligand from the photo-excited state (SN_1) or the interaction between the photo-excited state and the entering ligand (SN_2). The example given appears to be even more complex, because the product $[Fe(CN)_5N_3]^{3-}$ is apparently formed in an excited state and rapidly undergoes reverse ligand exchange in the dark, whereas it is known[17] that under normal conditions the azidopenta-cyanoferrate(III) is stable, even in the presence of CN^- ion.

(2) Photo-aquation.

This is probably the most common type of photo-substitution reaction.[18] Particular attention has been paid to Cr(III) complexes[19] since these are free from the simultaneous redox reactions which occur in many other systems. Typical complexes studied in aqueous solution have been $[Cr(NH_3)_2(NCS)_4]^-$,

$[Cr(Urea)_6]^{3+}$, $[Cr(NCS)_6]^{3-}$, and $[Cr(NH_3)_6]^{3+}$,

e.g. $[Cr(NH_3)_2(NCS)_4]^- + H_2O \xrightarrow{h\nu} [Cr(NH_3)_2(NCS)_3H_2O] + NCS^-$

Recently, Adamson[20] has discussed the theoretical implications of the experimental work on these systems and has shown that both doublet and quartet excited states of the central metal ion are involved in the various transitions.

(3) Geometrical photoisomerisation.

i.e. $\underline{cis}\,[ML_nX_m] \xrightarrow{h\nu} \underline{trans}\,[ML_nX_m]$

Balzani and Carassiti[21] have shown this type of reaction to occur in the case of $Pt(gly)_2$ (gly = glycinate ion). Using radioisotopic techniques they have shown that the isomerisation takes place via an intramolecular twisting mechanism which does not involve the breaking of any metal-ligand bonds.

(4) Photoracemization.

$d\text{-}[M(L\text{-}L)_3] \xrightarrow{h\nu} l\text{-}[M(L\text{-}L)_3]$

This type of reaction has been shown[22] to occur in the case of the $[Cr(C_2O_4)_3]^{3-}$ and $[Rh(C_2O_4)_3]^{3-}$ complexes, but it is not possible to say if the reaction is an intramolecular rearrangement, or involves a substitution type mechanism.

1.2.b Photo-oxidation-reduction Reactions

Redox reactions occur extensively in transition metal complex photochemistry, and the charge transfer may be either intermolecular (i.e. between the complex and some other species in solution), or intramolecular (i.e. between ligands and the central metal ion).

(1) Intermolecular.

These reactions are of the type

$$[ML_n]^z + X^- \xrightarrow{h\nu} [ML_n]^{z-1} + X$$

or

$$[ML_n]^z + Y \xrightarrow{h\nu} [ML_n]^{z+1} + Y^-$$

An example of the first kind is the hexammine cobalt(III) iodide ion pair

$$[Co(NH_3)_6]^{3+} + I^- \xrightarrow[\lambda < 4000\ \text{Å}]{h\nu} [Co(NH_3)_6]^{2+} + I$$

The overall result of this electron transfer is given[23,24] by the equation

$$[Co(NH_3)_6]^{3+} + I^- + 6H^+ + h\nu \longrightarrow Co^{2+}_{aq} + \tfrac{1}{2}I_2 + 6NH_4^+$$

That is, the primary photochemical act is the reduction of the central metal ion, and the subsequent decomposition of the complex is due merely to the lability of the $[Co^{2+}(NH_3)_6]$ species.

(2) Intramolecular.

In this case, since the oxidised ligand is originally coordinated directly to the central metal atom, electron transfer usually results in complete decomposition of the complex,

i.e. $[M^{z}L_{n}] \xrightarrow{h\nu} M^{z-1} + (n-1)L + \text{oxidised L}$

It should be noted that there is also the possibility of the electron transfer being from metal to ligand,

$$[M^{z}L_{n}] \xrightarrow{h\nu} M^{z+1} + (n-1)L + \text{reduced L}$$

but there are no known examples.

Endicott and Hoffman[25] have studied the photochemically induced redox reactions of a number of Co(III) complexes, and have shown that there are two types of reactions which occur, depending on the nature of the ligands. For the complexes containing only ammines, ammonia, or water, the mechanism is of the form

$$[Co(en)_3]^{3+} \rightleftharpoons {}^{*}[Co(en)_3]^{3+} \longrightarrow {}^{*}[Co(en)_2(en')]^{2+} + H^{+}$$

$${}^{*}[Co(en)_2en']^{2+} \longrightarrow Co^{2+} + 2\ en + en'$$

where en' = $HNCH_2\ CH_2\ NH_2$,

and in the case of complexes of the type $[Co(NH_3)_5Br]^{2+}$, $[Co(NH_3)_5I]^{2+}$, the proposed mechanism is

$$[Co(NH_3)_5I]^{2+} + h\nu \longrightarrow Co^{2+} + 5NH_3 + I$$

$$5H^+ + [Co(NH_3)_5I]^{2+} + I \longrightarrow Co^{2+} + I_2 + 5NH_4^+$$

Most oxalato complexes undergo a redox reaction of the type[26,27]

$$2\,[M(C_2O_4)_3]^{3-} \longrightarrow 2\,M(II) + 5(C_2O_4)^{2-} + 2\,CO_2$$

even when irradiated in the region of the d-d bands. It has been suggested[28] that even a small degree of overlap of the charge transfer and d-d bands is sufficient to allow a conversion from the latter to the former state, and lead to an overall redox reaction.

Photochemical electron transfer is also known to occur in labile metal complexes, for example,[24]

$$Ce\,NO_3^{3+} \longrightarrow Ce(III) + NO_3.$$

The largest group of complexes of this type to have been studied are the labile ferric halide and pseudo-halide complexes. These will be discussed further in Section 1.4.

1.2.c Simultaneous Reactions

Many examples are known of more than one type of photoreaction occurring simultaneously even when the incident radiation is monochromatic. In particular, Co(III) complexes may undergo

intramolecular redox reactions and aquation reactions at the same time,[30] with the relative magnitude of the quantum yields for the two processes depending on the wavelength of irradiation. However, it should be noted that the wavelength dependence is not such as to enable one to use unambiguously the criterion that irradiation in C.T. bands produces redox reactions and irradiation in d-d bands leads to substitution.

As discussed earlier (Section 1.1.c), it is apparent that the whole situation cannot be explained merely in terms of the primary photochemical absorption, but that transitions between various excited states are also important.

Mixed reactions may also occur when the complex consists of a mixture of ligands. For example, in an aquation type reaction, more than one species of ligand could be replaced

$$[MXY]^{z+} + H_2O \rightarrow [MX(H_2O)]^{z+1} + X^-$$

$$[MXY]^{z+} + H_2O \rightarrow [MY(H_2O)]^{z+1} + Y^-$$

With redox reactions, however, it is unlikely that more than one type of ligand would be oxidised, since the electron would normally come from the ligand having the lowest electron affinity.

1.3 Mechanism of Product Formation in Photoredox Reactions

Up to this point, mention has been made of the primary photo-act (i.e. light absorption causing the charge redistribution), and of the overall result of such reaction. However, in order to explain the differing quantum yields obtained in this type of reaction, it is necessary to discuss further the steps following the initial electron transfer.

In Section 1.1.b it was pointed out that the initial transition caused by the absorption of light in the C.T. band involves the transfer of an electron from one molecule to another. That is, in the general case of a transition metal complex of the type ML^{z+}, (where M^{z+1} = metal ion, L^{-1} = ligand)

$$ML^{z+} \longrightarrow M^{z+} + L^{\cdot}$$

In solution it is generally considered that the reactive species (reduced metal ion and ligand free radical) are surrounded by a solvent "cage". Noyes[31] has discussed the kinetics of reactions which occur when such reactive species are produced in pairs, and he has proposed that the following processes occur.

1.3.a Primary Recombination

The fragments may recombine by a process of back electron transfer before undergoing diffusive displacements. Because of the short time scale involved (10^{-13} - 10^{-11} sec.) it is unlikely that

the radicals could react with any other species within this time.

1.3.b Secondary Recombination

Following separation by random diffusive movements, it is possible that the fragments from a specific dissociation may eventually reencounter each other and undergo secondary recombination. Noyes has shown that this would have to occur within 10^{-9} seconds, otherwise the radicals would diffuse so far apart that the probability of such an encounter would be negligible. Both primary and secondary recombination are referred to as geminate recombination.

1.3.c Combination

If the fragments escape both primary and secondary recombination, it is possible that they may encounter, and subsequently combine with, reactive fragments from other dissociations.

1.3.d Scavenging Reactions

This term describes all other reactions of the fragments with other species present in the solution. As stated above, because of the short time scale, it is unlikely that a scavenging reaction will compete with primary recombination, and Noyes' treatment predicts that secondary recombination will only be competed with provided the scavenger is very reactive ($k_2 > 10^7$ l.mole^{-1}.sec^{-1}) and at high concentrations (> 0.01 M).

Under these conditions the scavenging reaction will be dependent on the square root of the scavenger concentration.

At low scavenger concentrations, there will only be competition with combination reactions (Section 1.3.c), and these will follow conventional kinetics.

1.3.e Reaction Scheme

In the general case being considered, the reduced metal ion and ligand radical may undergo back electron transfer (either as primary or secondary recombination), or the radical may react with some other species (scavenger) and so be destroyed while the metal ion remains in its reduced form.

i.e. The complete process may be written as

$$ML^{z+} \xrightarrow{h\nu} (M^{z+}.....L)\text{cage}$$

$$(M^{z+}....L)\text{cage} \longrightarrow ML^{z+} \qquad 1^{o} \text{ recombination}$$

$$(M^{z+}....L)\text{cage} \longrightarrow M^{z+} + L^{\bullet} \qquad \text{diffusive separation}$$

$$M^{z+} + L^{\bullet} \longrightarrow ML^{z+} \qquad 2^{o} \text{ recombination}$$

$$L^{\bullet} + S_{(\text{substrate})} \longrightarrow \text{products} \quad (\text{i.e. scavenging reaction})$$

In the absence of scavenger, there will be no overall reaction as the reactive fragments will eventually recombine, while at very high scavenger concentrations it will be possible to compete

with all except primary recombination, and so determine the primary quantum yield. i.e. the fraction of pairs of reactive fragments which escape primary recombination.

1.3.f Dependence of Primary Quantum Yield on Wavelength of Absorbed Light

Noyes[32,33] has also extended his theory so as to predict the quantum yield from values of the viscosity of the solvent, the sizes and masses of the fragments of dissociation, the energy of the bond that is broken (E), and the energy of the absorbed quantum ($h\nu$). In particular the theory predicts a linear relationship between the functions $(\phi/\phi - \phi)$ and $\sqrt{(h\nu - E)}$. Although the results of the photochemical dissociation of iodine agree reasonably well with this simple theory, it would not be surprising for it to be found that more refinements to the theory were necessary in order to achieve similar agreement in cases involving fragments of different size and mass, excited states, and charges. These points will be discussed with particular reference to the present work in Section 4.12.

1.4 Photochemistry of Labile Ferric Complexes in Solution

1.4.a Spectra

Rabinowitch[6] has interpreted the high intensity bands in the blue and U.V. regions of the spectra of labile ferric complexes in solution as electron transfer bands. That is, the light absorption

process may be described by

$$Fe^{3+}X^{-} \xrightarrow{h\nu} (Fe^{2+}....X)$$

where X = OH^{-}, Cl^{-}, Br^{-}, F^{-}, CNS^{-}, N_3^{-}.

Comparison of the electron affinity of X^{-} with the wavelength of the absorption maximum for each species FeX^{2+} shows that the peak is shifted almost quantitatively to higher wavelengths as the electron affinity decreases. This is to be expected as the energy change in the light absorption process is given[34] by (cf. Section 1.1.b)

$$h\nu = -\Delta H + Ex - I_{Fe^{2+}} + Q$$

where ΔH is the heat content change in the formation of the ion-pair FeX^{2+} from hydrated Fe^{3+} and X^{-} ions, Ex is the electron affinity of X in aqueous solution, $I_{Fe^{2+}}$ is the ionisation potential of the ferrous ion in solution, and Q is the repulsion energy in $(Fe^{2+}....X)$ with an interatomic distance identical with that in the ion pair $Fe^{3+}X^{-}$, and having the hydration shell in the corresponding non-equilibrium state. The value of Q is independent of the nature of the anion, and is of the order of 45 kcal.

In the spectrum of a solution containing Fe^{3+} and NCS^{-} ions we can assign the broad band of high intensity ($\varepsilon_{max} \simeq 4,500$) with $\lambda_{max} \simeq 460$ mμ as being due to the transition of an electron from an orbital associated predominantly with the anion, to a vacant

d orbital of the ferric ion. The weaker d-d bands which would be expected to be associated with the ferric ion are almost certainly obscured by the intense charge transfer band at 460 mμ.

1.4.b Photochemically Induced Reactions

Although Rabinowitch[6] had earlier suggested the charge transfer nature of the light absorption process, it was not until 1949 that Evans and Uri[35] demonstrated experimentally that radical formation was involved, by detecting the initiation of vinyl polymerisation when aqueous solutions of the ion pairs $FeOH^{2+}$, $FeCl^{2+}$ and FeF^{2+} were irradiated with light of wavelength >3000 Å. Evans, Santappa and Uri[36] extended this work to include FeN_3^{2+}, and were able to show that the polymerisation initiation step was of the form

$$X + CH_2{=}CHR \longrightarrow XCH_2\text{-}CHR\text{-}$$

and to derive quantum yields, chain lengths, and relative rate constants for the various steps proposed.

Bates, Evans and Uri[37] showed that organic substrates, such as benzoic acid and benzyl alcohol, could be oxidised by irradiating solutions containing both the substrate and the $FeOH^{2+}$ ion pair, presumably via a mechanism involving the hydroxyl radical. Uri[34] discussed this work more fully and proposed the following mechanism:

$$FeOH^{2+} \xrightarrow{h\nu} Fe^{2+}OH$$

$$Fe^{2+}OH \longrightarrow Fe^{2+} + OH$$

$$OH + C_6H_5COOH \longrightarrow .C_6H_4COOH + H_2O$$

$$.C_6H_4COOH + FeOH^{2+} \longrightarrow HOC_6H_4COOH + Fe^{2+}$$

Baxendale and Magee[38] demonstrated the oxidation of benzene by hydroxyl radicals and estimated a quantum yield of 0.13 for the reaction

$$FeOH^{2+} \xrightarrow[313\ m\mu]{h\nu} Fe^{2+} + OH$$

Dainton and Tordoff[39] reinvestigated the acrylamide polymerisation and found a value of 0.19 ± 0.05 for the quantum yield of the above reaction under their conditions. They also showed that after making suitable allowance for probable errors in acidity constants and extinction coefficients of the ferric species, the results of Baxendale and Magee[38] were in reasonable agreement with their own work.

Dainton and James[40] carried the work even further by considering other metal ion complexes, and showed evidence for the predicted relationship between the electrode potential of the M^{2+}/M^{3+} couple and the long wavelength limit of the electron transfer band of various M^{2+} species.

Adamson, Dainton and Baulch[41] attempted to use the Fe^{2+} ion as a radical scavenger in the $FeOH^{2+}$ system by measuring the isotopic exchange rate when mixtures of Fe^{2+}, Fe^{3+} and $FeOH^{2+}$ were irradiated with light of 2537 Å. Although their results were not in agreement with the mechanisms proposed above, and instead, necessitated that an excited state of the Fe^{3+} ion be proposed, Adamson et al. state that "a more detailed investigation of the exchange reaction in de-aerated solutions with highly purified water and much more intense radiation sources is clearly desirable".

1.4.c Photochemistry of the $FeNCS^{2+}$ Complex

Despite all of these investigations, it would appear that little is known of the photochemistry of the $FeNCS^{2+}$ complex. Evans and Uri[35] found no evidence for polymerisation following the irradiation of mixtures of $FeNCS^{2+}$ and vinyl monomers, even though one would expect it to behave in much the same way as the chloride, azide, etc. References to the use of $FeNCS^{2+}$ as a spectrophotometric method of analysis for iron, however, show the importance of excluding light from the system,[42] suggesting that the complex is photochemically active.

In view of this instability compared with other ferric complexes in solution (except for FeI^{2+} which is thermally unstable), it would appear as if the quantum yield for Fe^{2+} production from $FeNCS^{2+}$ in the absence of added radical scavengers, may be considerably

greater than for $FeOH^{2+}$, FeF^{2+} and $FeCl^{2+}$. This could be due either to a reduced efficiency of the back electron exchange (either as primary or secondary recombination)

$$Fe^{2+} + SCN^{\bullet} \longrightarrow FeNCS^{2+}$$

compared with dimerisation

$$SCN^{\bullet} + SCN^{\bullet} \longrightarrow (SCN)_2,$$

or to reaction of the radical with water, or to the ability of the radical to reduce ferric species such as

$$SCN^{\bullet} + FeNCS^{2+} \longrightarrow Fe^{2+} + (SCN)_2$$

as well as to oxidise Fe^{2+} ion.

The reaction between $SCN^{\bullet}$ radical and Fe(III) species has already been proposed by Betts and Dainton[43] in their study of the thermal bleaching of $FeNCS^{2+}$, and it can be shown to be thermodynamically favourable for $SCN^{\bullet}$ but not for $Cl^{\bullet}$.

It was decided therefore, to investigate the photochemical behaviour of the $FeNCS^{2+}$ species in aqueous solution, when irradiated in its charge transfer absorption band, in the absence of any added radical scavenger. In this way it was hoped to be able to measure the primary quantum yield for the reaction

$$FeNCS^{2+} \longrightarrow Fe^{2+} + SCN^{\bullet},$$

and the relative rate constants for any other reactions which the radical may undergo.

CHAPTER 2

Experimental

2.1 Materials

All solutions were prepared from demineralised water which was distilled from alkaline potassium permanganate and acidified potassium dichromate in all glass apparatus to ensure that no organic material remained to act as a radical scavenger.[44] A.R. perchloric acid (G. Frederick Smith) was used without further purification.

Ferric solutions were prepared from Ferric Perchlorate (Newton Maine Ltd. and G. Frederick Smith) which had been purified in order to remove a considerable amount of insoluble matter present in the purchased material.

The crystals were dissolved in excess 1 M $HClO_4$, and after boiling, the solution was filtered while still hot. Taking extreme care, the volume was then reduced by boiling until yellow needle-like crystals formed on cooling. These were separated and recrystallised twice more. The crystals were then made into a paste with concentrated $HClO_4$, and, after stirring for a few minutes, this was filtered using a Buchner flask and sintered glass funnel. The process was repeated until the crystals were a faint purple colour and the wash liquor (conc. $HClO_4$) was colourless. The crystals were finally sucked dry at the pump, and stored in a ground glass stoppered bottle.

Because of the extremely hygroscopic nature of "non-yellow" ferric perchlorate, it was not possible to remove all of the $HClO_4$ since atmospheric water formed both "yellow" ferric perchlorate ($Fe(ClO_4)_3.6H_2O$) and ferric-hydroxy species ($FeOH^{2+}$, $Fe(OH)_2^+$ etc.). Analyses showed that the product prepared in this way contained approximately 60-70% $Fe(ClO_4)_3$, the remainder being $HClO_4$.

In earlier experiments "Baker Analysed" ferric nitrate was used and there was no apparent difference in the kinetic measurements, but it was found to be more difficult to analyse reliably, probably because of the large quantities of nitrate ion present.

Ferrous solutions were prepared from A.R. ferrous sulphate or perchlorate. Experiments using A.R. sodium sulphate showed that sulphate ions did not alter the quantum yields.

The ammonium thiocyanate used was "Analar" reagent.

Sodium perchlorate solutions which were used to adjust the ionic strength were prepared from B.D.H., low in chloride, sodium perchlorate.

B.D.H. acrylonitrile was washed with 10% NaOH to remove inhibitor, then with distilled water and dried over anhydrous magnesium sulphate before being distilled in vacuo.

A.R. acetone was used as received.

Potassium ferrioxalate solutions, for use as an actinometer, were prepared by mixing equal volumes of a 0.3 M. A.R. ferric

ammonium sulphate solution in 0.2 N H_2SO_4, and 0.9 M potassium oxalate solution.

Both B.D.H. and Univar 1,10-phenanthroline were used in preparing the 0.1% solution in water as required for the ferrous analysis, and the buffer was prepared from A.R. sodium acetate and pure sulphuric acid.

2.2 Analyses

(Figures in brackets are the possible percentage error of each analysis.)

2.2.a Stock Solutions

Stock perchloric acid solutions were standardised against sodium tetraborate using methyl red indicator,[45] ($\pm$ 0.2%) and the sodium perchlorate solutions by carefully evaporating aliquots to dryness and weighing ($\pm$ 0.5%).

Ferric solutions were analysed by titration with potassium permanganate after reduction with stannous chloride ($\pm$ 0.2%).[46] In the case of ferric nitrate solutions the method had to be slightly modified, presumably because of the large quantities of nitrate ion present. This entailed acidification with concentrated hydrochloric acid and then boiling almost to dryness to remove the nitrate as oxides of nitrogen, followed by re-acidification with HCl before reduction.

The acid concentrations in the ferric solutions were analysed by titrating the total (Fe^{3+} + H^+) with freshly prepared standardised NaOH solution to pH = 9[70] using either phenolphthalein indicator or a Philips pH meter. For the determinations using the indicator it was necessary to take a 20-25 ml aliquot of solution, dilute to 150 ml with water and heat to 80-90°C before titrating. This enabled the indicator colour change to be easily seen, as the $Fe(OH)_3$ formed during titration quickly coagulated and settled, leaving a clear supernatant. Since the calculation of the H^+ concentration involved subtracting the number of equivalents of OH^- used up by the Fe^{3+} from the total number of equivalents used, the accuracy depended on both the ratio H^+/Fe^{3+} and the precision of the Fe^{3+} analysis. In most cases the percentage error in the H^+ concentration did not exceed $\pm$ 2%, although in a few of the solutions containing low H^+ and high Fe^{3+}, the error was up to $\pm$ 5%.

Stock ferrous solutions were titrated against permanganate,[46] and diluted accurately to the required concentration ($\pm$ 0.2%).

Thiocyanate analyses were done either gravimetrically[47] ($\pm$ 0.5%) as AgSCN, or argentometrically with potentiometric determination of the end point,[48] ($\pm$ 0.3%). The two methods gave results within 0.5% of each other. The freshly prepared silver nitrate solution used in the volumetric determinations was standardised against a weighed amount of A.R. sodium chloride which had been dried

in an oven at 300°C for 2 hours.

2.2.b Kinetic and Actinometric Solutions

For the kinetic measurements, the rate of reaction was followed by analysis of the Fe^{2+} produced, or in a few cases by the SCN^- destroyed. For the wavelengths at which the light intensity was measured by the ferrioxalate actinometer, the decomposition of the actinometer solution was followed by the measurement of the Fe^{2+} produced.

In both cases, ferrous ion was determined spectrophotometrically as the tris-1,10-phenanthroline complex.[49] For the most reliable results it was necessary that the pH be 4.0-4.5, and the analysis solution was adjusted to this pH using a sodium acetate/sulphuric acid buffer. Measurements were made on an SP600 spectrophotometer at 510 mμ and the extinction coefficient was found to be 1.086×10^4 using ferrous solutions which had been standardised against potassium permanganate. This compares well with the literature value[49] of 1.11×10^4. For the determination of concentrations less than 10^{-5} M, 4 cm spectrophotometer cells were used.

Since the ferric thiocyanate complex absorbs in the same region as the ferrous phenanthroline, it was necessary to add some anion to the reaction mixtures which would strongly complex the Fe^{3+} without affecting the formation of the Fe^{2+}-phen complex. It was thought that fluoride ion, added as NH_4F, would be suitable because of the

high formation constant of the colourless ferric fluoride complex. Unfortunately this interfered with the ferrous determination, either by increasing the pH too much, or else at pH = 4 (necessary for complex formation) other interfering species were formed (e.g. $FeOHF^{+}$).

At low ferric concentrations, when little fluoride was needed, the method worked reasonably well, but as the ferric increased it became necessary to add such high concentrations of fluoride that the analysis became unreliable. The problem could be overcome by adding a large excess of o-phen, but this was inconvenient because of the low solubility of the chemical, and the varying amounts needed for each analysis.

Attempts were made to remove the thiocyanate ion by passing the sample down a deacidite ion exchange column, but the size of the column found to be necessary was impracticable for use when a series of analyses were required in quick succession.

It was then decided to use oxalate as the complexing ion, knowing that this does not interfere with the ferrous determination in the photolysis of ferrioxalate.[49] In general, the oxalate concentration added was at least four times the ferric concentration, to ensure complete destruction of the $FeNCS^{2+}$ complex by removing the Fe^{3+} ion as the ferric oxalate complex. The one disadvantage of this method was that, due to the high photoactivity of the solution, the analysis solutions had to be made up and measured in

near darkness. However, this was more than compensated for by both the ease and reliability of analysis. Reproducibility was within $\pm$ 0.2%.

Early work involved ferrous analyses by measuring the potential of the Fe^{2+}/Fe^{3+} couple in the reaction mixture. Since the Fe^{3+} was to be in excess in all cases, its concentration remained virtually constant throughout the reaction, and hence the change in potential was dependent only on the Fe^{2+} concentration. Originally a calomel electrode was used as reference electrode, but it was eventually found more convenient to use a Fe^{2+}/Fe^{3+} solution as reference. At first the two cells were joined by an agar/2 M $NaClO_4$ salt bridge, but it was found that the gel in the bridge could be replaced by a plug of glass wool without affecting the results. i.e. no appreciable diffusion or mixing occurred between the two half-cells. This system was by far the easiest to handle as well as being extremely sensitive to Fe^{2+} production. Nitrogen gas passing through very fine glass bubblers acted as a stirring agent, and the platinum electrodes were wound around the bubblers (Figure 3).

Because of the high sensitivity, voltage measurements using a potentiometer could be made at half minute intervals for 5 minutes (corresponding to 1%-2% of reaction only) and an initial straight line of millivolts versus time could be obtained, the slope ($\partial E/\partial t$) of which could be related to the rate of production of ferrous ion, $R_{Fe^{2+}}$.

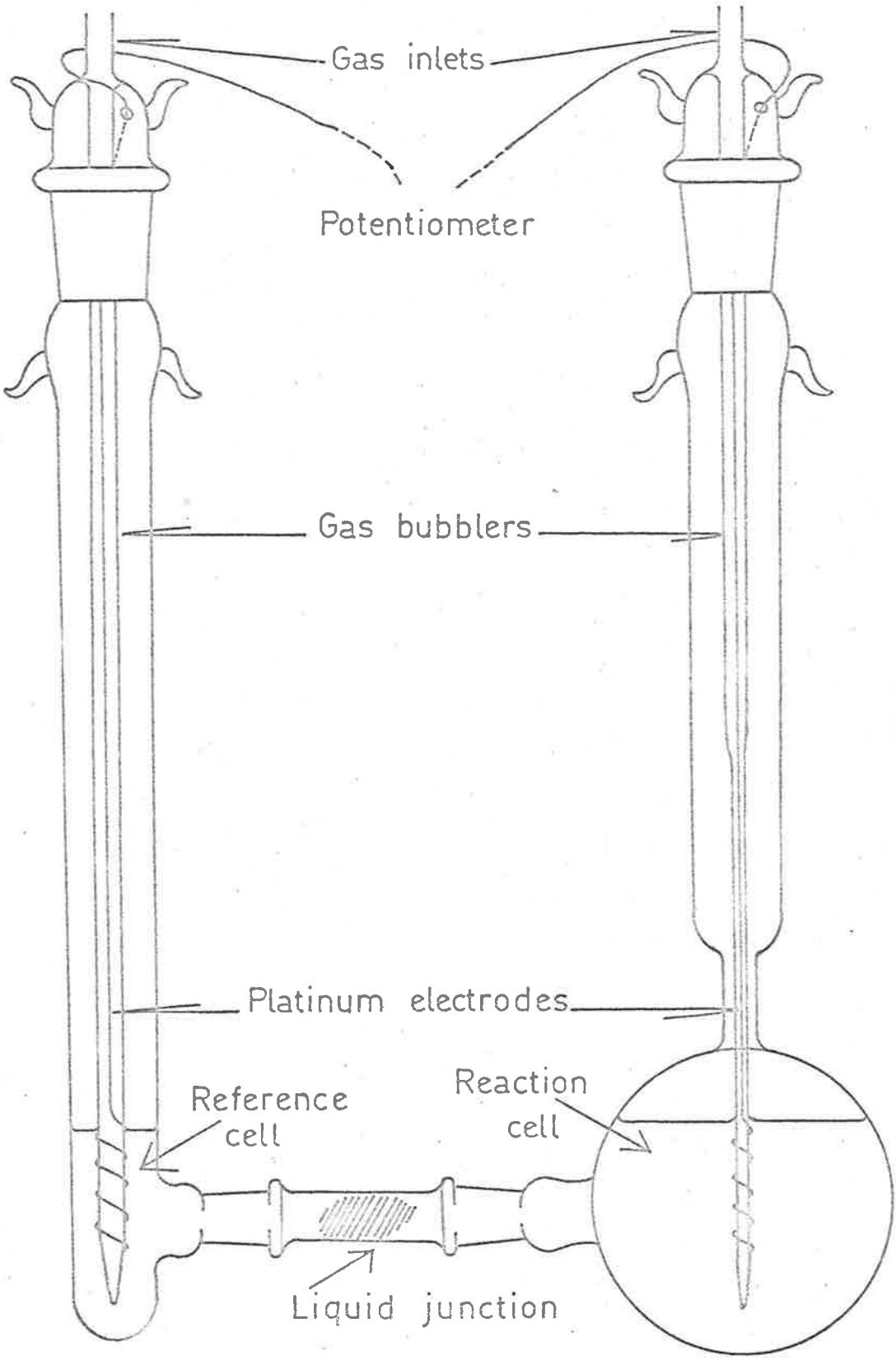

FIG. 3. Reaction Cell Set Up for Potentiometric Measurements.

Using the Nernst equation

$$E = E_o - \frac{RT}{F} \ln \frac{a_{Fe^{2+}}}{a_{Fe^{3+}}}$$

$$= E_o - \frac{RT}{F} \ln \frac{[Fe^{2+}]}{[Fe^{3+}]} - \frac{RT}{F} \ln \frac{\gamma_{Fe^{2+}}}{\gamma_{Fe^{3+}}} \qquad (2.1)$$

where a_x = activity of X, γ_x = activity coefficient of X. Since the concentration of Fe^{2+} produced was only a very small fraction ($\triangleq 1\%$) of the total Fe(III) concentration, then the total Fe(III) is effectively constant. At constant ionic strength, then, the last term in equation (2.1) is a constant, and differentiation leads to the expression

$$\frac{\delta E}{\delta t} = \frac{RT/F}{[Fe^{2+}]} \cdot R_{Fe^{2+}}$$

for small changes in E such that Fe^{2+} does not change considerably.

Unfortunately it was found that this relation did not hold experimentally. In the absence of SCN^-, a plot of millivolts versus log $[Fe^{2+}]$ gave a straight line of slope 2.303 RT/F as expected, but when SCN^- was present there was a marked, but reproducible deviation from the limiting slope at low ferrous concentrations (Figure 4).

At first sight this seemed to indicate the formation of a ferrous thiocyanate complex as there was apparently less Fe^{2+} ion giving rise to the E.M.F. than was known to be present. Attempts were made to calculate the formation constant of the complex by

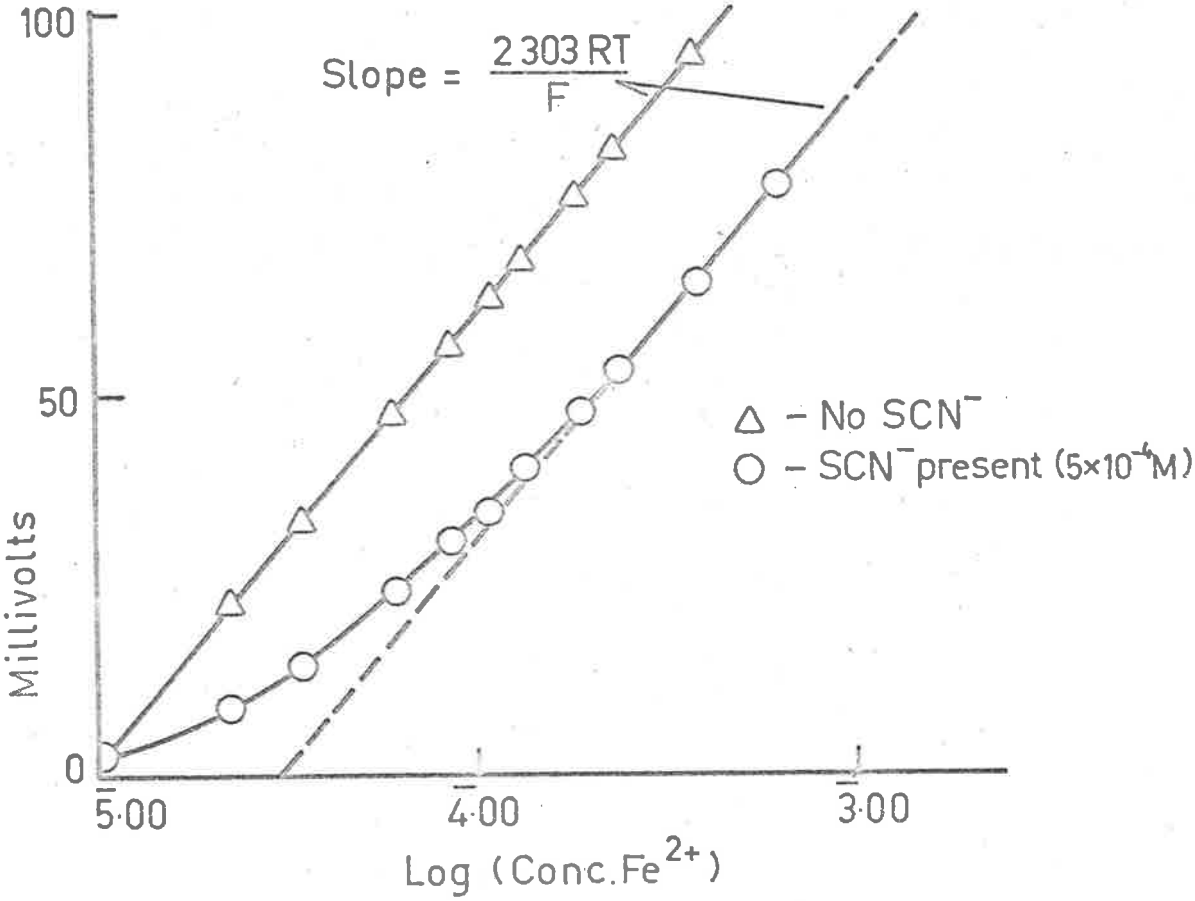

FIG. 4. Graph of Millivolts Versus Log (Fe^{2+} Concentration) Showing Deviation in Presence of SCN^- at Low Ferrous Ion.

adding varying amounts of SCN^- ion and measuring potentiometrically the apparent decrease in Fe^{2+} ion. After allowing for the SCN^- used in the formation of the ferric complexes, the free thiocyanate could be calculated and hence the equilibrium constant obtained from $K = [FeNCS^+] / [Fe^{2+}] [SCN^-]$.

Calculations over a wide range of concentrations of both Fe^{2+} (10^{-6}-10^{-3}), and SCN^- (10^{-5}-10^{-1}), gave a value for K of 2.5×10^4-4.0×10^4 which is not at all feasible since it is known that the formation constant of the ferric complex ($\simeq$120 at $\mu = 0.5$[50]) must be considerably larger than for the ferrous complex.

Another possible explanation for the observed effect was that SCN^- formed some other redox system, but regardless of the cause of the deviation, the problem was overcome by preparing an empirical calibration curve of millivolts versus concentration of Fe^{2+} for the conditions of the reaction being studied. This was done by adding 0.01 ml increments of 5×10^{-2} M Fe^{2+} solution to a known volume of reaction mixture (in the dark) and measuring the potential after each addition (Figure 4). A new calibration had to be made for all different conditions of concentration and temperature.

At the time, the kinetic results obtained by this method of analysis were unexpected, and it was therefore decided to repeat the work using the ferrous phenanthroline method discussed earlier. As it happened, both methods gave the same results, showing that the potentiometric method was in fact accurate ($\pm$ 1%) and reliable.

In addition, since it did not necessitate the removal of samples, it was much easier to use and could well be applied to many similar redox systems. The one disadvantage was that there always had to be at least a small amount (10^{-5} M) of Fe^{2+} present at the start of reaction, so as to make the electrode reversible.

2.2.c Ferric Thiocyanate Analysis

The ferric thiocyanate concentration was determined spectrophotometrically. Since most experiments were done on solutions whose optical densities at the absorption maxima (460 mμ) were ≥ 2, measurements were made at 540 mμ where the extinction coefficient was found to be 1.58×10^{3}, so that optical densities were in the range 0.7-0.1, thus giving rise to the least errors.

Preliminary work had shown that the Fe^{2+} ion produced during reaction slowed down the rate of reaction, and it was therefore necessary to measure initial rates. However, since the change in O.D. due to $FeNCS^{2+}$ was only of the order of 0.1/hour, it was difficult to obtain reliable readings for the change occurring in the first few minutes. A further difficulty was the need for accurate temperature control because of the temperature dependence of the equilibrium constant. Both of these problems were overcome using a Unicam SP700 spectrophotometer.

This had a thermostatted cell block and by using a standard solution with an O.D. approximately equal to the O.D. of the reaction solution at 540 mμas a blank, instead of water, readings could be made on the expanded 90%-110% transmission scale.

The blank was prepared by dissolving iodine in carbon tetrachloride. This solution has an absorption maximum near 500 mμ, and it was not difficult to adjust the O.D. to correspond closely to that of the reaction solution. Provided the spectrophotometer cell was well stoppered to prevent evaporation, the solution acted as a good standard reference for comparative O.D. measurements.

In this way, samples could be taken at 1 minute intervals for the first five minutes of reaction, and changes in O.D. of as little as 0.004 in 5 minutes were measured with 5%-10% accuracy.

The initial concentrations of the ferric species $FeNCS^{2+}$, $Fe(NCS)_2^{+}$ and $FeOH^{2+}$ in solution were calculated using values of the formation constants[50,51] measured at the ionic strength (0.5) of the reaction mixtures.

2.3 Apparatus

The light source was a medium pressure mercury lamp (A.E.I. type ME/D) operating from a solid state stabilised current D.C. power supply (see Figure 5). The lamp current was constant within

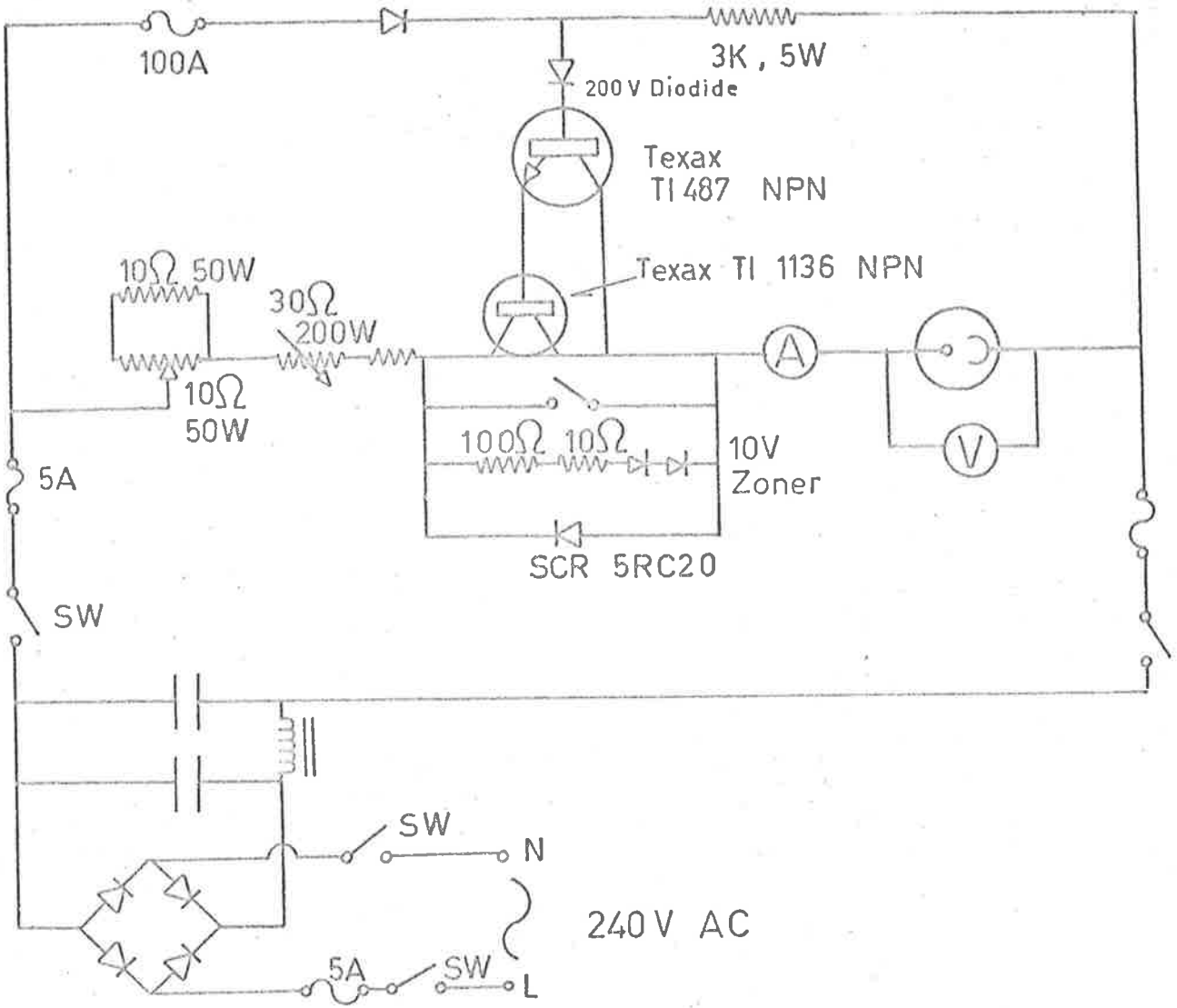

FIG. 5. Circuit Diagram for Stabilised Current D.C. Power Supply.

± 0.1%. Since the lamp did not correspond to a point source, it was very difficult to produce a parallel beam of uniform intensity, and experiments showed that the incident light intensity varied by as much as 20%-30% over the area of the cell. Most of the runs involved taking samples successively and as the level of liquid in the cell fell, then the rate of reaction varied, due to this change in intensity of the beam. After trying differing lens systems it was found that the best arrangement was to condense the beam to a small image, stop out the edge of this with a smaller iris and then use a 10 cm focal length, 6 cm diameter lens to give a parallel beam (Figure 6). By doing actinometry measurements (see later) with differing amounts of solution in the cell, it was shown that this arrangement gave a beam of even intensity to within 1%-2% across the 5 cm diameter face of the cell.

The 5461, 4358, and 3660 Å lines of the mercury arc were isolated by Zeiss Monochromat filters placed between the aperture and the 10 cm f.l. lens. The cylindrical pyrex glass reaction cell with polished windows was 5 cm in diameter and 2.5 cm thick. In addition to the long (22 cm) neck there was a short side arm which could either be stoppered or else used as a junction (via a salt bridge) to a reference cell in the case of potentiometric measurements (Figures 3 and 7).

"Oxygen-free" nitrogen, which had been passed through a chromous chloride tower to remove the remaining traces (10 p.p.m.) of oxygen,

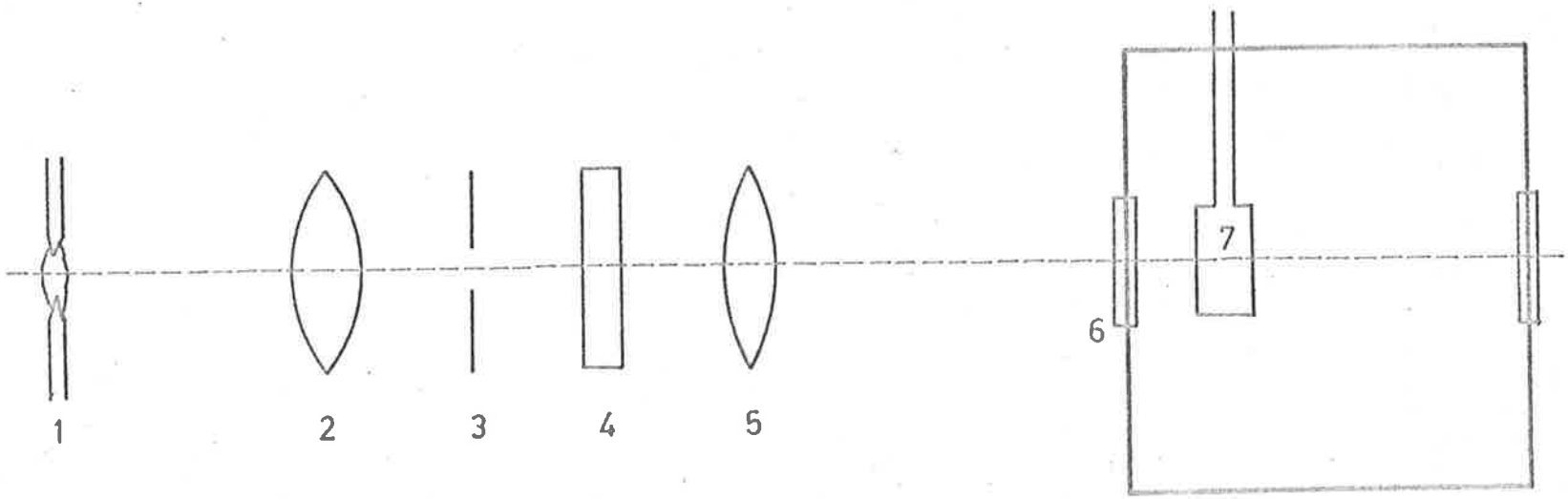

1. Hg Arc
2 Condensing Lens
3 Iris
4 Filter
5 Lens
6 Window
7 Cell
8 Water Bath

FIG. 6. Schematic Representation of Irradiation Apparatus.

was passed through the solution via the gas bubbler. As well as stirring the solution, this had the effect of excluding oxygen from the system.

The cell was held in a cradle which was placed reproducibly in a water thermostat bath controlled by a thermistor operated temperature controller to within $\pm$ 0.02°C. To exclude room light, the water bath was painted black except for an inlet window, and was covered with a close fitting lid.

The light intensity was varied over a range of 10:1 using a series of Kodak gelatin neutral density filters of different optical densities.

It was possible to estimate the light intensity approximately ($\pm$ 10%) in each case by considering the percentage transmittance of each filter, but it was necessary to make actinometry measurements (see Section 2.5) in all cases to obtain the required accuracy, ($\pm$ 1%), in the incident light intensity.

2.4 Procedure for Photolysis Experiments

The reaction mixtures were made up from the required quantities of stock solutions, including varying amounts of $NaClO_4$ solution so as to maintain a constant ionic strength of 0.5, pipetted into the reaction cell, and allowed to come to thermal equilibrium in the dark. In most cases, the concentration of Fe^{3+} ion was 5×10^{-2} M and SCN^- ion was 5×10^{-4} M. Under these conditions

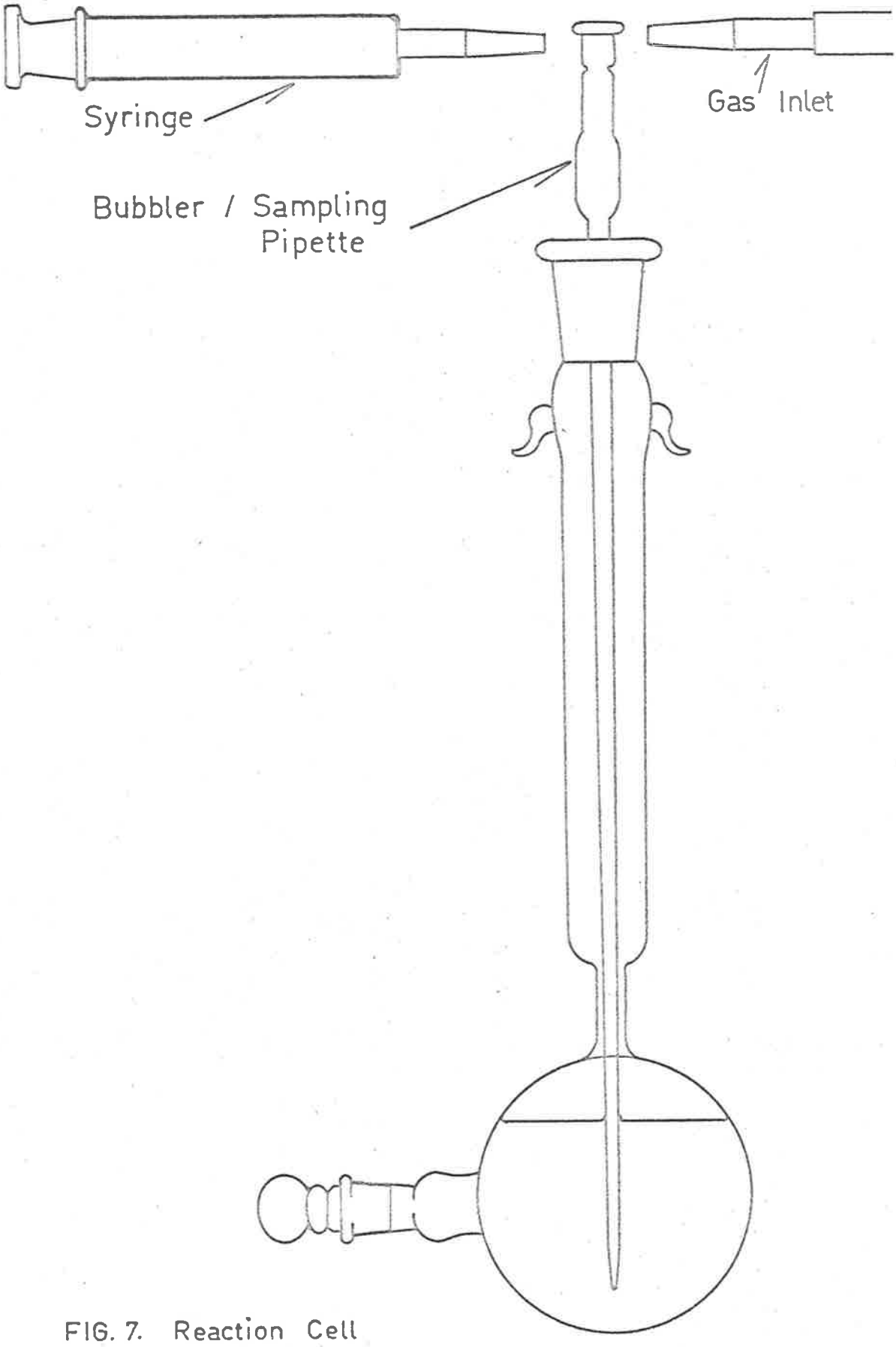

FIG. 7. Reaction Cell

the thermal reaction was only about 1% of the photochemical rate as determined by blank experiments. (Under the influence of room light the rate was considerably higher.) The thermal rates were in approximate agreement with those expected from an extrapolation of the data of Betts and Dainton.[43] At low light intensities and high SCN^- concentrations, however, a considerable correction had to be made to allow for the thermal rate. Whenever necessary, blank experiments were carried out in the dark.

For all experiments, oxygen-free nitrogen (see Section 2.3) was passed through the bubblers as a stirring agent, and when samples were to be taken, the gas inlet was removed from the top of the bubbler, a syringe connected in its place via a ground glass joint (Figure 7), the sample was drawn into bulk of the bubbler tube, and then transferred into a small beaker ready for accurate measurement into a volumetric flask for analysis. If there was to be any delay before analysing the samples, they were stored in a darkened cupboard to avoid undue photolysis by room light.

The lamp was always turned on at least $\frac{1}{2}$ hour before use to ensure complete warming up, and a shutter was placed across the face of the water bath window. At the start of the run, the shutter was removed and the time noted. After irradiating the cell for the appropriate time interval, the shutter was replaced and a sample removed as described except in the case of potentiometric ferrous determinations when a voltage measurement was made. The sample was then analysed either for Fe^{2+} or $FeNCS^{2+}$ as described in the

previous section. While this was being done, the shutter would be removed and the solution irradiated for a further time interval. It was possible to take ten 2 ml samples in any one run, from which to derive the initial rate of reaction.

2.5 Actinometry and Quantum Yield Calculations

The intensity of the 4358 Å and 3660 Å light incident on the reaction vessel was measured using the ferrioxalate actinometer as developed by Hatchard and Parker,[49] and at 5461 Å the light intensity was measured with a thermopile which was calibrated against the ferrioxalate actinometer at the lower wavelengths. Measurements were taken before and after each run, and the light intensity was found to be constant (for a given stabilised current) to within 1%-2% over several hours.

The technique used was that described by Hatchard and Parker[49] except that the ferrioxalate solution was prepared by mixing equal volumes of 0.30 M ferric ammonium sulphate and 0.90 M potassium oxalate solutions. The same cell, stirrer and sampling technique as described for the kinetic runs was used, and the optical density of the ferrous phenanthroline solution was measured in a 1 cm cell in a Unicam SP600 spectrophotometer.

Since the extinction coefficient for the ferrous phenanthroline was the same for both actinometry and kinetic measurements, and in most cases (see later) there was complete light absorption by both

actinometer and kinetic solutions, it was not generally necessary to calculate the absolute incident light intensity in quanta/cm^2/sec, but instead, the quantum yield for the production of Fe^{2+} in the reaction mixture ($\phi_{Fe^{2+}}$) was calculated from the relationship

$$\phi_{Fe^{2+}} = \frac{\text{moles of } Fe^{2+} \text{ produced in kinetic run}}{\text{moles of } Fe^{2+} \text{ produced in actinometer run}} \times \phi_{act}$$

which reduces to

$$\phi_{Fe^{2+}} = \frac{\text{O.D. change from kinetic run}}{\text{O.D. change from actinometer run}} \times \phi_{act} \times R$$

where R is the factor which allows for the different irradiation times, spectrophotometer cell lengths, and sizes of the samples analysed in the kinetic and actinometric runs, and ϕ_{act} is the known quantum yield for the ferrioxalate photolysis at the wavelength used.

In the case of the potentiometrically followed kinetic runs, the calibration curve (Figure 4) was used to determine the rate of production of Fe^{2+} in the reaction solution, and the quantum yield was calculated from

$$\phi_{Fe^{2+}} = \frac{\text{rate of production of } Fe^{2+} \text{ in kinetic run}}{\text{rate of production of } Fe^{2+} \text{ in actinometer run}}$$

For the runs which were followed by the analysis of $FeNCS^{2+}$

concentration, it was necessary to use the expression

$$\phi_{SCN^-} \text{ (quantum yield for } SCN^- \text{ disappearance)} = \frac{\text{rate of disappearance of } SCN^-}{\text{rate of production of } Fe^{2+} \text{ in actinometer run}} \times \phi_{act}$$

In this calculation, the extinction coefficients for both $FeNCS^{2+}$ and Fe^{2+}-phen were used.

For some runs, particularly at low SCN^- concentration, the $FeNCS^{2+}$ complex did not absorb 100% of the light incident on the cell, either because the O.D. due to $FeNCS^{2+}$ was too low, or the O.D. due to $FeOH^{2+}$ was too high, and so this species acted as an "inner filter". In these cases, the fraction of the light absorbed by $FeNCS^{2+}$ (I_{abs}/I_o) was calculated from the equation

$$\frac{I_{abs}}{I_o} = \frac{\varepsilon_1 \times [FeNCS^{2+}] \times l \times \left\{1-10^{-[(\varepsilon_1 \times [FeNCS^{2+}] \times l)+(\varepsilon_2 \times [FeOH^{2+}] \times l)]}\right\}}{(\varepsilon_1 \times [FeNCS^{2+}] \times l) + (\varepsilon_2 \times [FeOH^{2+}] \times l)}$$

where ε_1 = extinction coefficient of $FeNCS^{2+}$)
ε_2 = extinction coefficient of $FeOH^{2+}$) at λ of incident light.
$[FeNCS^{2+}]$ = concentration of $FeNCS^{2+}$
$[FeOH^{2+}]$ = concentration of $FeOH^{2+}$
l = path length of reaction cell.

Allowance for this fraction of light absorbed was then made in the calculation of $\phi_{Fe^{2+}}$ and ϕ_{SCN^-} as above.

The calibration of the thermopile for use in intensity measurements at 5461 Å was made by comparing the E.M.F. produced by the thermopile (detected as a galvanometer deflection), with the light intensity at the lower wavelengths at which actinometric measurements could be conveniently made.

The galvanometer deflection, (D), is a measure of the rate of energy absorption by the thermopile surface.

Therefore

$$D \propto Nh\nu \text{ ergs/sec/cm}^2$$

where N = No. of quanta

h = Planck's constant

ν = frequency of incident light

Therefore

$$N \propto D/\nu$$

i.e. $N \propto D.\lambda$ (λ = wavelength of incident light).

Measurements of the galvanometer deflection and Fe^{2+} produced by actinometry at 3660 Å and 4358 Å gave the same proportionality factor for the expression within 2.5%. The I_o at 5461 Å was then calculated from the measured galvanometer deflection and the known constant.

2.6 Errors

From the various rate plots of concentration versus time,

it was possible to obtain values for the initial rates within 1%-2%, except for the runs in which the change in $FeNCS^{2+}$ was measured using the SP700 spectrophotometer. The scatter of these points led to an overall deviation of 7-10% in the initial rate value.

Provided that care was taken to exclude room light, the actinometry measurements were reproducible to within 0.5%, and the values of ϕ_{act} as quoted by Hatchard and Parker were within 1%. As stated previously, the output from the lamp was constant within 1%-2% over several hours, and probably to within $\pm$ 0.5% for the duration of a run.

Any errors due to incorrect concentrations in the reactant mixtures would be less than 1%, since in nearly all cases, it is the concentration of only one species which is dominant in the mathematical expression for the quantum yields (see later).

It is therefore reasonable to assume that all calculated quantum yields are known with 4-5% precision except for the runs mentioned above which gave ϕ_{SCN} to within 10-12%.

CHAPTER 3

Results

3.1 Stoichiometry of the Reaction

Preliminary work on this system showed that $\phi_{Fe^{2+}}$, the quantum yield for the production of Fe^{2+} was always larger, by a factor of about six, than ϕ_{SCN^-}, the quantum yield for the disappearance of SCN^-.

In following the overall stoichiometry, reaction mixtures containing SCN^-, Fe^{3+} and H^+, but no Fe^{2+}, were irradiated at 4358 Å until all of the SCN^- was destroyed. The solutions were then analysed for total Fe^{2+} ion produced. The time required for complete bleaching of the $FeNCS^{2+}$ complex (taken as indicating $[SCN^-] = 0$), varied according to the initial concentrations of SCN^- and Fe^{3+}, and completion of reaction was not assumed until the optical density due to the remaining $FeNCS^{2+}$ measured in a 4 cm cell at 460 mμ, was less than 0.02. This corresponds to 10^{-6} M $FeNCS^{2+}$, and as the initial concentration was always greater than 10^{-4} M, showed that at least 99% of reaction was complete.

The ratio of [ferrous ion produced] to [thiocyanate ion destroyed] was found in nearly all cases to be 5.9 ± 0.2 (see Table 1), which suggests that the radical species is finally destroyed in a reaction analogous to the hydrolysis of thiocyanogen[52,53]

$$3(SCN)_2 + 4H_2O \longrightarrow 5SCN^- + SO_4^{=} + CN^- + 8H^+$$

so giving rise to a 6:1 stoichiometry (see Section 4.4).

Table 1

Typical Results of the Measurement of the Overall Stoichiometry of Reaction

Initial Concentrations			Final Concentrations		Ratio
SCN^-(M)	Fe^{3+}(M)	H^+(M)	SCN^-(M)	Fe^{2+}(M)	
4.99×10^{-4}	0.051	0.016	$\simeq 2 \times 10^{-6}$	2.93×10^{-3}	5.87
1.03×10^{-4}	0.050	0.080	$\simeq 1 \times 10^{-6}$	6.09×10^{-4}	5.91

Values for the ratio of up to 6.5 were obtained when solutions containing low acid concentrations (i.e. relatively high $FeOH^{2+}$ concentrations) were irradiated for 4 or 5 times longer than necessary to completely bleach the red colour.

This was probably due to light being absorbed by the $FeOH^{2+}$ complex, leading to Fe^{2+} production as a result of $FeOH^{2+}$ photolysis. In general, this did not introduce a significant error in the measured $FeNCS^{2+}$ stoichiometry, because even had the same rate of $FeOH^{2+}$ photolysis been maintained from the beginning of irradiation, there would have been a contribution due to $FeOH^{2+}$ photolysis of only 0.1 to the measured value of 5.9 ± 0.2 over the normal irradiation period. In the early stages of photolysis, before the SCN^- was destroyed, the $FeOH^{2+}$ absorbed a smaller fraction of the incident light and the rate of $FeOH^{2+}$ photolysis was slower because a much

larger fraction of the incident light was absorbed by the $FeNCS^{2+}$. In effect, $FeNCS^{2+}$ was acting as an "inner filter", reducing the rate of $FeOH^{2+}$ photolysis, and so in the normal irradiation time for these experiments the contribution of $FeOH^{2+}$ photolysis to the measured Fe^{2+} concentration was negligible.

Although analysis for other species in the bleached solution was made difficult by the high ferric concentration and ionic strength, both sulphate and cyanide ions were detected qualitatively. Attempts were made to detect sulphur, ammonia and cyanate ion, but there was no evidence for the formation of any of these species, all of which have been found previously as the oxidation products of SCN^-.[54,55,56]

3.2 Light Intensity Dependence

The rate of production of Fe^{2+} was measured over a range of light intensities of about 10:1. The results are given in Figure 8, which shows that the quantum yield is independent of the incident light intensity.

3.3 Dependence of $\phi_{Fe^{2+}}$ on Ferrous Concentration

In the thermal bleaching of $FeNCS^{2+}$,[43] the reaction was retarded by adding Fe^{2+} ion to the reaction mixture, and a corresponding reduction in $\phi_{Fe^{2+}}$ has been found in the photochemical reaction. Ferrous sulphate was added to the reaction mixtures, and the initial

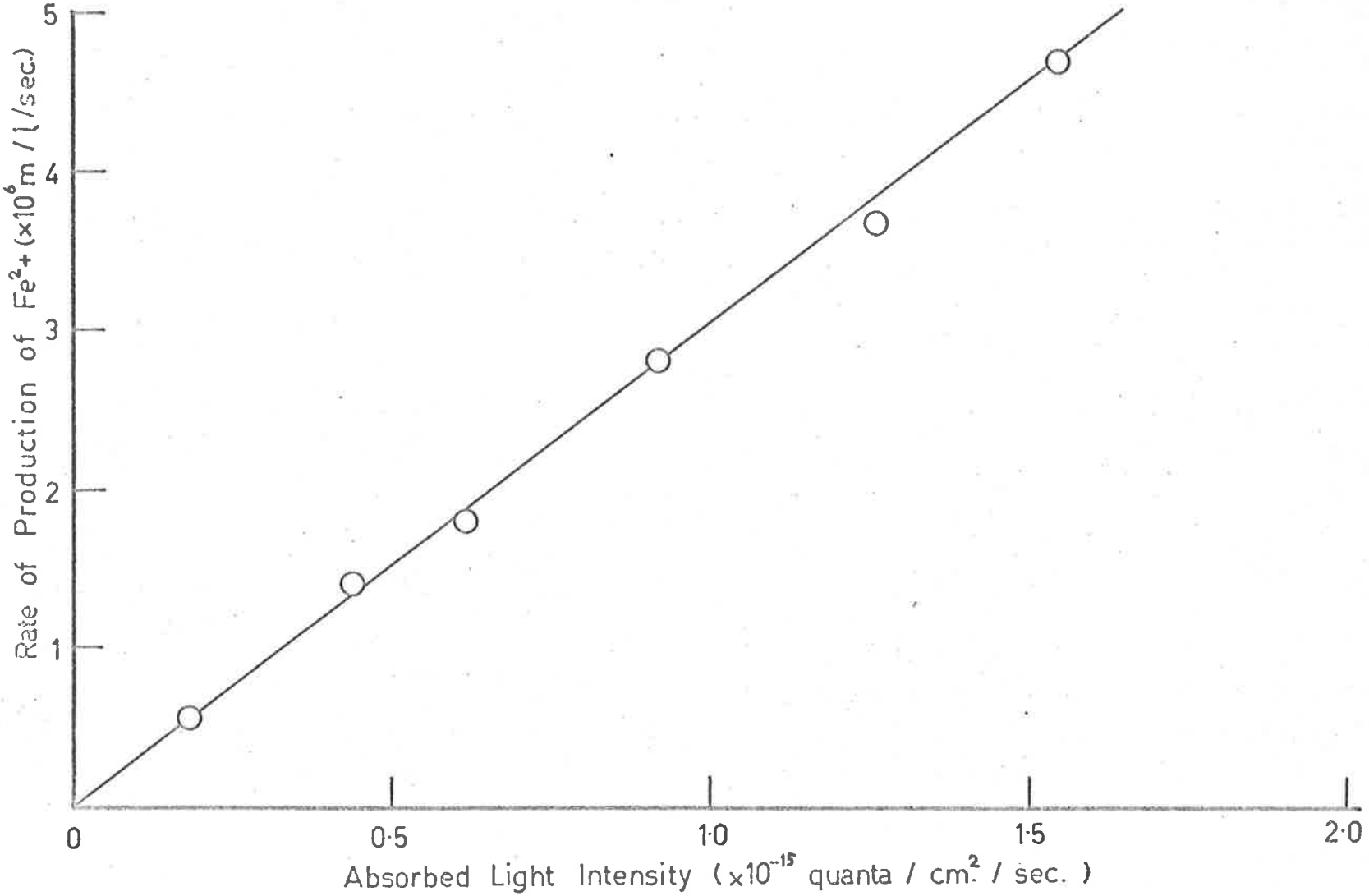

FIG. 8. Light Intensity Dependence.

rates (from which the quantum yields were calculated) were measured. Blank runs in which Na_2SO_4 was added showed that $SO_4^=$ ion had a negligible effect on the quantum yield. The variation of $\phi_{Fe^{2+}}$ with Fe^{2+} ion concentration is shown in Table 2.

As reaction proceeded the rate of production of Fe^{2+} slowed down even though there was still effectively 100% absorption of the incident light (Figure 9). This auto-retardation is most probably due to the accumulation of Fe^{2+} produced by the photolysis. A significant error was not introduced in any of the measured quantum yields by this since the maximum Fe^{2+} produced during any kinetic run was 0.5×10^{-4} M. The average Fe^{2+} concentration present during a kinetic run, and due to the accumulation of reactive products, was therefore of the order of $0.2\text{-}0.3 \times 10^{-4}$ M. Comparison with Table 2 shows that this may have affected the measured quantum yields at the lower added Fe^{2+} concentration by 2-3%, but at Fe^{2+} concentrations above 2×10^{-4} M, the effect would be negligible.

The lowering of the quantum yield on the addition of Fe^{2+} ions can be explained by assuming that the SCN$^\bullet$ radical species produced on photolysis are scavenged by Fe^{2+} ion, reacting to form $FeNCS^{2+}$

$$Fe^{2+} + SCN^\bullet \longrightarrow FeNCS^{2+} \qquad (3.1)$$

A similar type of reaction has been postulated in the thermal

Table 2

Dependence of $\phi_{Fe^{2+}}$ on Added Ferrous Ion Concentration

(a) $[Fe^{III}] = 0.05$ M; $[FeNCS^{2+}] = 4.50 \times 10^{-4}$ M; $[FeOH^{2+}] = 1.18 \times 10^{-3}$ M; $[H^+] = 0.0782$. Wavelength of Incident Light = 4358 Å.

$[Fe^{2+}] \times 10^4$ M	$\phi_{Fe^{2+}}$	$[Fe^{2+}] \times 10^4$ M	$\phi_{Fe^{2+}}$
0.00	0.064	5.09	0.041
1.02	0.058	7.13	0.037
2.04	0.047	10.18	0.032

(b) $[Fe^{III}] = 0.05$ M; $[FeNCS^{2+}] = 4.46 \times 10^{-4}$ M; $[FeOH^{2+}] = 4.22 \times 10^{-3}$ M; $[H^+] = 0.0202$. Wavelength of Incident Light = 4358 Å.

$[Fe^{2+}] \times 10^4$ M	$\phi_{Fe^{2+}}$	$[Fe^{2+}] \times 10^4$ M	$\phi_{Fe^{2+}}$
0.00	0.069	4.92	0.053
0.98	0.065	5.92	0.051
1.01	0.064	6.92	0.049
1.89	0.060	7.86	0.047
2.00	0.063	8.06	0.044
2.98	0.057	8.82	0.046
3.80	0.055	9.69	0.045
3.99	0.054	9.90	0.046
4.67	0.053		

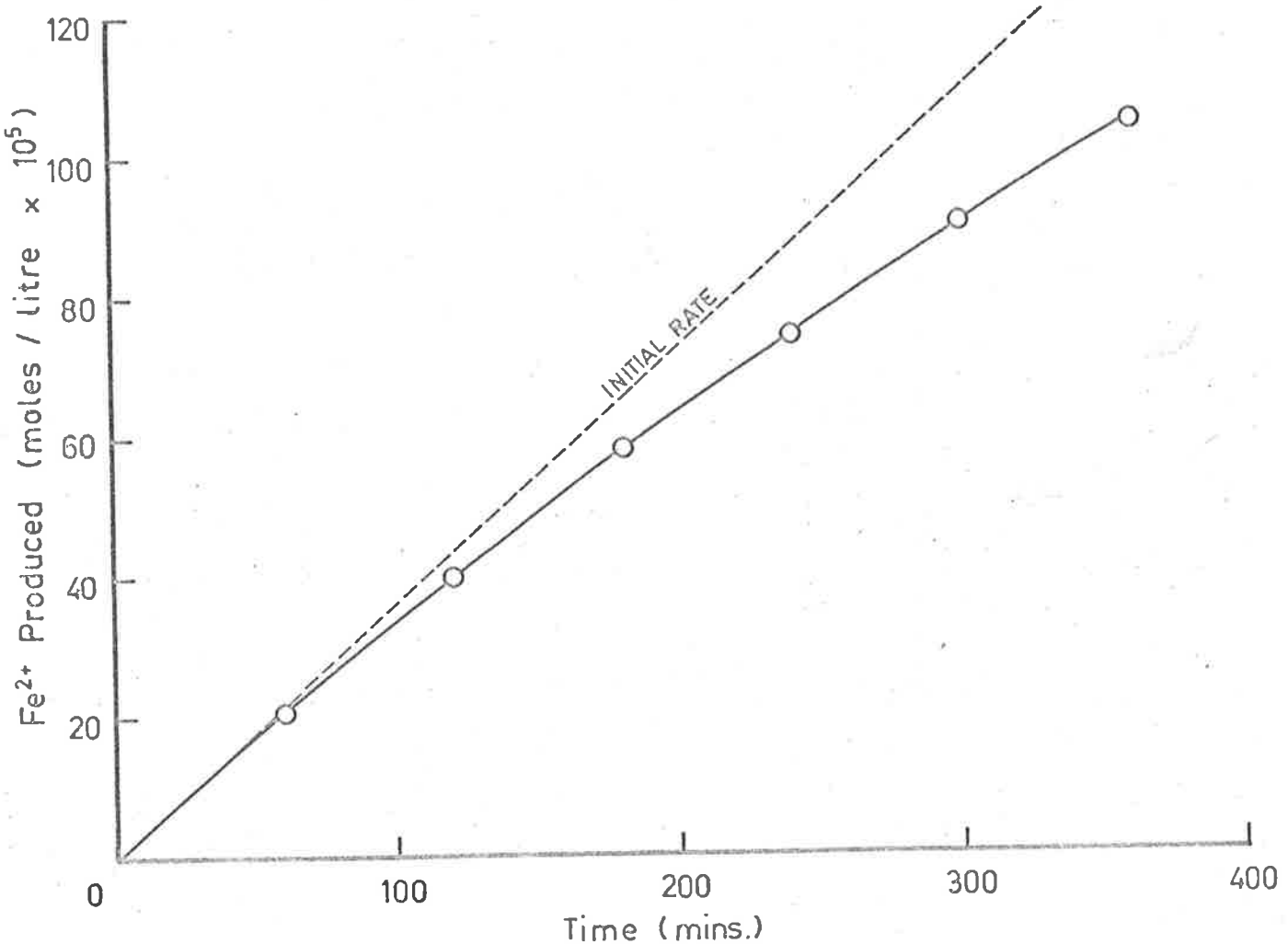

FIG. 9. Graph Showing Natural Retardation of the Reaction.

bleaching of $FeNCS^{2+}$,[43] and most photochemical investigations of labile ferric complexes,[34-40] as well as other metal complexes (e.g. $CeNO_3^{3+}$ [29]) have suggested the importance of this type of reaction.

3.4 Dependence of $\phi_{Fe^{2+}}$ on Acid Concentration

The results in Table 2 show that the extent to which $\phi_{Fe^{2+}}$ is diminished by adding Fe^{2+} is dependent on the acid concentration. If the reaction (3.1) is independent of $[H^+]$, then the variation is more probably due to a reaction involving the hydrolysed ferric species, $FeOH^{2+}$. In Table 3 and Figure 10, $\phi_{Fe^{2+}}$ increases as $FeOH^{2+}$ increases, as it would if a reaction such as (3.2) were contributing to the yield of Fe^{2+}.

$$SCN^{\bullet} + FeOH^{2+} \longrightarrow Fe^{2+} + HOSCN \qquad (3.2)$$

The species HOSCN has been previously suggested as an intermediate in both the hydrolysis of thiocyanogen[52,53] and the oxidation of thiocyanate by hydrogen peroxide.[54,55,56] By estimating the probable value of the O-S bond strength in HOSCN, it has been possible to show that reaction (3.2) is thermodynamically favourable, the estimated enthalpy change being -60 kcal/mole.

3.5 Dependence of $\phi_{Fe^{2+}}$ on $FeNCS^{2+}$ Concentration

Table 4 and Figure 11 show the effect on $\phi_{Fe^{2+}}$ of changing the

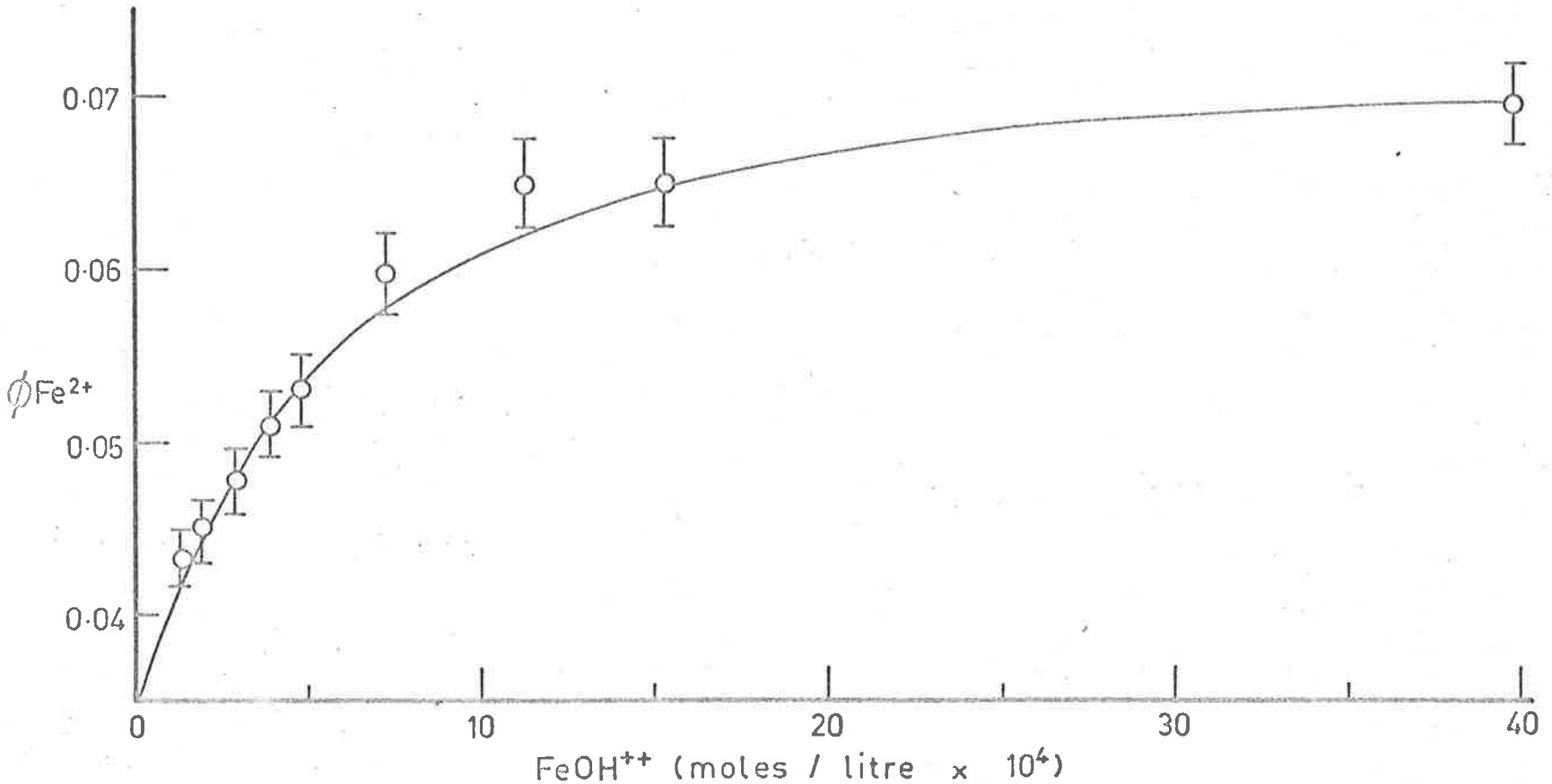

FIG. 10. Dependence of ϕFe^{2+} on $FeOH^{++}$ Concentration.

Table 3

The Dependence of $\phi_{Fe^{2+}}$ on Concentration of $FeOH^{2+}$

$[Fe^{III}] = 0.05$ M; $[FeNCS^{2+}] = 4.4 \times 10^{-4}$ M. Wavelength of Incident Light = 4358 Å.

Total $[H^+]$	$[FeOH^{2+}] \times 10^4$	$\phi_{Fe^{2+}}$	Total $[H^+]$	$[FeOH^{2+}] \times 10^4$	$\phi_{Fe^{2+}}$
0.602	1.36	0.0433	0.116	7.12	0.0599
0.497	1.65	0.0450	0.074	11.20	0.0651
0.284	2.88	0.0476	0.055	15.46	0.0650
0.221	3.71	0.0511	0.019	39.93	0.0690
0.180	4.58	0.0531			

$FeNCS^{2+}$ concentration, at two different acid concentrations. At the higher acid concentration (0.6 M), $\phi_{Fe^{2+}}$ increased as $FeNCS^{2+}$ increased, but at the lower acid concentration (0.020 M) $\phi_{Fe^{2+}}$ was almost independent of the complex concentration.

Changing the ratio of SCN^- to Fe^{3+} changes the $FeNCS^{2+}$ concentration but also changes the amount of the second complex, $Fe(NCS)_2^+$. If $Fe(NCS)_2^+$ played a significant part in the reaction scheme, this might alter the observed quantum yield. However, at the highest SCN^- concentration used, the concentration of $Fe(NCS)_2^+$ was calculated (using $K_2 = 15$ [57]) to be less than 1% of the $FeNCS^{2+}$ concentration.

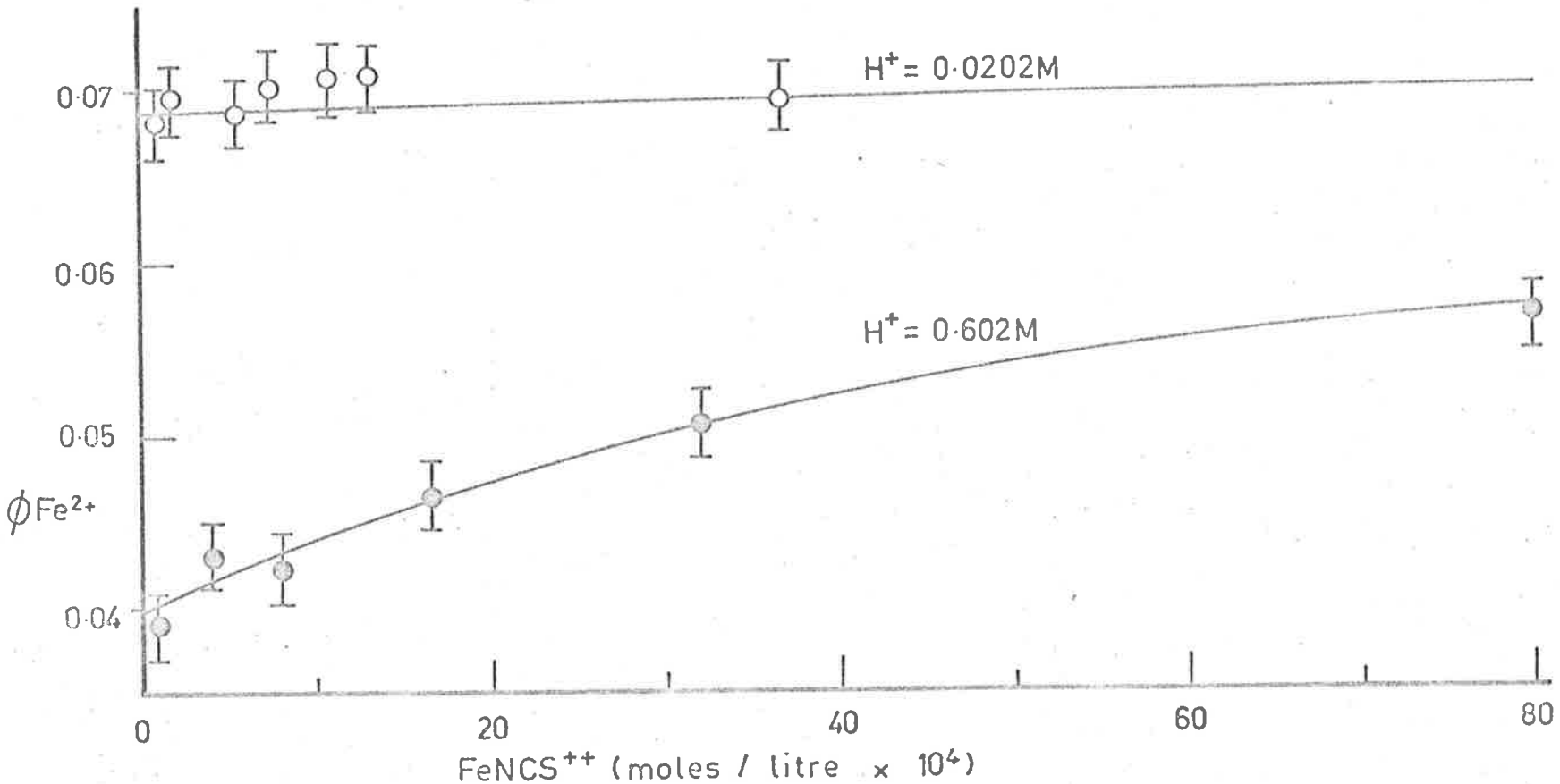

FIG. 11. Dependence of ϕFe^{2+} on $FeNCS^{++}$ Concentration.

Since the extinction coefficient at 460 mμ of the second complex is only twice that of the first complex,[57] there was very little light absorbed by $Fe(NCS)_2^+$, and it is unlikely that photolysis of this species is the cause of the observed variation in $\phi_{Fe^{2+}}$. In addition, the effect is unlikely to have been acid dependent if it were due only to the changing concentration of $Fe(NCS)_2^+$.

Table 4

The Dependence of $\phi_{Fe^{2+}}$ on Concentration of $FeNCS^{2+}$

(a) $[Fe^{III}] = 0.05$ M; $[FeOH^{2+}] = 1.36 \times 10^{-4}$ M; $[H^+] = 0.602$ M

Wavelength of Incident Light = 4358 Å

$[FeNCS^{2+}] \times 10^4$	$\phi_{Fe^{2+}}$	$[FeNCS^{2+}] \times 10^4$	$\phi_{Fe^{2+}}$
0.80	0.0388	16.30	0.0464
4.14	0.0430	32.30	0.0503
8.13	0.0420	79.30	0.0563

(b) $[Fe^{III}] = 0.05$ M; $[FeOH^{2+}] = 4.23 \times 10^{-3}$ M; $[H^+] = 0.020$ M

Wavelength of Incident Light = 4358 Å

$[FeNCS^{2+}] \times 10^4$	$\phi_{Fe^{2+}}$	$[FeNCS^{2+}] \times 10^4$	$\phi_{Fe^{2+}}$
0.90	0.0681	9.20	0.0705
1.48	0.0695	11.43	0.0709
4.61	0.0688	36.82	0.0692
6.38	0.0703		

The dependence on $FeNCS^{2+}$ can be accounted for by the reaction

$$SCN^{\bullet} + FeNCS^{2+} \longrightarrow Fe^{2+} + (SCN)_2 \qquad (3.3)$$

This is in competition with reaction (3.2) and so explains the variation of the $FeNCS^{2+}$ dependence with acid concentration, since at low acid the $FeOH^{2+}$ concentration is sufficiently large to scavenge virtually all of the radicals. Reaction (3.3) is also thermodynamically favourable, with an estimated standard enthalpy change of about -70 kcal/mole.

3.6 Dependence of $\phi_{Fe^{2+}}$ on Fe^{3+} Concentration

A series of runs was carried out in which the total Fe^{3+} concentration was varied while SCN^- and H^+ concentrations were kept constant (Table 8, Section 4.10). It is not possible to determine what change in $\phi_{Fe^{2+}}$ was due to changing Fe^{3+} concentration alone, as both the $FeNCS^{2+}$ and $FeOH^{2+}$ concentrations also vary with the total Fe^{3+} concentration and so lead to a change in the measured quantum yield. However, it is probable that if the thiocyanate radical species can react with $FeNCS^{2+}$ and $FeOH^{2+}$, then it will also react with free Fe^{3+}.

Reaction between thiocyanate radical and Fe^{3+} ion is therefore considered in the discussion of the overall reaction scheme.

3.7 Wavelength Dependence

The quantum yield for the production of Fe^{2+} was measured at 3660 Å, 4358 Å, and 5461 Å under concentration conditions such that $\phi_{Fe^{2+}}$ was a maximum. These concentrations have already been determined in Sections 3.4, 3.5, and 3.6. After allowing for the percentage light absorbed at each wavelength, the quantum yields were as shown in Table 5.

Table 5

Dependence of $\phi_{Fe^{2+}}$ on Wavelength at 25°C

$[Fe^{III}] = 0.050$ M; $[SCN^-] = 5 \times 10^{-4}$ M; $[H^+] = 1.6 \times 10^{-2}$ M.

λ (Å)	3660	4358	5461
ν (cm^{-1})	27320	22940	18320
$\phi_{Fe^{2+}}$	0.124	0.070	0.030

The decrease in $\phi_{Fe^{2+}}$ as the energy of the quantum of absorbed light decreases suggests that at least part of the energy absorbed by the $FeNCS^{2+}$ molecule appears as kinetic energy of the fragments, and so affects the extent to which the fragments can diffuse from the solvent cage and avoid primary recombination.

3.8 Temperature Dependence

The rate of reaction was measured at 25°C, 33°C and 40°C using identical solutions consisting of 0.05 M Fe^{3+}, 5 x 10^{-4} M SCN^- and 0.016 M H^+. The wavelength of the incident light was 4358 Å. The observed values of the rate of reaction gave an Arrhenius activation energy plot of log (rate) versus the reciprocal of the absolute temperature (Figure 12). From the slope of this straight line, the energy of activation was calculated to be 4.8 $\pm$ 0.5 kcal/mole.

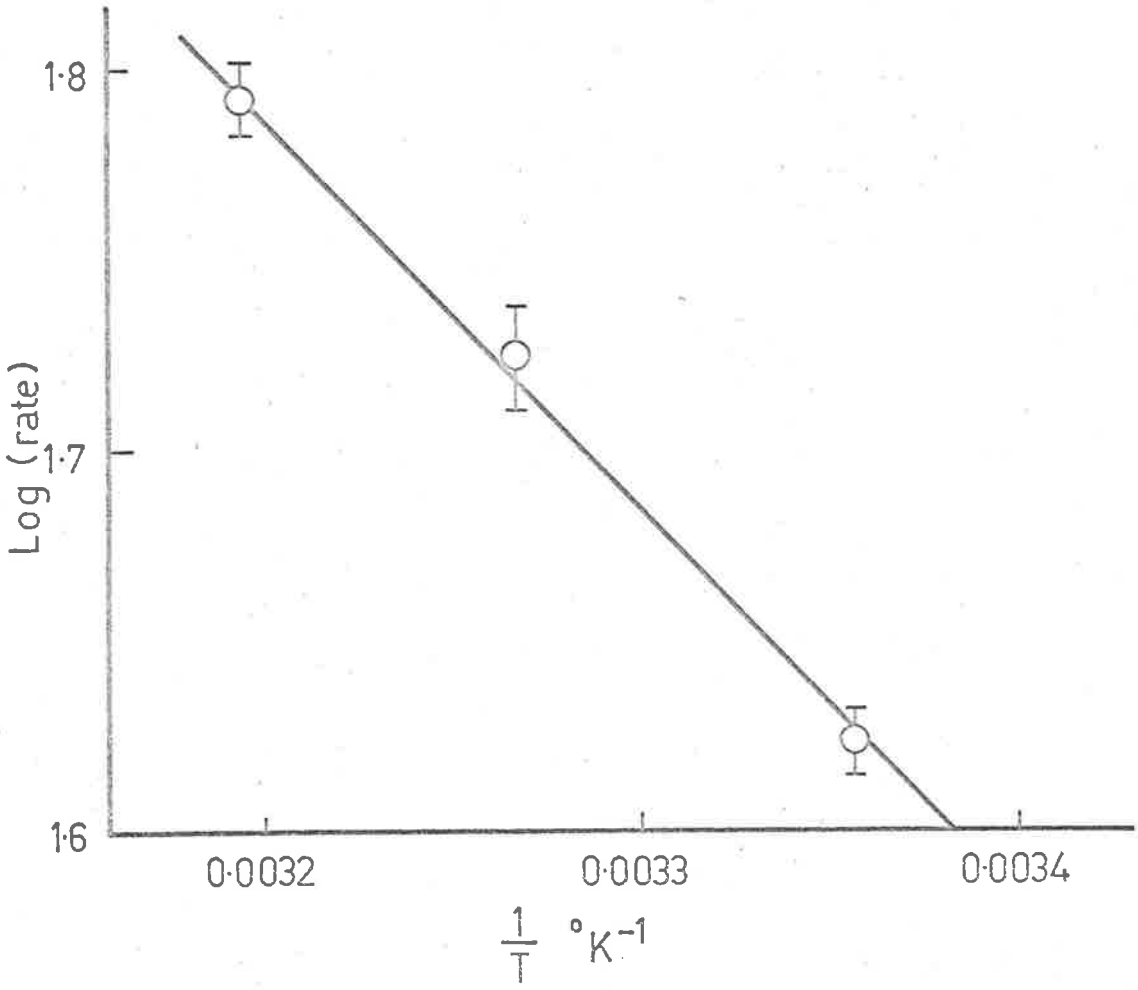

FIG. 12. Arrhenius Activation Energy Plot.

CHAPTER 4

Discussion

4.1 The Primary Photochemical Act

The results presented in the previous chapter show that the overall effect of the absorption of light by the $FeNCS^{2+}$ complex is the production of ferrous ion and oxidation products of thiocyanate ion. It is therefore evident that the primary chemical act following the absorption of light by the complex leads to the transfer of an electron from the thiocyanate ion to the ferric ion.

$$FeNCS^{2+} + h\nu \longrightarrow (Fe^{2+} \ldots\ldots {}^{\bullet}NCS)_{cage}$$

The ferrous ion and thiocyanate radical are initially produced in pairs within a solvent cage (a non-random distribution) and then undergo a variety of processes. Noyes[31,32] has discussed the kinetics of this type of reaction, and a description of his treatment has been given in Chapter 1. The present work will be described using his concepts and definitions.

Following the formation of the reactive fragments within the solvent cage, they may either undergo back electron transfer within the cage (primary recombination) or separate by diffusion. Since it is unlikely that primary recombination can be competed with (see Section 1.3.a), the fraction of radicals (or Fe^{2+} ions) escaping from the cage (ϕ_1) following the absorption of each quantum of light will be constant regardless of the addition of any other

material to the reaction mixture.

Subsequent to the diffusive separation, the fragments may undergo secondary recombination with their original partners, combine with the fragments from other dissociations, or undergo reactions with other species in solution. All of these possibilities will be discussed.

4.2 The Nature of the Thiocyanate Radical Species

So far in this thesis, the reactive thiocyanate species produced by the light absorption has been written as the thiocyanate radical $SCN^{\bullet}$, but the results are also consistent with the species being the radical ion $(SCN)_2^-$, produced by the reaction

$$SCN^{\bullet} + SCN^- \rightleftharpoons (SCN)_2^- \qquad (4.1)$$

The radical-ion has been suggested as an intermediate in the thermal bleaching of ferric thiocyanate,[43] and the γ—radiolysis of thiocyanate solutions,[58] and recent pulse radiolysis studies[59,60,61] have confirmed its existence in aqueous solution.

Pulse radiolysis has been used to measure both the rate constants and formation constants for the equilibrium

$$X^{\bullet} + X^- \underset{k_b}{\overset{k_f}{\rightleftharpoons}} X_2^-$$

where X = SCN, Br, and I. The values are given in Table 6.

Table 6

Measured Values of Rate and Formation Constants for the Reaction

$$X^{\bullet} + X^{-} \rightleftharpoons X_2^{-}$$

X	Rate Constant	Formation Constant	Ref.
Br	5.4×10^9	2.2×10^5	62,63
I	7.6×10^9	1.3×10^5	61,64
SCN	7.0×10^9	2.0×10^5	61

The minimum free thiocyanate concentration in any run was 5×10^{-5} M, and the steady state concentration of $SCN^{\bullet}$ and $(SCN)_2^{-}$ was very much less than 10^{-5} M. The ratio $(SCN)_2^{-}/SCN^{\bullet}$ was therefore at least 10 and in many cases was considerably more. As equilibrium in these systems is reached so quickly the majority of radicals which escape primary recombination will exist in solution as the radical-ion $(SCN)_2^{-}$. The identity of the radical species as $SCN^{\bullet}$ or $(SCN)_2^{-}$ does not affect the interpretation of the kinetic data if reaction (4.1) is assumed to be mobile compared with the other reactions which involve the radical species. With k_f close to diffusion controlled this is a reasonable assumption. Even if $SCN^{\bullet}$ and $(SCN)_2^{-}$ have different reactivities, then only the fastest reacting one will be important because of the speed at which equilibrium (4.1) is established. Within the limits of this assumption, the terms $SCN^{\bullet}$, $(SCN)_2^{-}$ and thiocyanate radical can

then be used synonomously.

4.3 The Reaction Scheme

In the preceding chapter qualitative evidence has been given for reactions of Fe^{2+}, $FeOH^{2+}$, $FeNCS^{2+}$ and Fe^{3+} with those radicals produced by the photochemically induced electron transfer which escape primary recombination within the solvent cage. These form the basis of the following reaction scheme.

$$FeNCS^{2+} \xrightarrow[I_{abs}]{\phi_1} Fe^{2+} + SCN^{\bullet} \qquad (4.2)$$

$$SCN^{\bullet} + SCN^{-} \rightleftharpoons (SCN)_2^{-} \qquad (4.1)$$

$$\left.\begin{aligned} (SCN)_2^{-} + Fe^{2+} &\xrightarrow{k_1} FeNCS^{2+} + SCN^{-} \\ SCN^{\bullet} + Fe^{2+} &\xrightarrow{k_1} FeNCS^{2+} \end{aligned}\right\} \qquad (4.3)$$

$$\left.\begin{aligned} (SCN)_2^{-} + FeNCS^{2+} &\xrightarrow{k_2} Fe^{2+} + (SCN)_2 + SCN^{-} \\ SCN^{\bullet} + FeNCS^{2+} &\xrightarrow{k_2} Fe^{2+} + (SCN)_2 \end{aligned}\right\} \qquad (4.4)$$

$$\left.\begin{aligned} (SCN)_2^{-} + FeOH^{2+} &\xrightarrow{k_3} Fe^{2+} + (SCN)_2 + OH^{-} \\ SCN^{\bullet} + FeOH^{2+} &\xrightarrow{k_3} Fe^{2+} + HOSCN \end{aligned}\right\} \qquad (4.5)$$

$$(SCN)_2^{-} + Fe^{3+} \xrightarrow{k_4} Fe^{2+} + (SCN)_2 \qquad (4.6)$$

4.4 Stoichiometry

Thiocyanogen, $(SCN)_2$ is known to be unstable in aqueous solution,

and hydrolyses[52,53] very rapidly to yield cyanide, sulphate and thiocyanate ions. The reaction scheme proposed for hydrolysis is

$$(SCN)_2 + H_2O \longrightarrow HOSCN + HSCN$$

$$2HOSCN \longrightarrow HSCN + NCSO_2H$$

$$HOSCN + NCSO_2H \longrightarrow NCSH + NCSO_3H$$

$$NCSO_3H + H_2O \longrightarrow NCH + H_2SO_4$$

i.e. the overall hydrolysis is

$$3(SCN)_2 + 4H_2O \longrightarrow 5SCN^- + SO_4^{=} + CN^- + 8H^+ \qquad (4.7)$$

The stoichiometry of the hydrolysis together with the photolysis reaction scheme given above (Section 4.3) leads to the value of six for the ratio $\phi_{Fe^{2+}}/\phi_{SCN^-}$. Initially, from every ferric thiocyanate ion there is formed one Fe^{2+} ion and one radical. The fraction of these escaping primary recombination is ϕ_1. The radicals must eventually be destroyed by a series of reactions analogous to the hydrolysis of thiocyanogen, since this is the only way in which a fraction of the radicals can be completely destroyed at the same time as some are reconverted to thiocyanate ion.

It is probable that each radical which escapes primary recombination reacts with another Fe^{III} species to produce another ferrous ion, and in doing so oxidises yet another SCN^- ion to

produce a molecule of thiocyanogen. That is, in the formation of two moles of Fe^{2+} ion and one mole of thiocyanogen, two moles each of Fe^{3+} and SCN^- are destroyed. However, because of the stoichiometry of reaction (4.7), each mole of thiocyanogen on hydrolysis regenerates $^5/_3$ moles of thiocyanate ion, so that overall only $^1/_3$ mole of thiocyanate ion is destroyed for every two moles of Fe^{2+} produced.

i.e. $$\frac{Fe^{2+} \text{ produced}}{SCN^- \text{ destroyed}} = \frac{2}{1/3} = 6.$$

4.5 Reaction of the Radical with Species Other Than Fe^{II} and Fe^{III} Complexes

If the reactions with Fe^{III} species are competing only with Fe^{2+} for the radicals, then for those runs in which no Fe^{2+} was initially added to the reaction mixture, $\phi_{Fe^{2+}}$ would be independent of acid or thiocyanate concentrations, as all of the radicals escaping primary recombination would react either with $FeOH^{2+}$, $FeNCS^{2+}$ or Fe^{3+}, so that $\phi_{Fe^{2+}} = 2\phi_1$. Likewise, in the absence of other radical reactions the Fe^{2+} dependence at fixed acid and thiocyanate concentrations would be such that $\phi_{Fe^{2+}}$ approached zero at sufficiently high Fe^{2+} concentrations.

The observed variations in the quantum yield with H^+, SCN^- and Fe^{2+} concentrations must therefore be due to competition for the radicals by a reaction which neither produces Fe^{2+}, nor any

other species which may act as an oxidising or reducing agent which can react either with Fe^{2+} or Fe^{III} species. It is unlikely that radical reactions with trace impurities are important because the use of reagents from widely differing sources had no noticeable effect on $\phi_{Fe^{2+}}$, and doubly distilled water (Section 2.1) was used in making up all solutions.

Two possible reactions which may compete in this way and still maintain the 6:1 stoichiometry are the hydrolysis of the $(SCN)_2^-$ radical-ion

$$(SCN)_2^- + H_2O \xrightarrow{k_5} X \qquad (4.8)$$

and a bimolecular termination step

$$2(SCN)_2^- \xrightarrow{k_6} (SCN)_2 + 2SCN' \qquad (4.9)$$

followed by

$$X, \text{ or } (SCN)_2 + H_2O \longrightarrow \text{hydrolysis products.}$$

The reaction scheme must therefore include either reaction (4.8) or (4.9), or both.

At first sight, equation (4.8) seems to be a vague description of the probable reaction, but considering recent flash photolysis and pulse radiolysis studies of the thiocyanate systems, one can see that the exact reaction pathways for the decay of the radical are difficult to define even when direct measurements of the

concentrations of the radical species itself can be made. Dogliotti and Hayon[65] have found that the decay of the transient produced on photolysis of CNS^- ion in N_2-saturated neutral and acidic solutions is first order, and independent of CNS^- concentration. The decay is also first order in neutral, acid or alkaline solutions saturated with N_2O gas, but in the presence of oxygen the decay rate approaches second order.

Baxendale et al.[61] in their pulse radiolysis work found exclusively second order decay of the transient species, but Adams et al.[59], also using pulse radiolysis techniques showed that in acid solutions in the presence of oxygen, the decay kinetics are even more complex.

Since there are differences in the observed decay kinetics of what is apparently the same species in these direct studies, it is not surprising that there is considerable uncertainty in defining the reaction in the present work when it is not possible to make direct measurements on the species in question. For example, reaction (4.8) may or may not be acid catalysed, but it is only by a detailed kinetic analysis (see Section 4.9) that any distinction can be made between the various possibilities.

4.6 Light Intensity Dependence

A steady state treatment of the kinetics (see Appendix I) shows that if reaction (4.9) occurs appreciably, there will be a

complex dependence on I_{abs}, the absorbed light intensity.

$$\phi = \phi_1 + \frac{A}{I_{abs}} \left[\frac{B \pm \sqrt{B^2 + 4k_6\phi_1 I_{abs}}}{2k_6} \right] \qquad (4.10)$$

where $A = k_1[Fe^{2+}] - k_2[FeNCS^{2+}] - k_3[FeOH^{2+}] - k_4[Fe^{3+}]$

and $B = k_1[Fe^{2+}] + k_2[FeNCS^{2+}] + k_3[FeOH^{2+}] + k_4[Fe^{3+}]$

whereas reaction (4.8) leads to a quantum yield independent of the absorbed light intensity

$$\phi = \phi_1 \left[\frac{2k_2[FeNCS^{2+}] + 2k_3[FeOH^{2+}] + 2k_4[Fe^{3+}] + k_5}{k_1[Fe^{2+}] + k_2[FeNCS^{2+}] + k_3[FeOH^{2+}] + k_4[Fe^{3+}] + k_5} \right] \qquad (4.11)$$

In the absence of added Fe^{2+} ion, since A = -B, equation (4.10) can be rewritten as

$$\frac{\delta[Fe^{2+}]}{\delta t} = \phi_1 I_{abs} - B \left[\frac{B \pm \sqrt{B^2 + 4k_6\phi_1 I_{abs}}}{2k_6} \right] \qquad (4.12)$$

The values of the terms which comprise B are not known for this reaction scheme and it is not possible to determine accurately the exact light intensity dependence to be expected. However, it is possible to discuss three distinct alternatives.

First, if $(4k_6\phi_1 I_{abs}) \gg B^2$, then equation (4.12) reduces to

$$\frac{\delta[Fe^{2+}]}{\delta t} = \phi_1 I_{abs} \pm \frac{B}{2k_6} \cdot \sqrt{4k_6\phi_1 I_{abs}} \qquad (4.13)$$

According to equation (4.13) the light intensity dependence would be curved due to the superimposition of the square root and linear terms unless the second term was much smaller than the first. The values of I_{abs} and k_6[59] are known to be approximately 10^{-8} Einstein.l^{-1}.sec^{-1} and 10^9 l.moles^{-1}.sec^{-1} respectively and ϕ_1 is of the order of 0.1. On substituting those values in equation (4.13)

$$\frac{\delta[Fe^{2+}]}{\delta t} \simeq 1 \times 10^{-9} \pm \frac{B}{2 \times 10^9} \sqrt{4 \times 10^9 \times 0.1 \times 10^{-8}}$$

$$\simeq 1 \times 10^{-9} \pm B \times 10^{-9}$$

Therefore it can be seen that B would have to be less than 0.1 for the second term to make a contribution of less than 10% to $\delta[Fe^{2+}]/\delta t$. Under the experimental conditions used ($[Fe^{3+}] = 0.05$; $[SCN^-] = 2 \times 10^{-4}$; $[H^+] = 0.077$) this would be extremely unlikely, since the prominent term in B is probably $k_4[Fe^{3+}]$, making k_4 = 2 litre/moles/sec at the most. The rate constants for a reaction such as (4.6) would be expected to be considerably larger than this, since it is known that rate constants for reactions between OH radicals and Fe^{2+} are of the order of 10^8 [66] and other workers[43,58] have shown that reaction (4.6) is faster than reaction (4.3). It is

reasonable then to assume that equation (4.13) would lead to a non-linear dependence on I_{abs}.

If, in equation (4.12), $B^2 \gg (4k_6\phi_1 I_{abs})$, then there are still two possibilities corresponding to the plus and minus signs in the last term.

Using the negative root, equation (4.12) becomes

$$\frac{\delta[Fe^{2+}]}{\delta t} = \phi_1 I_{abs}$$

but this is invalid as it corresponds to the steady state concentration of radicals being zero and is obviously an unreal solution.

The positive root gives rise to the expression

$$\frac{\delta[Fe^{2+}]}{\delta t} = \phi_1 I_{abs} - \frac{B^2}{k_6}$$

$$= \phi_1 I_{abs} - \text{const.} \qquad (4.14)$$

showing that the light intensity dependence, although linear, would have a negative intercept which would be of considerable magnitude using the estimated values of B and k_6.

As the experimentally determined light intensity dependence is linear, and passes through the origin, it is evident that none of these alternatives based on reaction (4.9) as the termination step offer a valid explanation of the system. It is concluded therefore that reaction (4.8) is the important

reaction by which the radical is destroyed without the formation of Fe^{2+} or some other oxidising species, even though there is considerable uncertainty as to its exact nature.

A stationary state treatment of the complete reaction scheme, including reaction (4.8) yields equation (4.11) (see Appendix I).

4.7 Effect of Ferrous Ion

Equation (4.11) on rearrangement gives

$$\frac{1}{\phi} = \frac{1}{\phi_1}\left[\frac{k_1[Fe^{2+}]}{2k_2[FeNCS^{2+}] + 2k_3[FeOH^{2+}] + 2k_4[Fe^{3+}] + k_5} + \frac{k_2[FeNCS^{2+}] + k_3[FeOH^{2+}] + k_4[Fe^{3+}] + k_5}{2k_2[FeNCS^{2+}] + 2k_3[FeOH^{2+}] + 2k_4[Fe^{3+}] + k_5}\right] \quad (4.15)$$

For a given set of Fe^{3+}, SCN^- and H^+ concentrations a plot of $1/\phi$ versus $[Fe^{2+}]$ should be linear, with a slope and intercept which are dependent on the concentrations of the various ferric species. The experimental results are shown in Figure 13, the solid lines being the calculated least square lines through the points.

4.8 Effect of $FeOH^{2+}$ and $FeNCS^{2+}$

In the absence of added Fe^{2+} ion, equation (4.11) becomes

$$\phi_{Fe^{2+}} = \phi_1\left[1 + \frac{k_2[FeNCS^{2+}] + k_3[FeOH^{2+}] + k_4[Fe^{3+}]}{k_2[FeNCS^{2+}] + k_3[FeOH^{2+}] + k_4[Fe^{3+}] + k_5}\right] \quad (4.16)$$

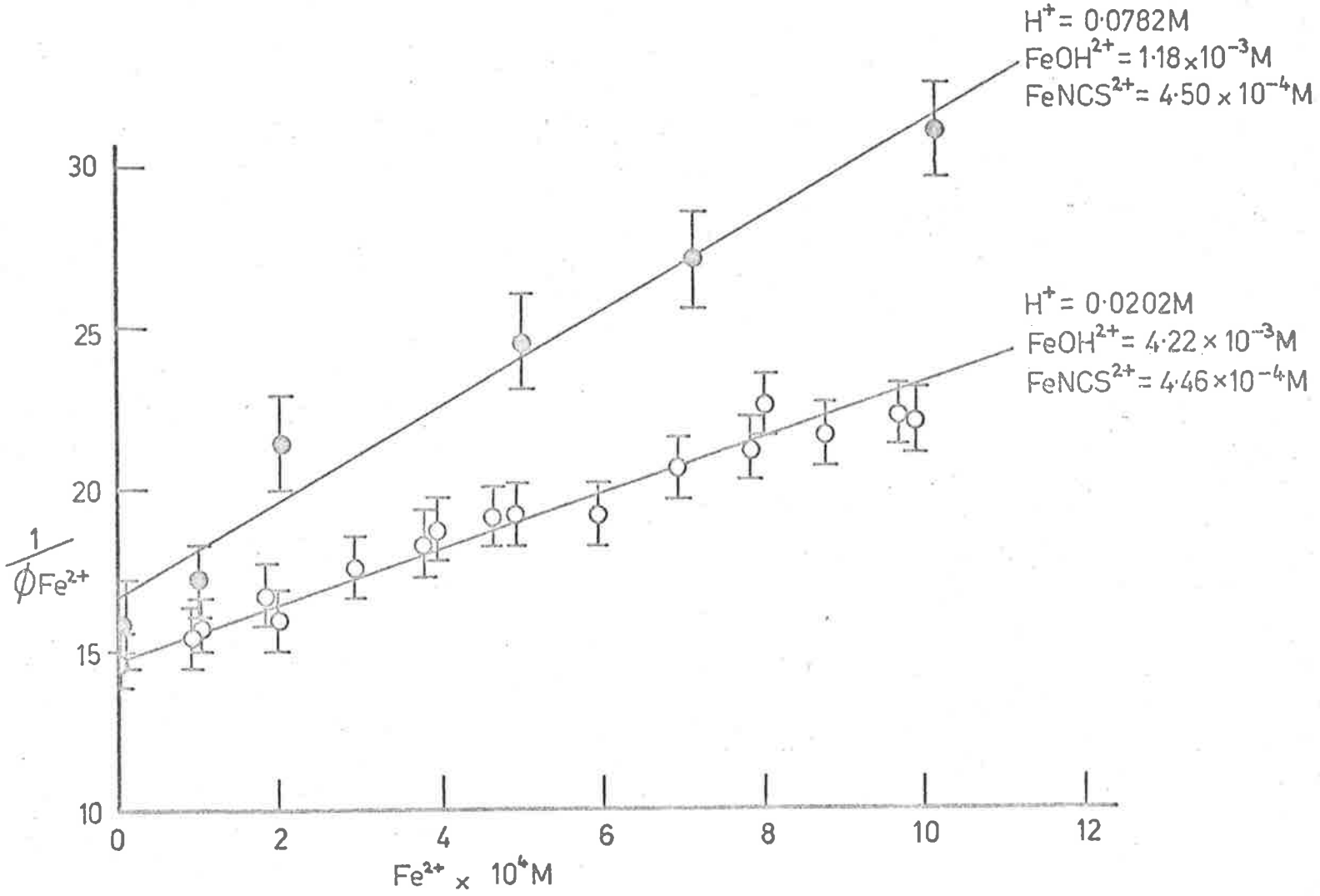

FIG. 13. The Dependence of $\frac{1}{\phi Fe^{2+}}$ on Ferrous Ion Concentration.

When the $FeOH^{2+}$, $FeNCS^{2+}$ and Fe^{3+} concentrations are sufficiently small, equation (4.16) reduces to

$$\phi_{Fe^{2+}} = \phi_1$$

but at the other limit, when these concentrations are sufficiently large to capture all of the radicals, then equation (4.16) becomes

$$\phi_{Fe^{2+}} = 2\phi_1$$

This behaviour can be seen in Tables 3 and 4, and Figures 10 and 11. At low acid (0.02 M) concentrations, $\phi_{Fe^{2+}}$ is 0.07 ± 0.002 and independent of SCN^- concentration, due to the concentration of $FeOH^{2+}$ (4.23×10^{-3} M) being large enough to make $\phi_{Fe^{2+}}$ equal to $2\phi_1$ within experimental error at all thiocyanate concentrations. Thus $\phi_1 = 0.035$. Under conditions of higher acid concentrations (0.6 M), the $FeOH^{2+}$ concentration is much lower ($\leq 2 \times 10^{-4}$ M) and the quantum yield increases from a value equal to ϕ_1 towards $2\phi_1$, as the SCN^- concentration increases. Similarly, at constant $FeNCS^{2+}$, $\phi_{Fe^{2+}}$ increases as the $FeOH^{2+}$ concentration is increased until a maximum value of $2\phi_1$ is reached.

4.9 Calculation of Relative Rate Constants

In order to calculate the relative values of the various rate constants, a set of equations relating them to each other were

derived. Using equation (4.15) and the slopes of the ferrous dependences (S), two equations of the form

$$S = \frac{k_1}{2k_2[FeNCS^{2+}] + 2k_3[FeOH^{2+}] + 2k_4[Fe^{3+}] + k_5}$$

were obtained, corresponding to the two separate Fe^{2+} dependences done at different concentrations of $FeOH^{2+}$, $FeNCS^{2+}$ and Fe^{3+}. In addition, a random selection of points from the $FeOH^{2+}$ and $FeNCS^{2+}$ dependences was made, and on substituting the appropriate values for measured quantum yields, concentrations and ϕ_1 in equation (4.16), a set of equations also containing k_2, k_3, k_4 and k_5 was obtained.

In attempting to solve these equations simultaneously to give values for the ratios k_2/k_5, k_3/k_5 and k_4/k_5, the ratios were found to vary depending on which set of values were used in setting up the equations. There was an apparent inverse dependence of the ratio k_3/k_5 on H^+ concentration, suggesting that the hydrolysis of the radical was acid dependent. On rewriting the reaction scheme including (4.17)

$$(SCN)_2^- + H_3O^+ \xrightarrow{k_5} X \qquad (4.17)$$

instead of (4.8), the expression for $\phi_{Fe^{2+}}$ becomes (see Appendix II)

$$\phi_{Fe^{2+}} = \phi_1 \left[\frac{2k_2[FeNCS^{2+}] + 2k_3[FeOH^{2+}] + 2k_4[Fe^{3+}] + k_5[H^+]}{k_1[Fe^{2+}] + k_2[FeNCS^{2+}] + k_3[FeOH^{2+}] + k_4[Fe^{3+}] + k_5[H^+]} \right] \quad (4.18)$$

Using the same method as already described, the values of the ratios were found to be much more self-consistent. The ratios were finally computed by a method of successive approximations in which the value of $\phi_{Fe^{2+}}$ at each experimental point was computed from the rate expression (4.18), (after first calculating the concentrations of complexes, free ferric, and free acid) for varying values of the ratios, until the best fit to the experimental results was found. The best agreement between the experimental and calculated quantum yields was obtained using the figures quoted in Table 7.

In Figures 10 and 11, the solid lines represent the variation of $\phi_{Fe^{2+}}$ with acid and SCN^- concentrations calculated using these values of the ratios.

4.10 Ferric Dependence

Further support for these values of the ratios is given by the series of experiments in which $[Fe^{III}]$ was varied while H^+ and SCN^- concentrations remained constant. The experimentally determined quantum yields are compared with the calculated values in Table 8. Apart from run No. 6, there is again reasonable agreement between

Table 7

Values of the Primary Quantum Yield at 436 mμ and the Relative Rate Constants of Reactions of Thiocyanate Radicals at 25°C, 0.5 ionic strength.

$FeNCS^{2+} \longrightarrow Fe^{2+} + SCN^{\bullet}$	$\phi_1 = 0.035 \pm 0.002$
$Fe^{2+} + (SCN)_2^- \xrightarrow{k_1} FeNCS^{2+} + SCN^-$	$k_1/k_5 = 305 \pm 30$
$FeNCS^{2+} + (SCN)_2^- \xrightarrow{k_2} Fe^{2+} + (SCN)_2 + SCN^-$	$k_2/k_5 = 115 \pm 10$
$FeOH^{2+} + (SCN)_2^- \xrightarrow{k_3} Fe^{2+} + (SCN)_2 + OH^-$	$k_3/k_5 = 90 \pm 10$
$Fe^{3+} + (SCN)_2^- \xrightarrow{k_4} Fe^{2+} + (SCN)_2$	$k_4/k_5 = 2.0 \pm 0.5$
$(SCN)_2^- + H_3O^+ \xrightarrow{k_5} X$	

the experimental and calculated values of the quantum yields. It is not surprising that run 6 shows a greater deviation, since k_4/k_5 is the least accurately known ratio, and yet in the expression for $\phi_{Fe^{2+}}$ the term $k_4[Fe^{3+}]$ is most significant for this run.

4.11 Comparisons with Other Works

From their measurements on the thermal bleaching of $FeNCS^{2+}$ Betts and Dainton[43] obtained the ratio of the rate constants for

Table 8

Comparison of the Experimentally Determined Values of $\phi_{Fe^{2+}}$ with Those Calculated from the Ratios of Rate Constants Given in Table 7

Run No.	$[Fe^{III}]$ M	$[FeNCS^{2+}]$ M	$[FeOH^{2+}]$ M	$[H^+]$ M	$\phi_{expt.}$	$\phi_{calc.}$
1	0.01	2.82×10^{-4}	0.99×10^{-3}	0.017	0.066	0.066
2	0.10	4.82×10^{-4}	5.17×10^{-3}	0.031	0.065	0.068
3	0.01	2.93×10^{-4}	7.26×10^{-5}	0.25	0.040	0.042
4	0.10	5.00×10^{-4}	7.48×10^{-4}	0.25	0.052	0.055
5	0.20	5.00×10^{-4}	1.50×10^{-3}	0.25	0.055	0.059
6	0.25	5.00×10^{-4}	1.87×10^{-3}	0.25	0.054	0.061

the reactions

$$Fe^{2+} + (SCN)_2^- \xrightarrow{k_7} Fe^{3+} + 2SCN^-$$

and $$Fe(III) + (SCN)_2^- \xrightarrow{k_8} Fe^{2+} + (SCN)_2$$

Their value of k_7/k_8 was 3.5 ± 1.0.

At the high acid and thiocyanate concentrations used by these workers, the predominant Fe^{III} species was the $FeNCS^{2+}$ complex. Their value can therefore be compared with the present value for k_1/k_2, 2.7 ± 0.3, from Table 7.

Again, at 15°C Duflo-Plissonier[58] obtained a value of 2.0 ± 0.2

for this ratio under similar conditions.

Mention must also be made of the paper by Ellis and Laurence.[67] Recent recalculations have shown the necessity for including reaction (4.6) in the scheme, and this leads to the different values for the ratios of the rate constants presented here.

4.12 Wavelength Dependence

The treatment according to Noyes[32,33] utilises the assumption that if a molecule absorbs light of energy $h\nu$ greater than E (the average energy necessary to dissociate the molecule) then the two fragments separate with a total kinetic energy $h\nu - E$. Thus, as $h\nu$ increases, the fragments will gain greater kinetic energy, leading to larger separation outside the cage and hence a higher quantum yield. For the case of iodine dissociation (both fragments are identical) it is found that a plot of $\phi/(1 - \phi)$ versus $\sqrt{h\nu - E}$ is linear as is to be expected from the expression derived by Noyes.

In the present work, although there is a decrease in ϕ_1 with the energy of light absorbed, Figure 14 shows that the results cannot be made to fit the Noyes equation, but this is not surprising, for a number of reasons. Firstly, there is considerable doubt as to the value of E. According to the electrode potentials of the two couples concerned, the free energy change should be close to zero, and in the thermal study, Betts and Dainton[43] found there to be an activation energy in excess of 25 kcal/mole, but it can be seen

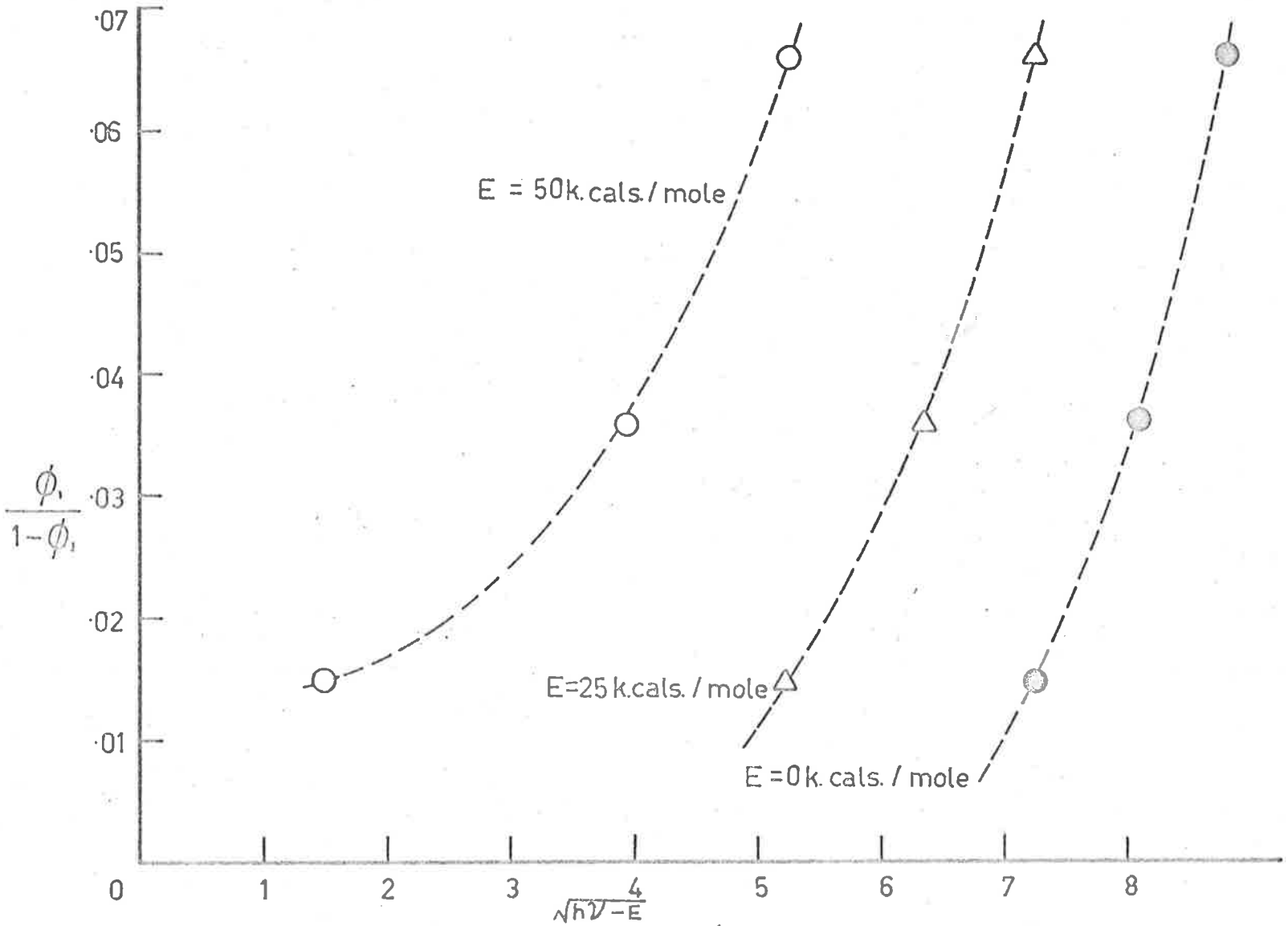

FIG. 14. "Noyes" Plots for the Dependence of ϕ_1 on the Wavelength of Absorbed Light

from Figure 14, neither of these values leads to a straight line. Secondly, the theory was derived for two identical fragments, but in this case they are vastly different in size, shape, and mass. Finally, and probably most important of all, it is unlikely that all of the excess energy does appear as kinetic energy. Although the absorption band at 4600 Å has been assigned as a charge transfer band, this only means that an electron moves from the thiocyanate to the iron and does not consider whether or not the resultant fragments are in an excited state. In particular, a considerable fraction of the excess energy could well be used to raise the thiocyanate radical to an excited electronic or vibrational level.

4.13 Temperature Dependence

This series of runs was carried out under conditions of high $FeNCS^{2+}$ and $FeOH^{2+}$ concentrations such that equation (4.18) reduces to

$$\phi_{Fe^{2+}} = 2\phi_1 \qquad (4.19)$$

Since the concentrations of the various Fe^{3+} complexes do not appear in this expression, it is unnecessary to make any allowance for the changes in formation constants of $FeNCS^{2+}$ and $FeOH^{2+}$ as the temperature is altered.

The rate determining step under these conditions then, is the diffusion of the radicals from within the solvent cage, as ϕ_1 is

the only variable in equation (4.19). The experimentally determined value of the activation energy (4.8 ± 0.5 kcal/mole) supports this concept, as diffusion controlled reactions are found to have low (2-6 kcal/mole) activation energies in aqueous solution.

CHAPTER 5

Qualitative Experiments

5.1 Effect of Radical Scavengers

5.1.a Acetone

It was suspected that acetone would scavenge $SCN^{\bullet}$ radicals by a reaction similar to that between bromine or iodine atoms and acetone.

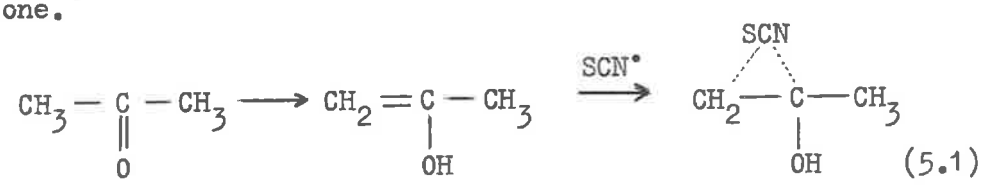

(5.1)

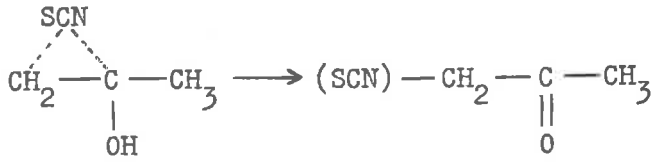

(5.2)

i.e. No SCN^{-} is regenerated as in the reaction of the radical with water.

Qualitative measurements only were made, since these experiments were merely to act as confirmatory evidence for the reaction mechanism proposed previously (Section 4.9). The results are shown in Table 9.

At zero Fe^{2+} concentration there is negligible secondary back reaction occurring, and since the scavenger cannot enter the cage and compete with primary recombination, it is to be expected that $\phi_{Fe^{2+}}$ will not be changed upon the addition of acetone. However, scavenging

Table 9

Qualitative Effect of Adding Acetone

$[Fe(III)] = 5 \times 10^{-2}$; $[SCN^-] = 5 \times 10^{-4}$; $[H^+] = 0.016$; $[Acetone] \doteq 1.3$ M

Fe^{2+} Concentration	ϕ_{SCN^-}	$\phi_{Fe^{2+}}$
0	increased	no effect
5×10^{-4} M	increased	increased

of the radical by acetone instead of H_2O will effectively change the stoichiometry in such a way that ϕ_{SCN^-} will increase.

In the presence of higher ferrous concentrations, there will be competition with the back reaction, leading to higher values of ϕ_{SCN^-} and $\phi_{Fe^{2+}}$. Once again the change should be greater for ϕ_{SCN^-} than for $\phi_{Fe^{2+}}$ because of the change in stoichiometry. In fact it is found experimentally that $\phi_{Fe^{2+}}$ is increased by 20% and ϕ_{SCN^-} by 60%.

5.1.b Manganous Ion

Addition of manganous ion (as $MnSO_4$) to the reaction mixture made no noticeable difference to the observed quantum yield.

5.1.c Acrylonitrile

Uri et al.[34,35,36] have used the polymerisation of vinyl compounds as a mechanistic criterion for showing the existence of

free radicals, but claimed that polymerisation does not occur in the $FeNCS^{2+}$ system. Despite this, it was felt that a vinyl monomer should compete with water for the $SCN^{\bullet}$ radical, and acrylonitrile was tested as a possible scavenger. Although polymerisation was not at first detected, there was a noticeable effect on the rate as shown in Table 10.

Table 10

Effect of Adding Acrylonitrile

$[Fe(III)] = 5 \times 10^{-2}$; $[SCN^-] = 5 \times 10^{-4}$; $[H^+] = 0.016$;

[Acrylonitrile] = satd. soln.

Fe^{2+} Concentration	ϕ_{SCN^-}	$\phi_{Fe^{2+}}$
0	increased	no effect
5×10^{-4}	increased	decreased

Except for the case of $\phi_{Fe^{2+}}$ at high ferrous concentrations, the results are the same as when using acetone as scavenger, and are as expected.

Since ϕ_{SCN^-} does increase at high ferrous concentration, it is obvious that acrylonitrile does scavenge the radicals (so affecting the stoichiometry) but to explain the decrease in $\phi_{Fe^{2+}}$ it is necessary to postulate the oxidation of Fe^{2+} to Fe^{3+}. The obvious step to consider is that the growing polymer may oxidise ferrous ion

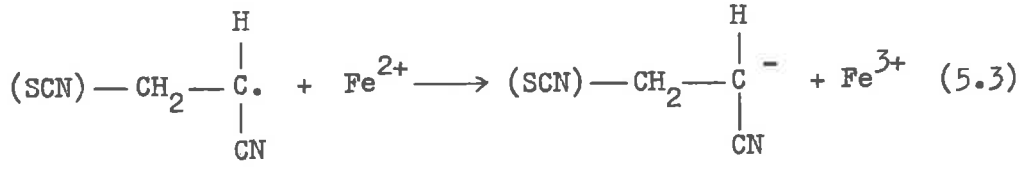

(5.3)

Theoretically this is feasible, as the product is a carbanion stabilised by an ∝-nitrile group. Comparison was made by heating azobis-isobutyronitrile to 60-70°C in the presence of ferrous ion. This compound is known to decompose on heating to produce a free radical,

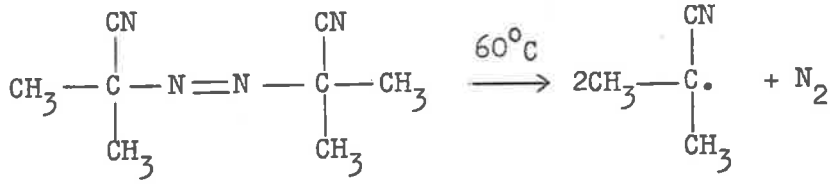

(5.4)

and it was found that ferrous ion was indeed oxidised by this radical. In this case, the product is a secondary carbanion, whereas in the postulated reaction (5.3) a primary carbanion is formed. Since a primary carbanion is known to be more stable than a secondary carbanion, it is likely that the postulated reaction between ferrous ion and the growing polymer (5.3) does indeed occur, leading to a decrease in $\phi_{Fe^{2+}}$. The effect is not noticed at low added Fe^{2+} because the probability of collision between Fe^{2+} and the radical is much diminished, and the polymer chain is more likely to be terminated by some other means.

5.2 Initiation of Polymerisation

Since acrylonitrile does scavenge $SCN^{\bullet}$ radicals, it should be

possible to observe polymerisation under some conditions, and it was found that concentrated aqueous solutions of acrylonitrile containing 5×10^{-2} M ferric ion and 5×10^{-2} M of thiocyanate ion, when irradiated with 4358 Å light, precipitated polymer during irradiation. Polymerisation was not initiated in these solutions in the dark, nor by irradiating solutions from which one of the reactants had been removed, showing that the polymerisation was neither ionically nor photo-induced.

Samples of the polymer were collected, purified by repeated solution and precipitation from dimethyl formamide and its properties compared with those of polymer initiated by radicals obtained by warming potassium persulphate, and also by the action of H_2O_2 on thiocyanate ion. The infrared spectra in all cases showed strong absorptions at 2250 cm^{-1} characteristic of a saturated nitrile group and were similar to that reported by Oster and Mizutane[68] for polyacrylonitrile. However in addition, the sample from the photochemically induced reaction gave a small peak at 2165 cm^{-1} which could be attributed to the SCN group attached to the end of the polymer chain. From the relative size of the peaks the ratio SCN/CN groups was found to be approximately 1:15. Assuming there to be one SCN group per chain, the average molecular weight would therefore be 700-800. The small peak was not noticeable in the spectrum of the H_2O_2/SCN^- induced polymer, indicating that the polymer chain is probably much longer than when produced by the

photolysis reaction.

5.3 Low Temperature Irradiation

Using the experimental arrangement shown in Figure 15, two identical samples (except for one being liquid and the other in solid glass) were irradiated at 20°C and -196°C. On melting, it was found that the optical density (at 460 mμ) of the irradiated sample at -196°C had not changed whereas the 20°C sample had undergone a considerable change. The difference was not merely due to differences in the thermal reaction, as shown by blank experiments with the light turned off, but was probably due to the resulting ferrous ion and $SCN^{\bullet}$ radical being held close together in the rigid ice lattice, so enhancing the probability of the back electron transfer. Although the radical would have been formed in close proximity of water molecules, it was probably oriented in an unfavourable direction for reaction with water, and in the absence of diffusion it would be unlikely that it could be reoriented.

Horne[69] has shown that the Fe^{2+}/Fe^{3+} electron exchange still proceeds in ice, and proposes that the electron can travel considerable distances through the lattice. However, I do not think there is any conflict with the $FeNCS^{2+}$ reaction, since for the initial step to occur, the electron has merely to move between the two ions which are held in close proximity, whereas in the Fe^{2+}/Fe^{3+}

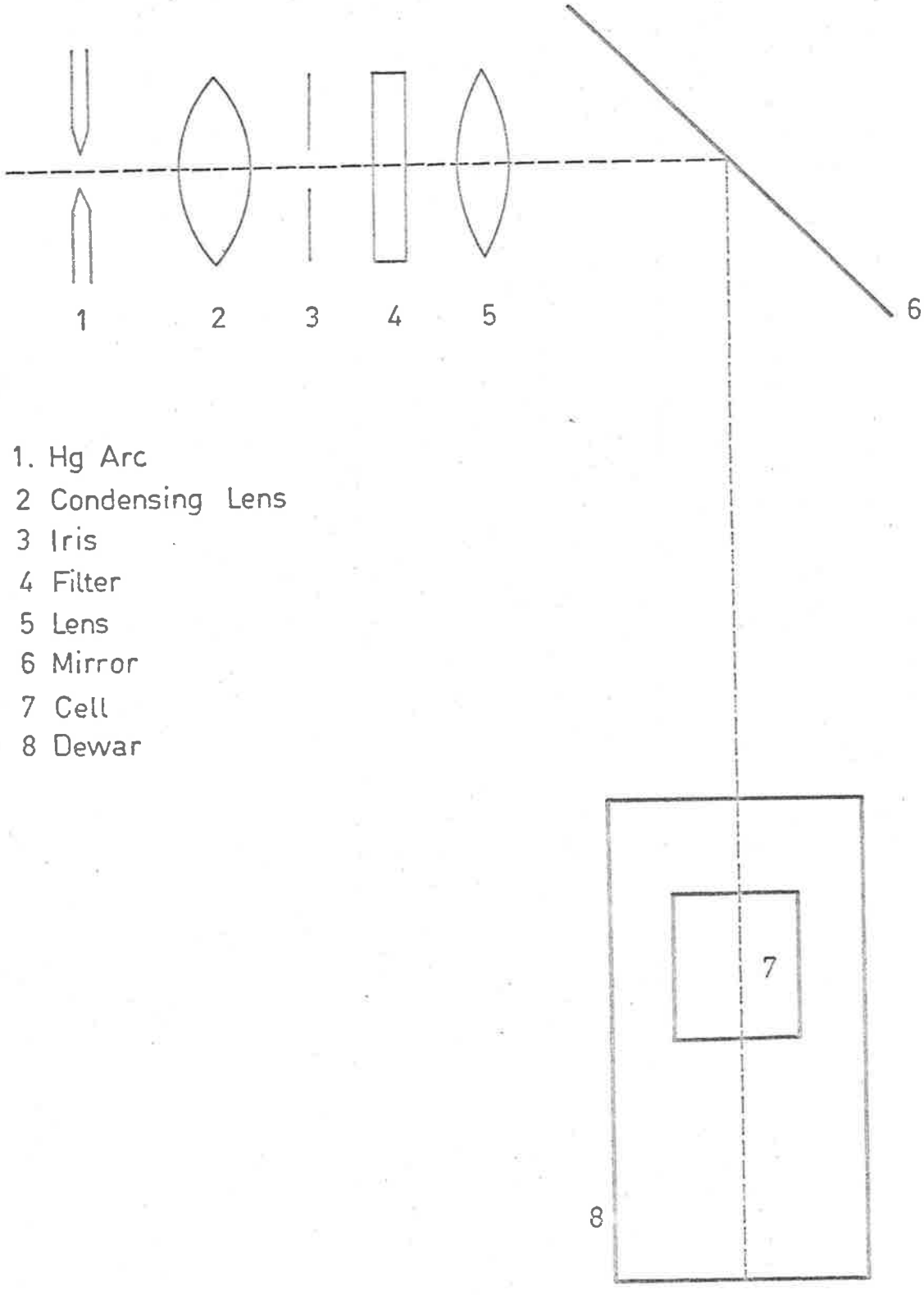

1. Hg Arc
2 Condensing Lens
3 Iris
4 Filter
5 Lens
6 Mirror
7 Cell
8 Dewar

FIG. 15. Schematic Representation of Apparatus for Low Temperature Irradiations.

exchange, the electron may travel considerable distances through the lattice via a water bridged mechanism anyway.

5.4 Effect of Nitrous Oxide

Several runs were carried out in which nitrous oxide was used as the gas for stirring. Since the gas is a very good scavenger for hydrated electrons, it would be expected that the quantum yields would be altered considerably if free electrons were produced during photolysis. In fact, neither $\phi_{Fe^{2+}}$ nor ϕ_{SCN^-} showed any noticeable change, as would be expected from the proposed mechanism for photo-reduction.

5.5 The $FeCl^{2+}/FeNCS^{2+}$ Reaction

From values of the electron affinities for the chloride and thiocyanate radicals,[71] it is expected that the following reaction would occur

$$Cl^{\bullet} + SCN^{-} \longrightarrow SCN^{\bullet} + Cl^{-}$$

The chloride radical is known to be formed by the irradiation of $FeCl^{2+}$ with light of 3660 Å,[35] and it was suspected that in the presence of thiocyanate ion under concentration conditions in which the red $FeNCS^{2+}$ complex did not absorb more than a small fraction of light at 3660 Å, the red colour would gradually disappear due to the formation of the thiocyanate radical as above, followed by

reaction with water.

This was found to be the case, and solutions of $FeNCS^{2+}$ which faded only slightly in 24 hours irradiation at 3660 Å were completely bleached in 2 hours on the addition of 1 M sodium chloride.

i.e. $$FeCl^{2+} \xrightarrow{h\nu} Fe^{2+} + Cl^{\bullet}$$

$$Cl^{\bullet} + SCN^{-} \longrightarrow Cl^{-} + SCN^{\bullet}$$

Since the $SCN^{\bullet}$ radical apparently reacts readily with H_2O, whereas the chloride radical does not, it was also expected that the rate of production of Fe^{2+} would be increased in the presence of thiocyanate ion, since the hydrolysis step would compete with the recombination reaction. This was found to be so as shown in Table 11.

Table 11

Comparison of Rate of Production of Ferrous in the Photochemistry (at 3660 Å) of $FeCl^{2+}$ in the Presence and Absence of Thiocyanate Ion

$[Fe(III)] = 0.05$ M; $[H^+] = 1$ M; $[Cl^-] = 2$ M.

SCN^- Concentration	Rate of Fe^{2+} Production
0	5.6×10^{-6} mole/litre/hr
10^{-4} M	5.0×10^{-5} mole/litre/hr

5.6 Production of the $SCN^{\cdot}$ Radical by Oxidising Agents

It has been stated previously that polymerisation of acrylonitrile can be initiated by the action of H_2O_2 on thiocyanate, presumably via the formation of the thiocyanate radical. When a 4-5 M solution of potassium or ammonium thiocyanate was treated with H_2O_2, there was a very vigorous exothermic reaction, producing sulphate, cyanide and a yellow solid

$$SCN^- + H_2O_2 \longrightarrow \text{yellow solid} + HCN + SO_4^{=}.$$

The same result was obtained using HNO_3 instead of H_2O_2.
Analysis of the solid gave the following figures:

C = 21%, H = 1.5%, N = 25%, S = 46%.

These values correspond closely to an empirical formula of $(HNCS)_n$, suggesting that the product is a polymeric thiocyanate molecule of some sort. There are many known compounds with this empirical formula, a large proportion of which have cyclic structures.

The solid was insoluble in all types of solvents, and it was difficult to carry out any tests which would help identify the product. Both infrared and mass spectral measurements were made, but it was impossible to characterise the substance.

Of more interest, however, was the observation that immediately following the mixing of H_2O_2 and SCN^-, and before a large amount of the yellow solid was formed, the reacting solution turned to a noticeable pink colour. The whole reaction was slowed down

considerably at low temperatures, and it was possible to retain the pink colour indefinitely by freezing the solution in liquid nitrogen soon after mixing. The spectrum was measured using a fast scanning rate on the SP700 spectrophotometer, and although it was difficult to make accurate measurements because of the formation of yellow solid as the solution warmed up, it was obvious that the pink colour was due to an absorption maximum at 500 mμ. This is in agreement with the work of Boag et al.[72,73] on the production of $SCN^{\bullet}$ by the action of hydroxyl radical on thiocyanate ion.

Using the low temperature attachment of the Varian E.S.R. spectrometer, the E.S.R. spectrum of the frozen pink solution was measured. A signal was obtained at 3200 g (Figure 16) indicating the presence of a free radical species, but detailed interpretation of the spectrum has not been attempted. However, it is likely that it is due to the thiocyanate radical, which would be expected to give more than one signal peak because of the many electronic interactions possible within the molecule.

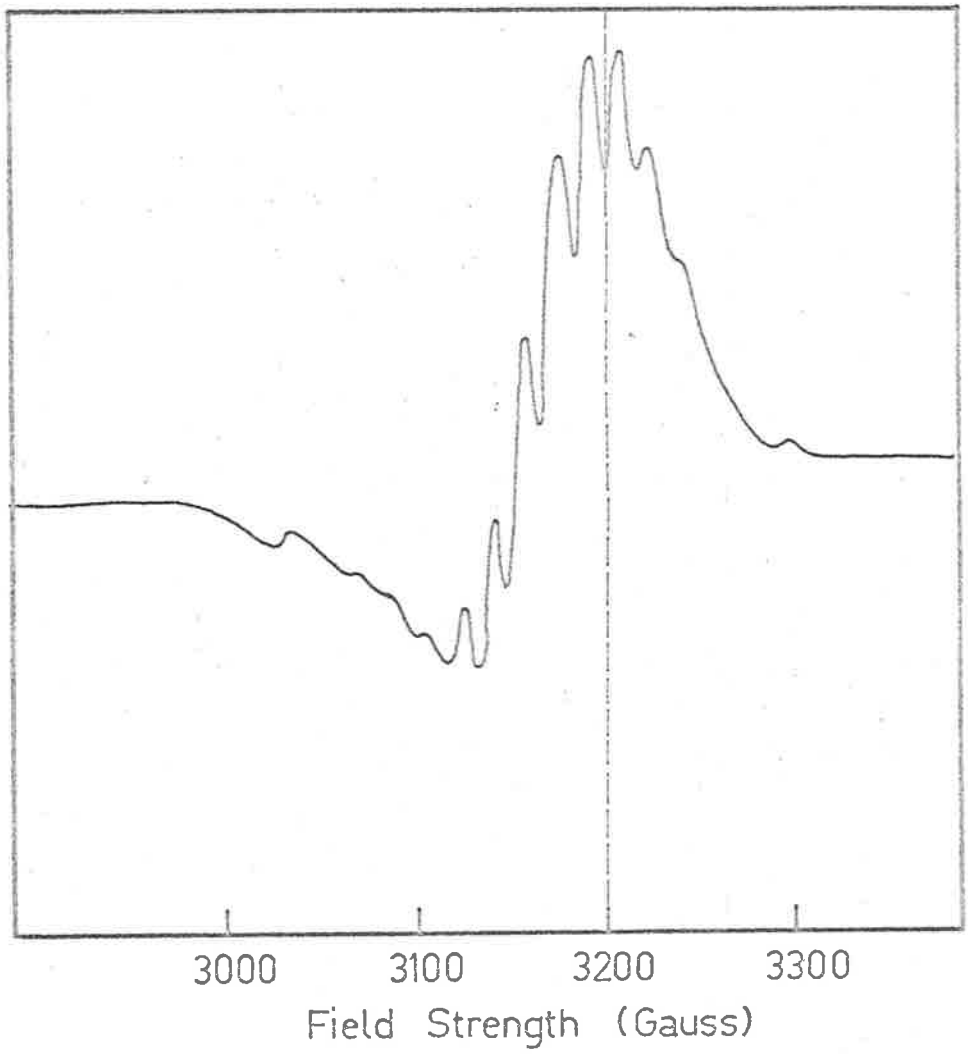

FIG. 16. E.S.R. Spectrum of Thiocyanate Radical.

PART 2

THERMAL OXIDATION-REDUCTION REACTIONS

CHAPTER 1

Introduction

In Part 1 of this thesis the mechanism of the photochemical reduction of the $FeNCS^{2+}$ complex in aqueous solution was suggested, the absorption of light in the complex causing intramolecular electron transfer.

There are many thermal oxidation-reduction reactions between metal ions and both inorganic and organic ions or molecules, in which the path of the electron transfer is not immediately obvious. Part 2 will deal briefly with the mechanisms of thermal oxidation-reduction reactions, particular attention being paid to the detection and identification of any intermediate complexes which may be formed.

Broadly speaking, there are considered[74,75] to be two types of mechanism operating in electron transfer reactions, the main difference lying in the nature of the transition state or activated complex. The two mechanisms were first suggested by Taube. The first class of mechanism is the "outer-sphere" type, in which the first coordination shell of each reactant remains unchanged and the electron transfer occurs through an "extended" activated complex: the interaction to form the transition state is mainly in the outer coordination sphere of the central atoms. An example of this type of reaction is given by the oxidation of $[Cr(bip)_3]^{2+}$ by $[Co^{III}(NH_3)_5L]$,[7] (where bip = bipyridyl and L = NH_3, H_2O, OH^-, Cl^-, or Br^-) in which

it can be shown that the coordination spheres of both the oxidant and reductant remain unchanged because of the inertness to substitution of Cr(III) and Co(III).

The second type is the "inner-sphere" reaction in which electron transfer is preceded by substitution into the coordination shell of one of the ions to form a "bridged intermediate" transition state in which the two central atoms are linked by a common ligand group. For example[77]

$$[(NH_3)_5Co^{III}X] + [Cr(H_2O)_6^{2+}] \longrightarrow [(NH_3)_5Co^{III}\text{-}X\text{-}Cr^{II}(H_2O)_5] + H_2O$$

$$\downarrow$$

$$Co^{II} + 5NH_4^+ + Cr^{III}X$$

where X = F^-, Cl^-, Br^- or I^-.

The criteria by which these mechanisms can be distinguished are presented fully by Halpern.[74]

In considering oxidation-reduction reactions of the type,

$$M^{z+} + A^- \longrightarrow M^{(z-1)+} + A$$

we may again postulate both types of mechanisms. In an outer-sphere type reaction, the two species will be held close together by ionic interaction, with perhaps a solvent molecule separating them, while in an inner-sphere type reaction, the coordination shells will overlap and an incipient chemical bond will be formed. Provided that the intermediates in these mechanisms are relatively

long lived, it should be possible to distinguish between them by their differing absorption spectra. The effect of outer-sphere complex formation would be to perturb the d orbitals of the metal ion and so affect the d-d transition, so that the absorption maximum of the complex would probably be at the same position, but of higher extinction coefficient (a less forbidden transition) than that of the free metal ion (see Part 1, Section 1.1.a). The inner-sphere complex, however, would exhibit a charge-transfer spectral band of much higher intensity and at a wavelength which depended on the nature of both the oxidant and reductant (see Part 1, Section 1.1.b).

It would appear then, that spectrophotometric detection of the intermediates formed in the metal ion oxidation of inorganic and organic ions or molecules may give some idea of the pathway by which electron transfer occurs. If the rate of the oxidation-reduction step is small compared with the rate of complex formation, it would be a relatively simple matter to study the complex, but in many cases the half-life of the overall reaction is only of the order of seconds or less, so that the "non-detection" of an intermediate does not necessarily mean that an inner-sphere complex is not formed on the way to the transition state.

Even though a complex of the type $MA^{(z-1)+}$ may be detected, attention must also be paid to the stoichiometry and kinetics of the overall oxidation-reduction reaction, particularly for a reaction

of the type

$$2M^{z+} + 2A^{-} \longrightarrow 2M^{(z-1)+} + A_2$$

Two possible reaction paths in this case are

(1) $$M^{z+} + A^{-} \longrightarrow M^{(z-1)+} + A^{\bullet}$$

$$2A^{\bullet} \longrightarrow A_2$$

or

$$A^{\bullet} \longrightarrow \text{other reactions.}$$

i.e. first order in both species

$$R = k\left[M^{z+}\right]\left[A^{-}\right]$$

(2) $$M^{z+} + A^{-} \longrightarrow MA^{(z-1)+}$$

$$MA^{(z-1)+} + A^{-} \longrightarrow M^{(z-1)+} + {}^{\bullet}A_2^{-}$$

$$M^{z+} + {}^{\bullet}A_2^{-} \longrightarrow M^{(z-1)+} + A_2$$

i.e. $R = k\left[M^{z+}\right]\left[A^{-}\right]^2$

In the first case, detection of an intermediate complex, $MA^{(z-1)+}$, would infer an inner-sphere mechanism, since the transition state would be formed from this complex, but in the second case, although $MA^{(z-1)+}$ may form, it cannot be the species leading directly to the transition state because of the requirement of second order kinetics in $\left[A^{-}\right]$, and so does not necessarily imply that the reaction mechanism is of the inner sphere type. Unless evidence could be

given for the existence of the $[MA^{(z-1)+} \cdot A^{-}]$ complex, it would not be possible to say definitely whether the final electron transfer takes place via an inner or outer-sphere mechanism.

For example, in the ferric/thiosulphate system Page[78,79] has detected the $FeS_2O_3^+$ complex and has measured its formation constant and extinction coefficient. Since the extinction coefficient is fairly low ($\varepsilon_{5893} = 120$), and the absorption maximum is close to that for Fe^{3+}_{aq}, the absorption can be attributed to a "forbidden" d-d transition becoming slightly allowed due to the perturbation of the orbitals by ion-pair formation. That is, an outer-sphere type complex is formed. Patnaik, Nanda and Bakshi[80] claim the reaction to be first order in Fe^{3+} and second order in $S_2O_3^{=}$, and have suggested the formation of $Fe(S_2O_3)_2^{-}$, but although they have spectrophotometric evidence for the first complex, it is only the kinetic results which lead to the postulation of the second complex. It would seem possible, then, that an outer-sphere complex between Fe^{3+} and $S_2O_3^{=}$ does form, and this species forms yet another outer-sphere complex with the second $S_2O_3^{=}$. Since the second complex is probably the precursor of the transition state, it is relatively short lived and as such is unobservable spectrophotometrically, although Bildea and Niac[81] claim to have measured its absorption spectrum recently.

Page[82] later reinvestigated the mechanism of the reaction, and postulates the step

$$FeS_2O_3^+ + S_2O_3^= \rightleftharpoons FeS_2O_3 + S_2O_3^-$$

i.e. two more reaction intermediates are proposed; a singly charged thiosulphuryl ion, $S_2O_3^-$, and an uncharged ferrous thiosulphate complex. However, this step corresponds to the reduction of the ferric species and could well involve the $Fe(S_2O_3)_2^-$ intermediate mentioned above. In most other examples of metal ion oxidation of common anions (see Table 12), the first complex at least has been suggested from the kinetic analysis, although $FeNCS^{2+}$ and $FeS_2O_3^+$ are the only ones to have been observed spectrophotometrically.

Table 12

Examples of Oxidation-Reduction Reactions Between Metal Ions and Inorganic Anions Involving Complex Formation

Oxidant	Reductant	Intermediates	Ref.
Mn^{3+}	$C_2O_4^=$	$Mn(C_2O_4)^+$, $Mn(C_2O_4)_2^-$, $Mn(C_2O_4)_3^{\equiv}$	83
Mn^{3+}	Br^-	$MnBr^{2+}$	84
Cr^{VI}	I^-	Cr^{VI}, I^-	85
Fe^{3+}	$S_2O_3^=$	$FeS_2O_3^+$, $Fe(S_2O_3)_2^-$	78-82
Fe^{3+}	SCN^-	$FeNCS^{2+}$	43
Fe^{3+}	I^-	FeI^{2+}	86

Despite the lack of evidence, it would appear that all of these cases, with the exception of $Mn(C_2O_4)^+$ which undergoes direct decomposition, involve the primary formation of either an inner or outer-sphere type complex, MA, followed by the formation of the outer-sphere second complex MA.A from which the electron transfer transition state is formed.

Oxidation of organic compounds by metal ions has also been the subject of interest in recent years. Sengupta,[87] Mehrotra and Ghosh,[88] and McAuley and Brubaker[89] have studied the oxidation of a series of organic acids (citric, tartaric, malonic, mandelic, pyruvic, malic, and lactic) by Ce(IV) in both sulphuric and perchloric acids, and in most cases have found evidence for complex formation between the metal and the dissociated acid. McAuley and Hill[90] also have evidence for the formation of a cobalt(III) malate complex. Guibault and McCurdy[91] have studied the oxidation of glycerol by cerium(IV) and have shown the existence of an intermediate complex, but in the case of the ceric-fructose reaction,[92] there was no evidence for complex formation. McAuley, Hill and Pickering[93,94,95] have recently studied the oxidation of α-mercaptocarboxylic acids by vanadium, cobalt and cerium, and have measured the absorption spectrum of the intermediate complex in each case.

Most of these reactions of organic substrates are first order with respect to both metal ion and substrate suggesting the first complex is a direct precursor of the transition state. That is, the

electron transfer occurs within the complex and produces the reduced metal ion and an organic free radical. It is the subsequent reactions of this radical with other metal ions which leads to the unusual stoichiometry, e.g.

$$HOOC.CH(OH).CH(OH).COOH + 8Ce(IV) + 2H_2O \longrightarrow 3CO_2 + HCOOH + 8H^+ + 8Ce(III)$$

There are also many known examples of the oxidation of other organic molecules (e.g. oxidation of olefins by Tl(III)[96]) and free radicals by transition metal ions. A review of the mechanisms involved has been given by Kochi.[97]

The difficulty experienced in observing and making accurate measurements on these intermediates can be attributed mainly to the speed at which they decompose. If the rate of the redox step were small compared with the rate of the complex formation (as in $FeNCS^{2+}$ for example), it would not be difficult to make accurate measurements on the complex, but this is often not possible by conventional means. Page[78,79,82] used a "capacity flow" method of studying this type of system, but this has not been used a great deal by other workers.

In Part 2 of this thesis a method by which stopped-flow measurements can be used to obtain spectral information about short lived intermediates will be described. McAuley et al.[93,94,95] have also discussed this use of a stopped-flow apparatus recently.

It was decided to study the ferric/ascorbic acid and ferric/iodide

systems, as both of these are known to undergo rapid oxidation-reduction reactions in aqueous solution. In neither case has there been any direct evidence for complex formation, although in the light of kinetic results, past investigations have suggested that a transient intermediate may well be formed.

CHAPTER 2

The Oxidation of Ascorbic Acid by Ferric Ion in Aqueous Solution

2.1 Introduction

For many years it has been known that the oxidation of aqueous ascorbic acid solutions by molecular oxygen is catalysed by reducible metal ions, and that under certain conditions the reduction of metal ion and oxidation of ascorbic acid occurs quantitatively. This fact has been used in devising methods of analysis for both ascorbic acid and the metal ions.[98,99,100]

Several attempts to study the kinetics andmechanism of the reaction, particularly with Cu^{2+} as catalyst, have led to conflicting opinions of the mechanism. Weissberger and Luvalle[101] suggested that the rate-determining step in the copper catalysed oxidation is:

$$HA^- + Cu^{2+} \longrightarrow HA + Cu^+.$$

(HA^- = monodissociated ascorbic acid; HA = semiquinone.)
Nord,[102] however, points out that this does not account for the dependence of the rate on the concentration of dissolved oxygen. From a consideration of all the available data, he suggests that the complete mechanism is:

$$H_2A \rightleftharpoons H^+ + HA^-$$

$$HA^- + Cu^{2+} \rightleftharpoons HA + Cu^+$$

$$HA \rightleftharpoons A^- + H^+$$

$$A^- + Cu^{2+} \longrightarrow A + Cu^+$$

$$2Cu^+ + 2H^+ + \tfrac{1}{2}O_2 \longrightarrow 2Cu^{2+} + H_2O$$

$$H_2A + \tfrac{1}{2}O_2 \longrightarrow A + H_2O$$

(H_2A = ascorbic acid; A = dehydroascorbic acid.)

Grinstead,[103] in a study designed mainly to test the 'model' peroxidase system, consisting of the iron chelate of EDTA, ethylenediaminetetraacetic acid, investigated the oxidation of ascorbic acid by H_2O_2 and the reduction of Fe(III)-EDTA by ascorbic acid. It was shown that the rate of the metal chelate reaction was independent of H_2O_2 concentration, and was determined by a step involving a one-electron oxidation of ascorbic acid to a radical intermediate. It was suggested that the reaction proceeded via a ferric chelate/ascorbic acid intermediate complex, but the existence of this complex could not be proved.

Taqui Khan and Martell[104,105] studied the metal ion and metal chelate catalysed oxidation of ascorbic acid by molecular oxygen using Cu(II) and Fe(III) complexes. By measuring the change in pH when Cu^{2+} ions were added to a solution of ascorbic acid, equilibrium evidence for the formation of the complex $CuHA^+$ ($\log K \triangleq 1.57$) was obtained, and it was suggested that Fe^{3+} formed a similar complex which could not be detected because of the faster oxidation step. In order to account for the oxygen dependence of the overall reaction, they proposed that a metal-ascorbate oxygen complex was formed (Figure 17a). However this was not necessary in the ferric chelate reaction as the reaction rate was independent of dissolved oxygen concentration.

In a further study[106] involving a series of Fe(III) chelates

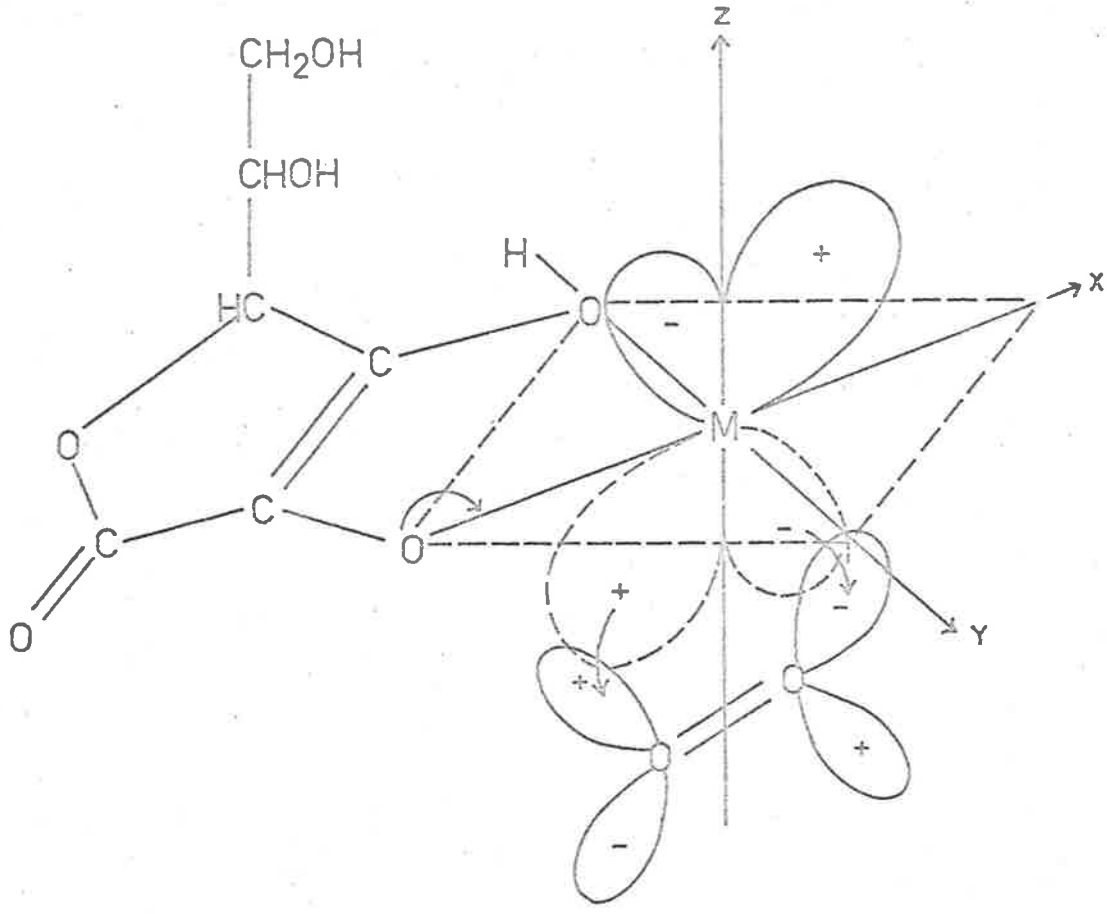

FIG. 17(a). Proposed Metal-Ascorbate-Oxygen Complex (from Ref. 104).

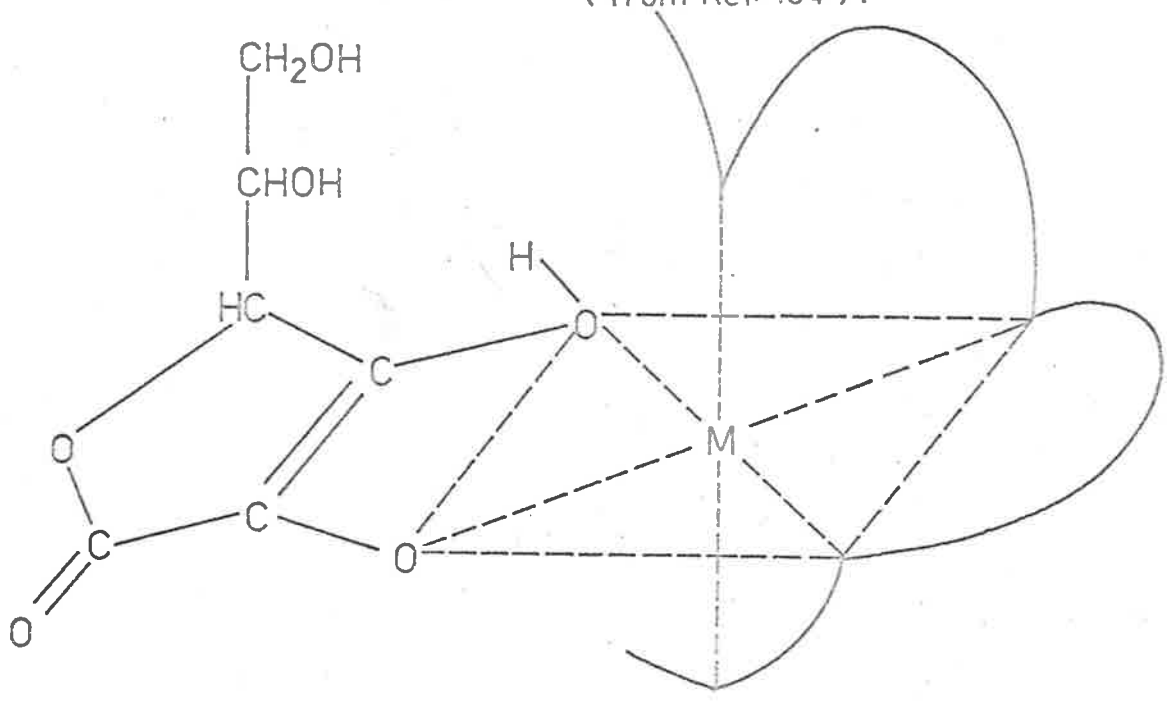

FIG. 17(b). Proposed Ferric Chelate-Ascorbate Complex (from Ref.105)

of aminopolycarboxylic acids in the absence of oxygen, they proposed a mechanism involving a loose combination of the ascorbate anion and the oxidising agent with subsequent electron transfer to the metal chelate. This also suggests that the ferric chelate-ascorbate complex (Figure 17b) may exist for a short time in solution.

The slight differences in the proposed mechanism may be partly due to the reasonably high pH used in some studies which would lead to a variety of reactive metal species in solution, especially when buffer solutions were used to control the pH. It would also appear that in the presence of oxygen there may be two distinct paths by which the oxidation of ascorbic acid proceeds. One of these is the direct oxidation-reduction reaction between metal ion and ascorbate, (the type of reaction discussed in Part 2, Chapter 1), and the other is the metal ion catalysed oxidation of ascorbic acid by molecular oxygen.

It was decided in the present study to investigate the reaction between ascorbic acid and the free hydrated Fe^{3+} ion in the absence of oxygen, hoping that under these conditions there would only be one reaction path. Particular care was taken in attempting to detect and study any intermediate complex which may have been formed.

2.2 Experimental

2.2.a Materials and Analyses

The ascorbic acid used in all experiments was B.D.H. biochemical grade L-Ascorbic Acid. This was stored in a tightly stoppered bottle which was inserted into an airtight plastic container with a small amount of silica gel to absorb any moisture, and the whole was kept in a deep-freeze unit. When required, the plastic container was removed from the refrigerator and allowed to equilibrate to room temperature, condensed moisture was wiped from its surface, and the bottle containing the acid removed. While taking a sample of ascorbic acid, the stock bottle was kept open as little as possible so as to avoid any decomposition or the taking-up of water. The required sample was removed, weighed accurately, and quickly dissolved in a known volume of the solution, to give an ascorbic acid solution of known concentration.

All other chemicals and the distilled water were the same as described in Part 1 (see Section 2.1). Similarly, the analyses are described in Section 2.2.

2.2.b Apparatus

All kinetic runs were carried out using a spectrophotometric stopped-flow apparatus as designed by Sturtevant[107] and modified by Tregloan and Laurence.[108,108A] A pneumatic drive operating at 50-60 lbs. per square inch through a quick-opening valve ensured a steady,

reproducible push-time and flow profile of solution through the apparatus. At each push 0.5 ml of each reactant was injected, and the total length of the push was 100 milliseconds. Since the volume between the mixing chamber and the observation point was about 0.05 ml, the time interval between mixing and observation (dead time[98]), was about 5 milliseconds. The flow was stopped within 1-2 milliseconds by driving the pushing trolley against a rigid metal stopping-pin. Tests showed the mixing of reactants to be efficient and reproducible and the rates of reactions with half-lives down to 10-20 milliseconds could be measured within 1-2%.

The spectrophotometric system consisted of a Philips 12 volt, 100 watt quartz-iodine lamp (Type 7023), operating from a stabilized D.C. power supply, a series of lenses, a grating monochromator (F 11, Hilger and Watts), a further system of lenses to focus the image of the monochromator entrance slit on the front face of the observation cell, and an E.M.I. Type 6256S photomultiplier tube to detect the light transmitted through the cell. The E.H.T. supply for the photomultiplier was supplied by an Isotopes Developments E.H.T. Unit, Type 532/D, and the output was measured on a Tektronix Type 541 storage cathode ray oscilloscope (C.R.O.) fitted with a Type 2A63 differential amplifier and a Type 2B67 time base. Photographs of the traces were taken on 4" x 6" Kodak Tri-X film using the Tektronix oscilloscope camera.

For the measurement of small changes in the transmitted light, a stabilised D.C. power supply in conjunction with a "multipot" potentiometer was used to back off the voltage output from the photomultiplier tube enabling the use of a much higher sensitivity scale on the cathode ray oscilloscope amplifier to follow the changes in transmittance.

To prevent cavitation when reactant solutions flowed at high velocities through the apparatus, the solutions were degassed by melting 50 ml of frozen solution under vacuum in 100 ml closed vessels. According to vapour pressure and gas solubility data, the concentration of dissolved gases is lowered by more than 98% after one freezing/melting cycle under these conditions, but the effect of this on the solution concentration is less than 0.001%.

Accurate thermostatting was achieved by circulating water from a thermistor-controlled water bath through the hollow copper blocks which surround the whole of the flow apparatus. For temperatures above 5-10°C, the temperature was maintained constant to within 0.05°C, and the difference between the temperatures of the water bath and the reaction solution in the instrument was negligible. At lower temperatures, however, there was a slight difference; when the water bath was maintained at 0°C, the temperature of the reacting solution was 0.3-0.5°C. This was measured by inserting a thermistor into one of the driving syringes or into a specially drilled hole in the mixing chamber block.

2.2.c Design and Construction of Long Path Length Cells

The standard observation cells used in the stopped flow apparatus are of either 1 or 2 mm path length.[109] Since the rate of formation of the intermediate in the ferric/ascorbic acid system was extremely fast, it was necessary to use low concentrations of reactants so that reactions proceeded at an observable rate. This meant, however, that the concentration of intermediate formed was very low, and the observed optical densities in the 2 mm cell were often only 0.01 or less. In an attempt to increase the measured optical density changes, two types of long path length cells were designed and constructed.

Multi-path-Length Cell.

The front and back faces of a standard sized observation cell were "silvered" by vacuum evaporation of aluminium onto the entire surfaces except for entrance and exit slits placed as shown in Figure 18. The light beam was reflected upwards at an angle of approximately 5.5° by passing it through a small prism of angle 3°. The optical system is shown in Figure 18. To ensure that all of the light reaching the exit slit had passed through the solution for its complete path, and not through the glass sides of the cell, a standard sized cell was made with polished stainless steel sides and optically flat silica glass windows, as shown in Figure 19. Using a thin layer of Araldite as adhesive, the four components were carefully assembled so as to give parallel faces.

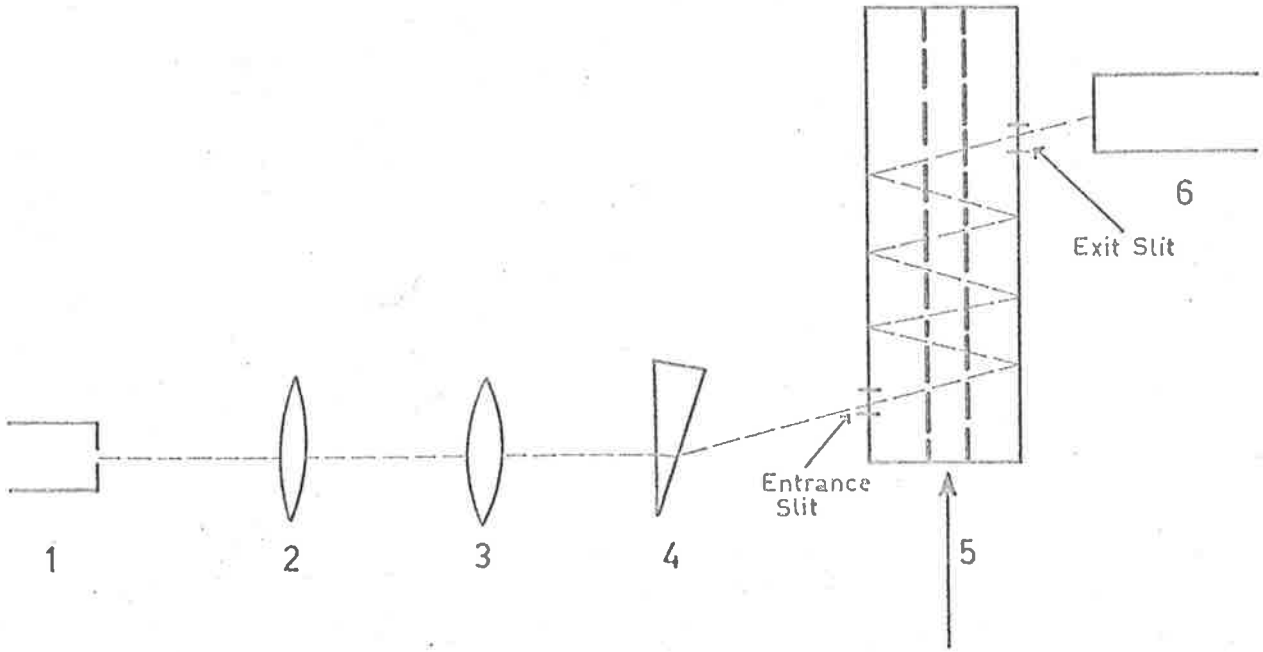

1 Monochromator
2 Lens ; f = 5 cm.
3 Lens; f = 10 cm.
4 Prism
5 Solution from Mixing Chamber
6 Photo-Multiplier Tube

FIG. 18. Diagramatic Representation of the Multi-Pathlength Cell.

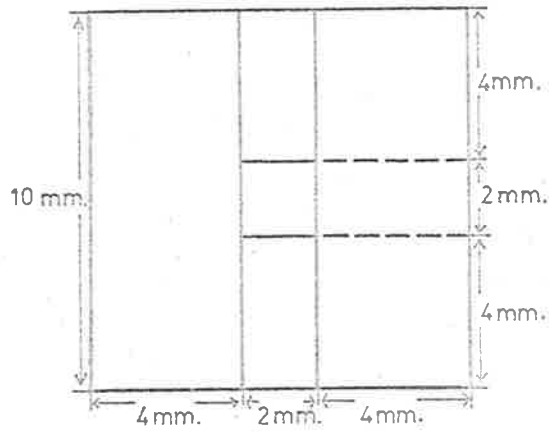

Cross Section.

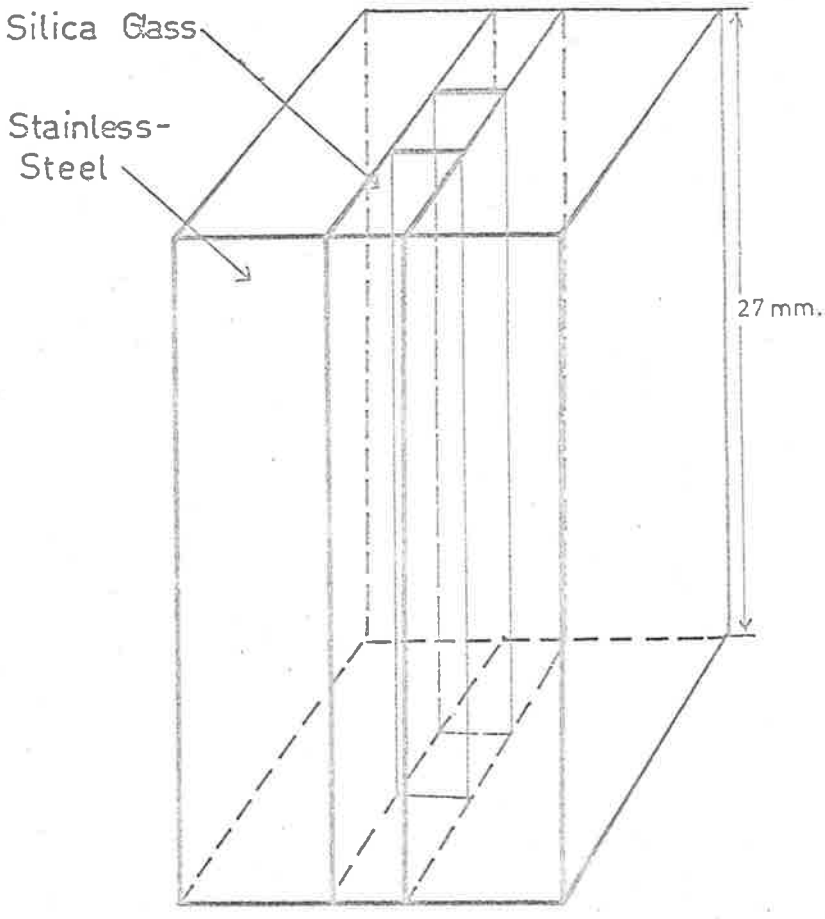

FIG. 19. Plan of Stainless-Steel / Silica Glass Cell.

The path length (1) of this cell was determined by measuring statically the light transmitted (I) by solutions of $KMnO_4$ and $K_2Cr_2O_7$ of known concentrations ([c]) and extinction coefficients (ε), compared with the light transmitted when the cell was full of H_2O (I_o). These quantities are related by the expression:

$$1 = \frac{\log I_o/I}{\varepsilon \cdot [c]}$$

It was found that the value of $\varepsilon \cdot [c]$ obtained in this way varied with the concentration of the solution used; as the value of $\varepsilon \cdot [c]$ increased, so the apparent path length decreased. The explanation for the effect was thought to be as follows.

The light beam entering the cell could not be made completely parallel, and was diverging at approximately 3^o. Had the exit slits been infinitely small this would not have mattered as there would, in effect, have been only one ray of light to consider. However, because of the light losses at each reflection, it was necessary to have fairly large ($\triangleq$ 2 mm) slits and this meant that some rays traversed the cell more times than others (Figure 20a). A geometrical construction of the light paths, allowing for refraction at the glass/solution interfaces, and considering three rays representing the two extreme edges of the light beam and the central ray, shows that these rays make 7, 13 and 9 passes of the cell respectively.

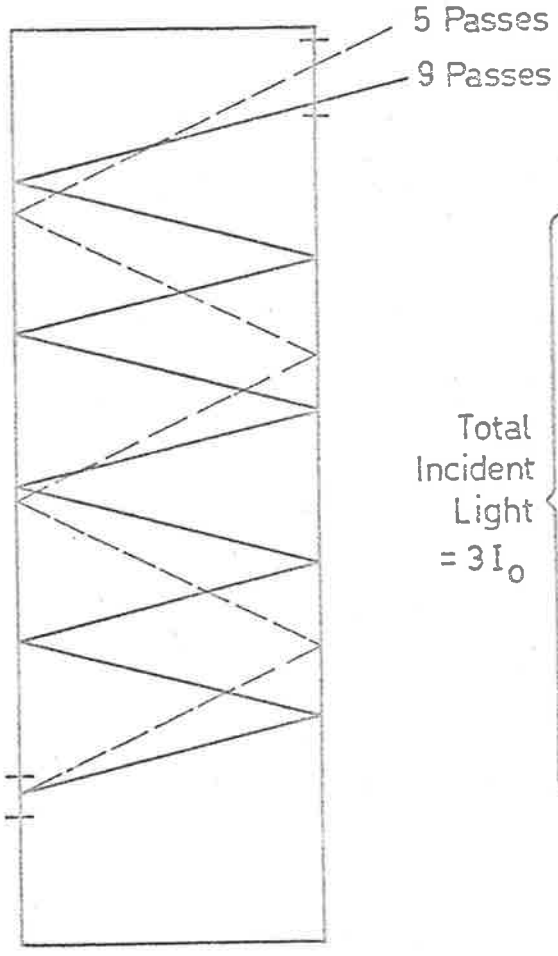

FIG. 20(a). Schematic Representation of the Effect of a Divergent Light Beam on the Number of Passes of the Cell Made By Each Light Ray.

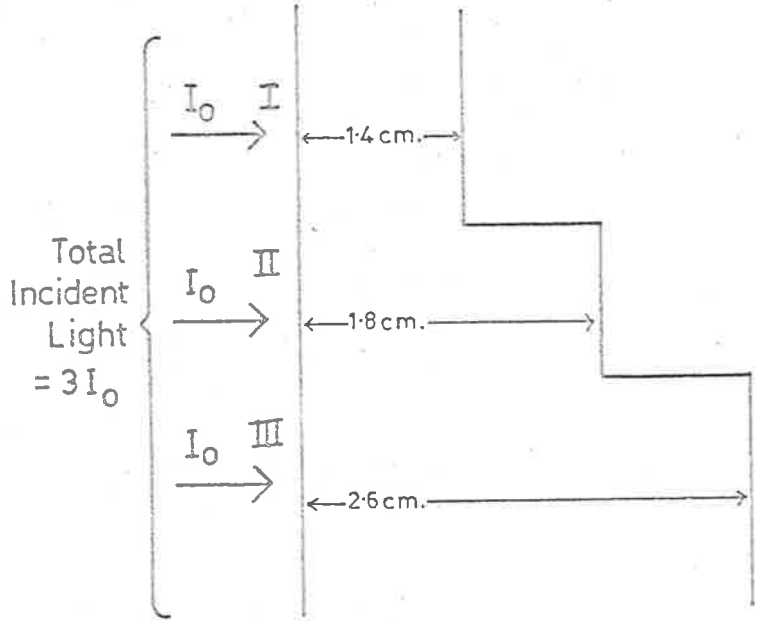

FIG. 20(b). Diagramatic Representation of the Effective Light Path.

Thus for a cell of 2 mm bore, the system can be represented diagramatically by a cell such as in Figure 20b.

Now consider solutions such that $\varepsilon \cdot [c] = 0.01$.

Path I O.D. = 0.014 $I_o/I = 1.033$ $I = 0.968\ I_o$

Path II O.D. = 0.018 $I_o/I = 1.042$ $I = 0.960\ I_o$

Path III O.D. = 0.026 $I_o/I = 1.062$ $I = 0.941\ I_o$

i.e. total incident light = $3I_o$.

total transmitted light = $2.869\ I_o$

$$\text{O.D.} = \log\left[\frac{3.000}{2.869}\right] = 0.0196$$

$\therefore$ apparent path length = 1.96 cm.

For a solution such that $\varepsilon \cdot [c] = 0.1$

Path I O.D. = 0.14 $I = 0.725\ I_o$

Path II O.D. = 0.18 $I = 0.661\ I_o$

Path III O.D. = 0.26 $I = 0.550\ I_o$

O.D. = 0.1903

$\therefore$ apparent path length = 1.90 cm.

Similarly, if $\varepsilon \cdot [c] = 1.0$, apparent length = 1.71 cm.

It can be seen from the results, that during any kinetic run, although the accuracy would be somewhat increased due to the longer path lengths of the cell (and therefore larger overall optical density change), the continual variation of l would considerably complicate the treatment of results and introduce further

possibilities of error. A further disadvantage of the cell, particularly when applied to reactions with short half-lives, was due to the different "dead times"[98] associated with the solution at the bottom and top of the cell. Again, because of the different path lengths of each ray of light, the observed dead time would not be a simple average of the times corresponding to the distances from the mixing chamber to the entrance and exit slits.

Because of these factors, it was decided that little was gained by adopting the use of this type of cell.

Two-way, Long Path Length Cell.

The complete cell block in the stopped flow apparatus was replaced by a solid stainless steel block (2" x 2" x 1"), drilled as shown in Figure 21, and with glass windows attached to the ends of the lower horizontal channel. The block was made in two halves as shown for more careful drilling. The windows were recessed into the block so that the vertical channels A were only a few thousands of an inch from the windows. This was to ensure that the flow of liquid would completely flush out the channel B. Channels A, B and C were all $^{60}/_{1000}$" in diameter, and the optical path length was 4 cm. The average distance between mixing and observation was about 3 cm, and this corresponded to a dead time of only 6 milliseconds. That is, only marginally longer than in the original model.

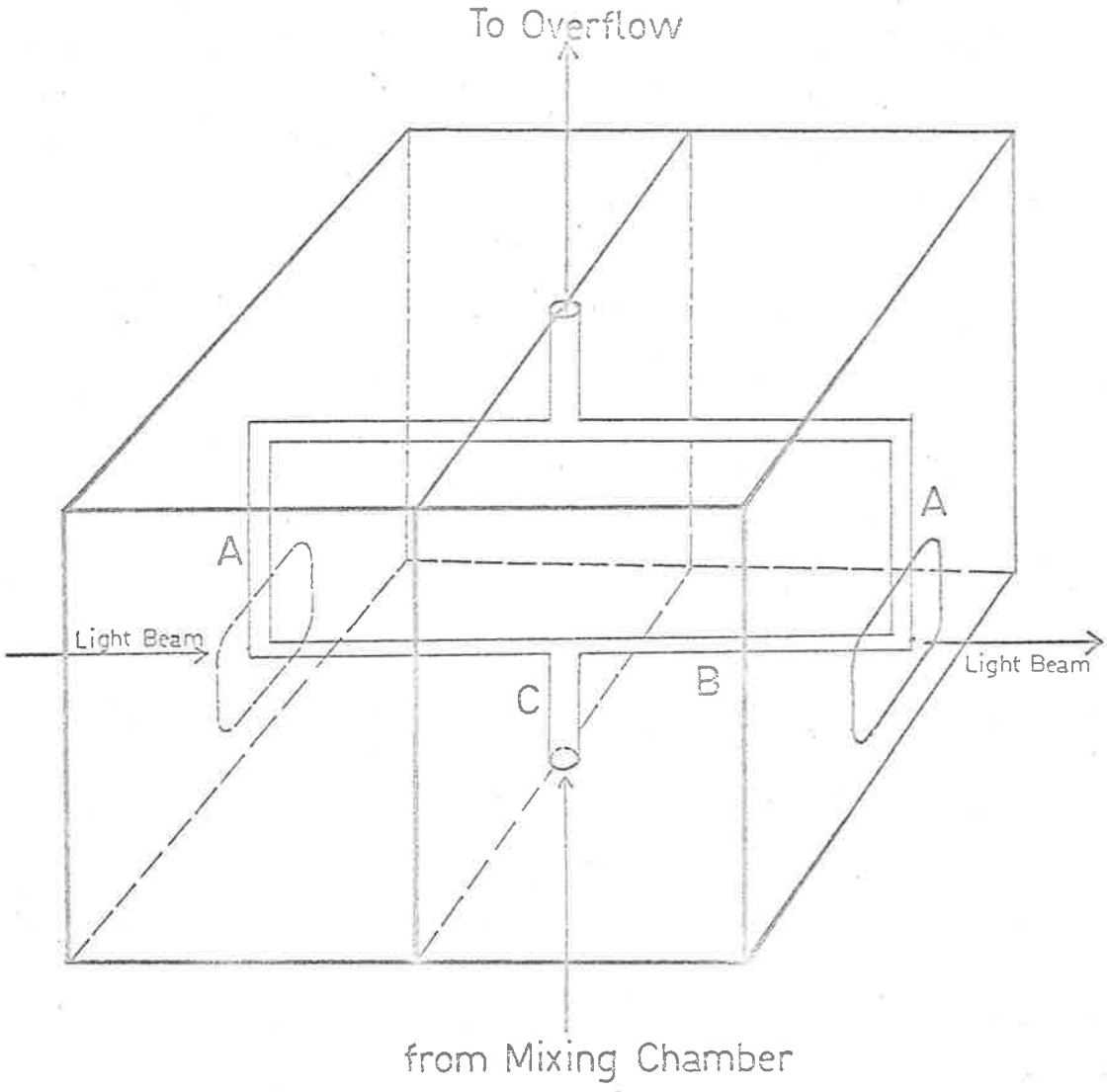

FIG. 21. Two-Way Long Pathlength Cell.

LIBRARY OF THE UNIVERSITY OF ADELAIDE

Preliminary tests showed that the path length of this cell could be determined accurately, that a sufficient quantity of light could be passed through the cell, and that solution from the previous run was easily removed from the observation channel by one push. Unfortunately, at high sensitivities there was an observable change in the transmitted light even when water was pushed from both syringes. This change was of the order of 0.005 optical density units, and took about 0.2 seconds to form and 2 seconds to decay, but was not at all reproducible. In many cases the effect was equivalent to 10-20% of the reaction to be studied and this would also have introduced large errors into the measured rates.

A firm explanation of the effect could not be given. The only two obvious causes are:

(1) cavitation within the observation tube, particularly at the intersection of channels C and B, due to the effective cross-section of the channel becoming larger.

(2) movement of the observation hole relative to the light beam and the photomultiplier tube.

Both of these are unlikely, however, because of the long time of decay. Sturtevant[98] suggests that cavitation may only last for 10 milliseconds (as against 2 seconds in this case), and it is difficult to imagine a slow movement of the whole assembly relative to the light beam. Some form of shock movement could be involved,

but would not be expected to last for more than a very short time either.

In view of the difficulties encountered in constructing a longer path length cell, it was decided that the accuracy of the kinetic results could not be improved upon beyond that obtained using the usual 2 mm cell.

2.2.d Treatment of Results

Figure 22 shows a typical oscilloscope trace obtained for a reaction in which the initial optical density at mixing is zero and steadily increases. During the time of the push, the optical density and hence the voltage from the photomultiplier tube remains constant, but as the push stops, the optical density begins to increase, and so the voltage corresponding to the transmitted light decreases. It was sometimes necessary to extrapolate back to zero time to allow for the elapsed dead time between mixing and observation, depending on the time scale involved.

If, for example, the time scale were 10 milliseconds/div., the extrapolation would be shown by the dotted line in Figure 22. In general, the required extrapolation was much smaller than in this example, and the error introduced was not so significant. The base line corresponds to the value of the backing-off potential. For example, (in Figure 22) if the backing-off voltage were 4 volts and the scale 20 millivolts/div. point A corresponds to 4.056 volts,

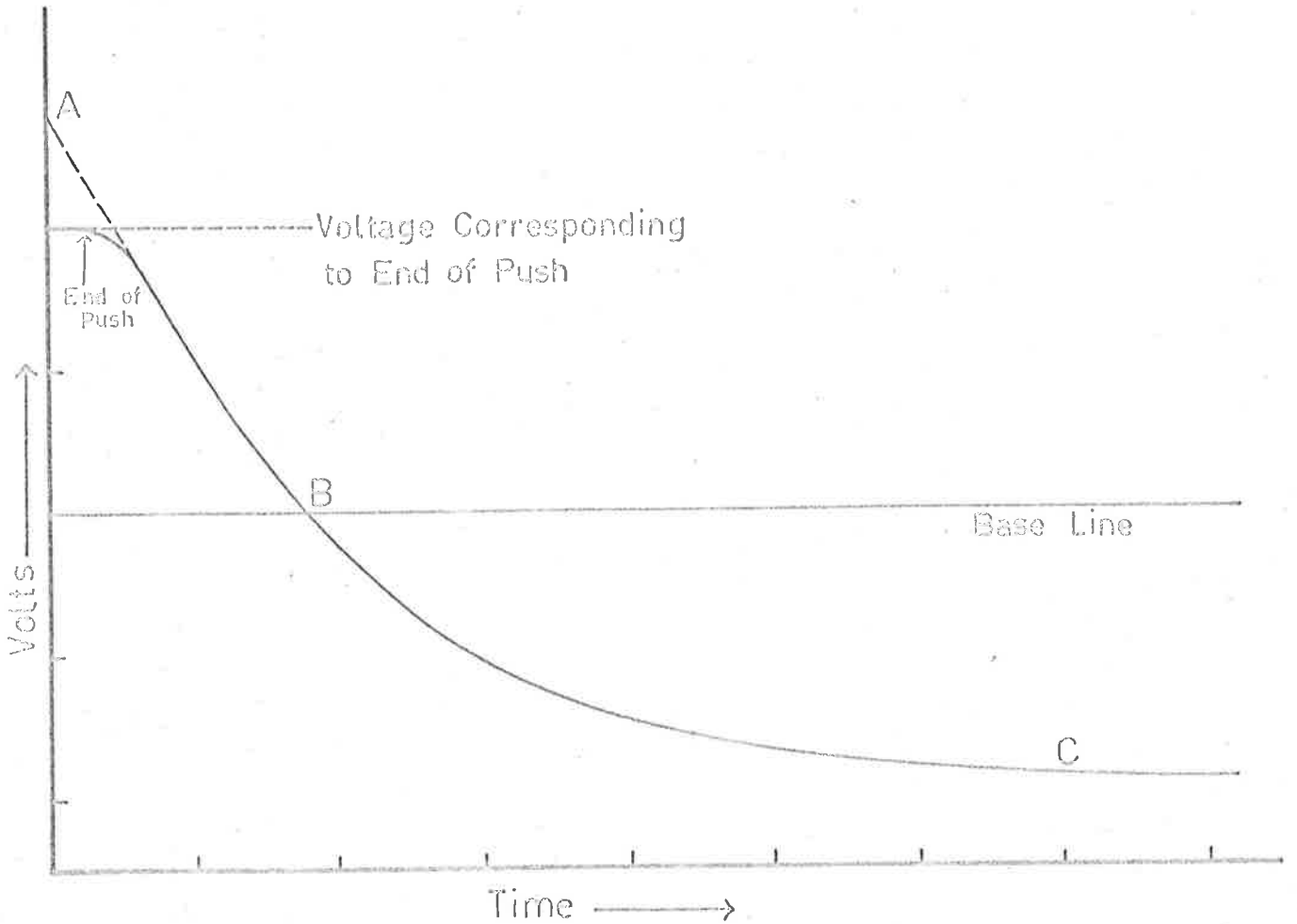

FIG. 22. Typical Oscilloscope Trace.

point B to 4.000 volts and point C to 3.963 volts. Assuming point A to correspond to zero optical density, it is then possible to calculate the optical density at point B from the expression:

$$O.D. = \log \frac{(\text{incident light intensity})}{(\text{transmitted light})}$$

$$= \log \frac{(\text{volts at point A})}{(\text{volts at point B})}$$

$$= \log \frac{(4.056)}{(4.000)}$$

$$= 0.0060.$$

In this way the optical density corresponding to any time could be calculated.

In practice, the traces were enlarged by a known factor ($\simeq$3-5) by projecting the photograph on to graph paper and drawing the curve by hand. Measurements along the Y-axis were then taken at known intervals and the corresponding optical densities for each point calculated on the C.D.C. 6400 computer. The program could be modified to calculate initial rates, rate constants etc. directly from these values.

Under certain conditions in the ferric ascorbate system there were found to be two distinct processes, one corresponding to a rapid increase in optical density followed by one due to a slower decrease in optical density (see Figure 23). The maximum optical density reached was found to be wavelength dependent, but always

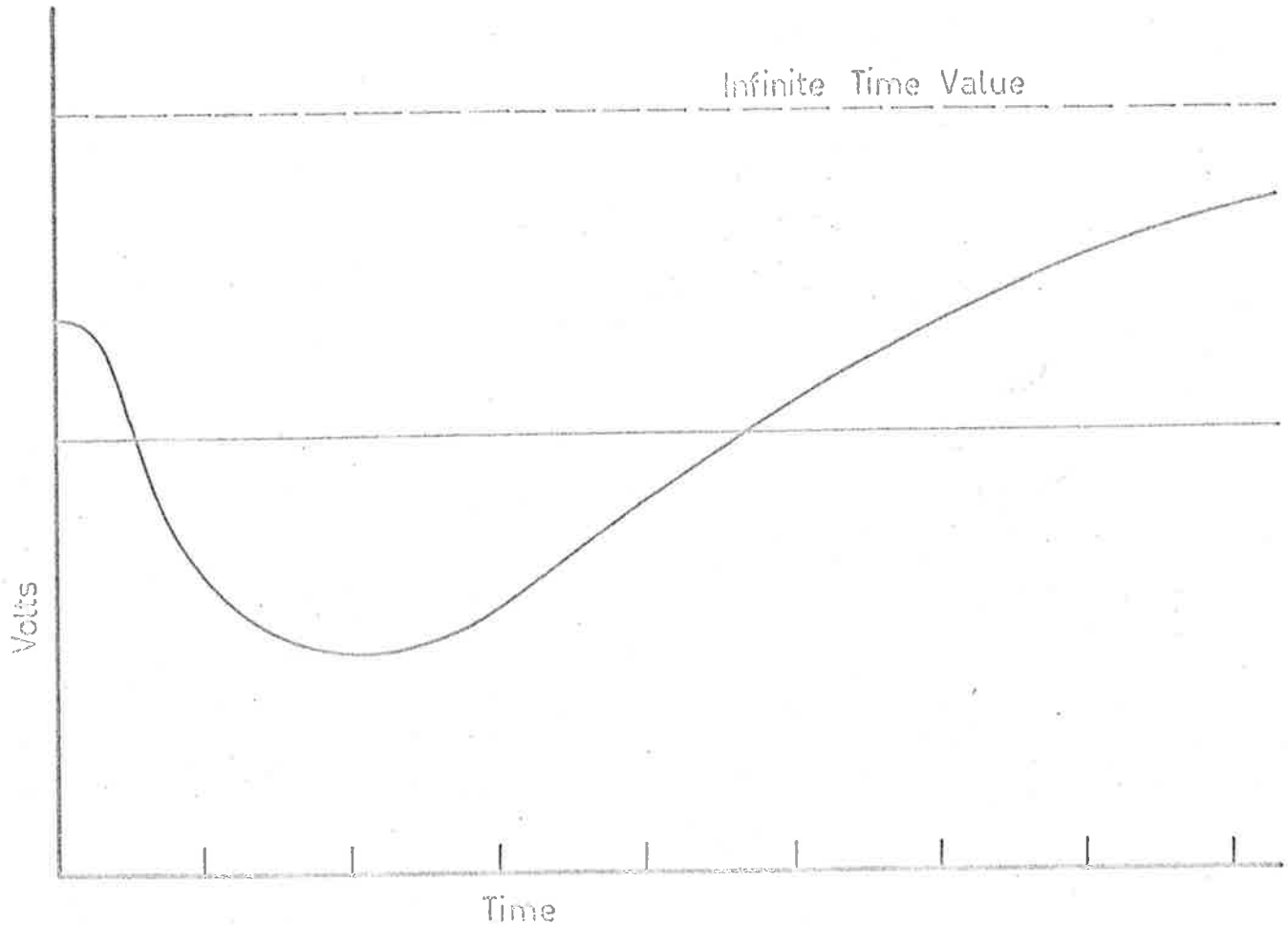

FIG. 23. An Oscilloscope Trace Showing Two Consecutive Processes During Reaction.

occurred at the same time from mixing for a given set of reactant concentrations. By carrying out the reaction under identical conditions of concentration, temperature, etc., but following the change at a series of wavelengths, the spectrum of the intermediate at any given time after mixing could be compiled by plotting the optical density at that particular time, against the wavelength at which the measurement was made. It was only possible to do this reasonably accurately because of the high reproducibility of the injected volumes of reactants, mixing times, and optical density determinations associated with the stopped-flow apparatus. These factors have been discussed in Section 2.2.b and the review by Sturtevant.[107]

In some cases a large extrapolation was necessary because of the high speed of the colour formation, but this could be done reasonably accurately since the optical density at infinite time is also zero, and the Y value at $t = 0$ should be the same as at $t = \infty$. That is, the initial part of the trace was extrapolated back for 5 msec in time, and to the same voltage as reached at $t = \infty$.

2.3 Results

2.3.a Preliminary

The spectra of solutions of ferric ion and ascorbic acid were measured independently in 4 cm cells in an SP600 spectrophotometer. Both species showed absorption peaks of high extinction coefficients at wavelengths below 400 mμ, but although it is known that the free ferric ion does have very weak d-d absorption at about 550 mμ, neither solution exhibited any measurable absorption in the concentration range used ($Fe^{3+} \leqslant 10^{-1}$; ascorbic acid $\leqslant 0.5$), at wavelengths above 400 mμ. Similarly, after mixing these two solutions and allowing sufficient time for the oxidation-reduction reaction to go to completion, the resultant solution showed no appreciable absorption at $\lambda > 350$ mμ.

A few preliminary kinetic runs were carried out on the stopped-flow apparatus. The course of reaction was followed by monitoring the light absorption at 340 mμ. The experimental conditions for these runs are shown in Table 13, and the values of the optical densities at various times are given in Appendix III.

Table 13

Preliminary Runs Monitored at 340 mμ; T = 25°C; $\Gamma = 0.5$.

Run No.	$[Fe^{3+}]$ M	$[H^+]$ M	[Ascorbic Acid] M
K15	2.5×10^{-2}	0.2	5×10^{-2}
K16	2.5×10^{-2}	0.2	4×10^{-2}
K17	2.5×10^{-2}	0.2	3×10^{-2}
K18	2.5×10^{-2}	0.2	2×10^{-2}

2.3.b Determination of Spectrum of Intermediate

A series of runs was carried out at 25°C using the same reactant solutions, but following the change in light absorption at different wavelengths. The concentrations of Fe^{3+}, ascorbic acid, and H^+ were 2.5×10^{-2} M, 5×10^{-2} M, and 0.2 M respectively, and the wavelength was increased from 380 mμ to 640 mμ in steps of 10 mμ. In many cases (particularly for the runs between $\lambda = 500$ mμ and $\lambda = 600$ mμ) a large extrapolation to zero time was required, and although the individual points on the extrapolated part of the curve were not accurate enough for a kinetic treatment to be carried out, the zero value could at least be obtained accurately by comparison with the infinite time value (see Section 2.2.d). By treating the data in the manner described in Section 2.2.d it was possible to obtain the spectrum of the intermediate as shown in Figure 24. The individual points are tabulated in Appendix III.

Blank runs from which either reactant was excluded showed no change in light absorption over the range 380-460 mμ, indicating that the above effect was due to some reaction caused by the mixing of the two reactants.

2.3.c Variation of Ascorbic Acid

The effect of changing the ascorbic acid concentration on the formation of the intermediate was studied in two series of runs, the conditions for which are given in Table 14. There was

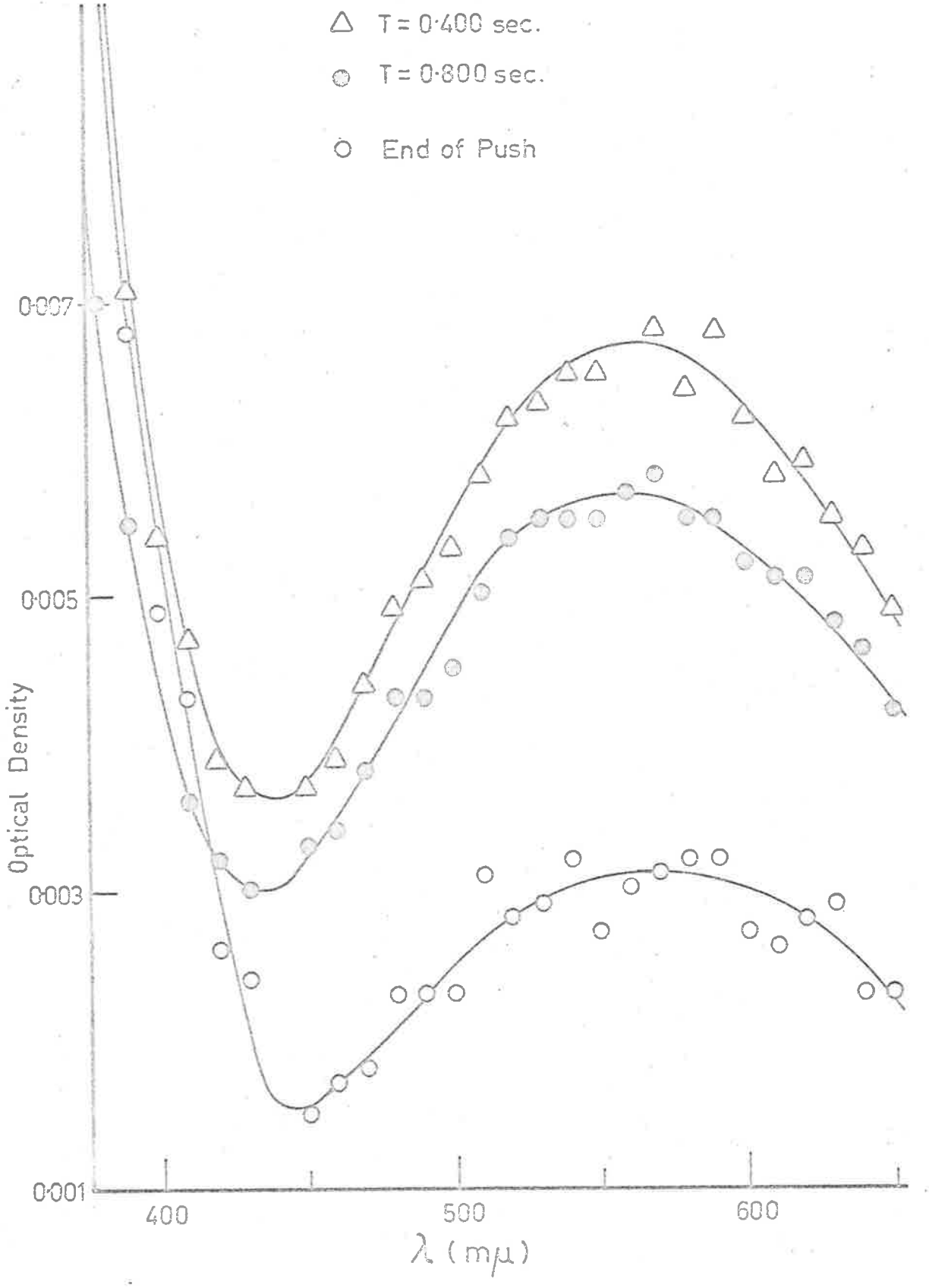

FIG. 24. Spectrum of Intermediate in Ferric / Ascorbate Reaction.

again considerable reaction during the time the solution took to travel from the mixing chamber to the observation point and the optical density corresponding to the end of the push is given in Table 14 along with the maximum optical density reached.

Table 14

Variation of Ascorbic Acid in Intermediate Formation

$T = 25^{\circ}C$ $\lambda = 560$ mμ.

Run No.	$[Fe^{3+}]$ M	$[H^+]$ M	[Ascorbic Acid] M		O.D. at end of push	O.D. max.
K19	2.5×10^{-2}	0.2	5×10^{-2}	0.5	0.0024	0.0063
K20	2.5×10^{-2}	0.2	2.5×10^{-2}	0.5	0.0017	0.0033
K21	2.5×10^{-2}	0.2	1.25×10^{-2}	0.5	0.0011	0.0017
K22	2.5×10^{-2}	0.2	10×10^{-2}	0.5	0.0054	0.0112
K23/1	5×10^{-2}	0.2	50×10^{-2}	1.0	0.0478	0.0749
K23/2	5×10^{-2}	0.2	40×10^{-2}	1.0	0.0419	0.0660
K23/3	5×10^{-2}	0.2	20×10^{-2}	1.0	0.0207	0.0395
K23/4	5×10^{-2}	0.2	8×10^{-2}	1.0	0.0116	0.0204
K23/5	5×10^{-2}	0.2	6×10^{-2}	1.0	0.0070	0.0125
K23/6	5×10^{-2}	0.2	4×10^{-2}	1.0	0.0050	0.0090
K23/7	5×10^{-2}	0.2	2×10^{-2}	1.0	0.0028	0.0041

2.3.d Variation of Fe^{3+}

The effect of changing Fe^{3+} ion concentration at constant ascorbic acid concentration is shown in Table 15. Again the kinetics of the formation of the intermediate could not be followed accurately, and the optical densities at two significant points only are given. The complete data for these runs is presented in Appendix III.

Table 15

Variation of Fe^{3+} Ion in the Intermediate Formation

$T = 25^{\circ}C$ $\lambda = 560 m\mu$ $\Gamma = 1.0$

Run No.	$[Fe^{3+}]$ M	$[H^{+}]$ M	[Ascorbic Acid] M	O.D. at end of push	O.D. max.
K26/1	10×10^{-2}	0.2	20×10^{-2}	0.0439	0.0781
K26/2	8×10^{-2}	0.2	20×10^{-2}	0.0332	0.0629
K26/3	6×10^{-2}	0.2	20×10^{-2}	0.0200	0.0439
K26/4	4×10^{-2}	0.2	20×10^{-2}	0.0158	0.0303
K26/5	2×10^{-2}	0.2	20×10^{-2}	0.0070	0.0120

2.3.e Complex Formation at $0^{\circ}C$

In an attempt to observe the kinetics of the early stages of the formation of the intermediate, runs corresponding in concentration to K23/1 were carried out at $0^{\circ}C$ (Runs K25/1-6 in Appendix III). Figure 25 shows that under these conditions, reaction could be followed

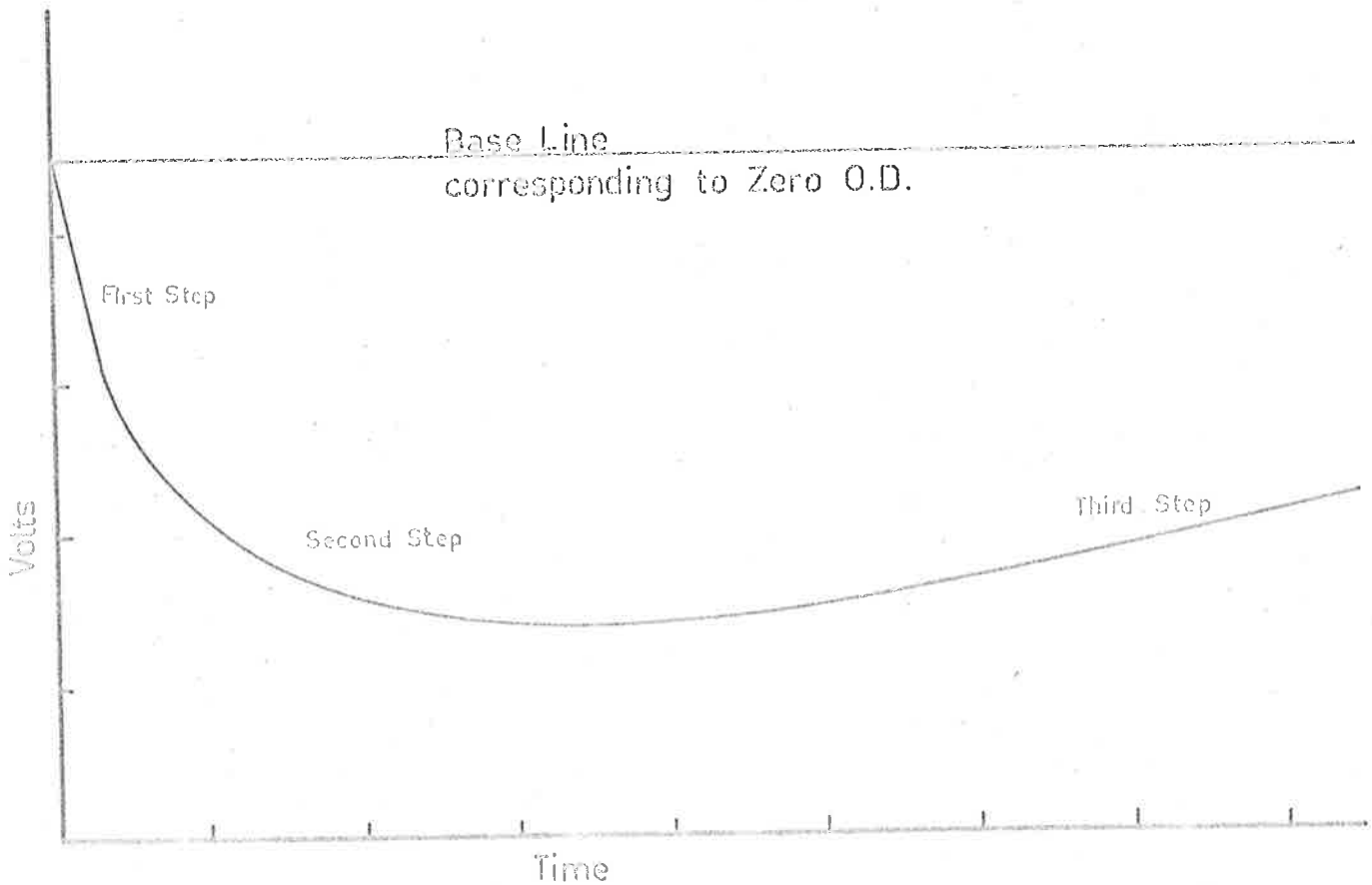

FIG. 25. Oscilloscope Trace of Run at 0°C Showing the Three Steps in the Overall Reaction.

virtually from the beginning (i.e. only a small extrapolation to zero time was necessary).

2.3.f Variation of Ferric and Ascorbic Acid Concentrations at 0°C

The dependence of the first step in the intermediate formation on both Fe^{3+} and ascorbic acid concentrations was studied in runs K27-K32. There were apparently two steps involved in the intermediate formation, and although the initial rate of the first step could be measured, the final optical density reached by this step alone could be estimated only very approximately because of the interaction between the first and second step of the formation. Even less information could be gained from the second step in the intermediate formation as there was initially interaction with the first step, followed by the removal of the intermediate by the final (oxidation-reduction) process, which leadsto a reduction of the absorption produced by the intermediate.

The conditions and important results of this series are shown in Table 16, the complete set of data appearing in Appendix III.

Table 16

Study of First Step of Intermediate Formation at 0°C

λ = 560 mμ; Γ = 1.0.

Run No.	$[Fe^{3+}]$ M	[Ascorbic Acid] M	$[H^+]$ M	Initial Rate	Estimated max. O.D.
K27	2×10^{-2}	50×10^{-2}	0.2	0.75	0.0075
K28	5×10^{-2}	50×10^{-2}	0.2	2.20	0.0200
K29	10×10^{-2}	50×10^{-2}	0.2	4.24	0.0400
K30	10×10^{-2}	5×10^{-2}	0.2	1.25	0.0140
K31	10×10^{-2}	3×10^{-2}	0.2	0.135	0.0024
K32	10×10^{-2}	1×10^{-2}	0.2	0.098	0.0017

2.4 Discussion

2.4.a Preliminary Runs

The preliminary spectral measurements on the reactants and products show that the course of the overall oxidation-reduction reaction may be studied spectrophotometrically only at wavelengths shorter than 350 mμ. However, this presents some practical difficulties; the optical system used in the present model stopped-flow apparatus allows considerable stray light to pass through the observation cell, and although the amount is quite negligible at wavelengths greater than 400 mμ, the percentage of stray light increases rapidly at shorter wavelengths (0.5% at 380 mμ, 10% at 320 mμ). The change with wavelength is due to the differing light output of the lamp and the sensitivity of the photomultiplier tube, so that at low wavelengths the slit width of the monochromator must be increased significantly. Because of this, the present apparatus is not well suited to the study of reactions which can only be followed spectrophotometrically at wavelengths below 400 mμ.

In addition, since both reactants, and to a lesser extent the products, absorb in the same region, any optical density measurements will contain contributions from more than one species. It is probably because of these factors, rather than the kinetics of the chemical system, that runs K15-K18 appear to give almost identical results, despite the change in ascorbic acid concentration.

The results of these runs serve merely to show that under these conditions, complete reaction between ferric ion and ascorbic acid occurs in about 10-20 seconds at 25°C, and a complete analysis has not been attempted.

2.4.b The Transient Intermediate

The detection during reaction of an absorption band other than those due to reactants or products shows that some other species is present in solution during the course of the overall oxidation-reduction reaction. Figure 24 shows that this species exhibits a broad absorption band with $\lambda_{max} \simeq 560$ mμ, and that it is formed very rapidly at 25°C as there is already a considerable quantity of it present by the time the reacting solution reaches the observation point, which is only 5-6 milliseconds after mixing. The absorption reaches a maximum (under these conditions of concentration, temperature, etc.) in only 0.4-0.5 seconds and then decays more slowly.

Because of the speed with which it forms the first 40-50% of reaction occurs in the "inaccessible" time interval between the points of mixing and observation, and so it is not possible to study the rate of formation of the intermediate at 25°C with any precision, particularly as experiments at 0°C show that at least two steps are involved in the formation of the intermediate.

Of interest however, is the dependence on the two reactants of

the concentration of intermediate formed. From the results in Tables 14 and 15, it can be seen that the amount of the intermediate formed is dependent on the concentrations of both ferric and ascorbic acid, indicating that the species observed is a product of a reaction between these two substances. Since λ_{max} corresponds very closely to that of the d-d absorption of the aquated ferric ion, it is not unreasonable to suggest that the intermediate is a ferric species in which the d orbitals are perturbed such that the d-d transition becomes more "allowed" than in the aquo Fe^{3+} ion. The most obvious ligand to consider in the system is ascorbic acid, and it is therefore proposed that the observed intermediate may be a complex formed by an association of a ferric ion with some form (associated molecule or dissociated anion) of ascorbic acid.

From the available experimental data it is possible to estimate values for the extinction coefficient and formation constant at $25^{o}C$ of this complex by considering the maximum optical densities reached under the different concentrations of Fe^{3+} and ascorbic acid. For an accurate determination of these quantities it is necessary to know the optical densities corresponding to the equilibrium concentrations of complex, but because the oxidation-reduction step occurs to an ever-increasing extent as more and more complex is formed, equilibrium is never fully reached. If the overall reaction were completely understood, it would be possible to extrapolate the

curve of complex formation versus time to an equilibrium value by allowing for the amount of complex destroyed by the redox step. However, since the dependence of the third step in the overall reaction (see Figure 25) on the concentration of complex is not known with certainty, any extrapolation would be subject to very large errors.

The observation that two steps are involved in the complex formation has also been mentioned but it will be shown later (Section 2.5) that the second step may merely involve a rearrangement of the species formed in the first step.

The following treatment considers that the intermediate corresponding to the maximum optical density (at 560 mμ) reached during reaction between ferric ion and ascorbic acid is due to a 1:1 complex of ferric and ascorbic acid, and the approximation is made that the maximum optical density reached corresponds to the equilibrium concentration of complex. Since this approximation may only be good to within 10-20%, it is only possible to obtain a rough estimate of the extinction coefficient and formation constant.

2.4.c Determination of Extinction Coefficient and Formation Constant of the Proposed Ferric-Ascorbate Complex

There are two possible reaction schemes to consider

(1) $$Fe^{3+} + H_2A \rightleftharpoons FeHA^{2+} + H^+$$
$$H^+ + HA^- \rightleftharpoons H_2A$$
$$Fe^{3+} + HA^- \rightleftharpoons FeHA^{2+}$$

where H_2A = ascorbic acid

HA^- = ascorbate anion

(2) $$Fe^{3+} + H_2A \rightleftharpoons FeH_2A^{3+}$$
$$H^+ + HA^- \rightleftharpoons H_2A$$
$$Fe^{3+} + H^+ + HA^- \rightleftharpoons FeH_2A^{3+}$$

It was noticed that decreasing the acid concentration caused an increase in complex formation, and although this could have been due to several factors, it is felt that it probably indicates that mechanism (1) is operative. Previous investigators have also suggested that the intermediate is $FeHA^{2+}$ and not FeH_2A^{3+}.

Now,

$$Fe^{3+} + H_2A \rightleftharpoons FeHA^{2+} + H^+$$

Initial concentration	a	b		o	c
Equilibrium	"	a-x	b-x	x	c+x

$$\therefore \quad K = \frac{x.(c+x)}{(a-x)(b-x)}$$

Assume $(c+x) \triangleq c$, (under conditions of high acid and low complex formation this is valid).

$$ab\left(1 - \frac{x}{a}\right)\left(1 - \frac{x}{b}\right) = \frac{x.c}{K}$$

$$\frac{x.c}{ab} \cdot \frac{1}{K} = 1 - \frac{x}{a} - \frac{x}{b} \text{ (taking only 1st powers in x)}$$

Since the only species absorbing at 560 mμ is the $FeHA^{2+}$ complex

optical density = $D = \varepsilon.x.l$

where ε = extinction coefficient, l = path length

$$\therefore \frac{Dc}{\varepsilon.l.ab} \cdot \frac{1}{K} = 1 - \frac{D}{\varepsilon.l}\left(\frac{1}{a} + \frac{1}{b}\right)$$

i.e. $$\frac{ab}{D} = \frac{c}{\varepsilon.l.K} + \frac{1}{\varepsilon.l}(a + b)$$

Therefore a plot of ab/D versus (a + b) should give a straight line of slope $1/\varepsilon.l$ and intercept $c/\varepsilon.l.K$.

Figure 26 shows this treatment applied to runs K19-K22. The values for ε and K calculated from the slope and intercept are 11.0 and 0.55 respectively. Using this value for ε, the maximum concentration of complex formed in run K22 is of the order of 5×10^{-3} M. Since this is only $2\frac{1}{2}\%$ of the H^+ concentration, and is the run which forms the most complex in this series, then the approximation that $c \triangleq c+x$ is valid.

There are two sources of error to consider in relation to the quoted values. Since the measured optical densities are only 0.01

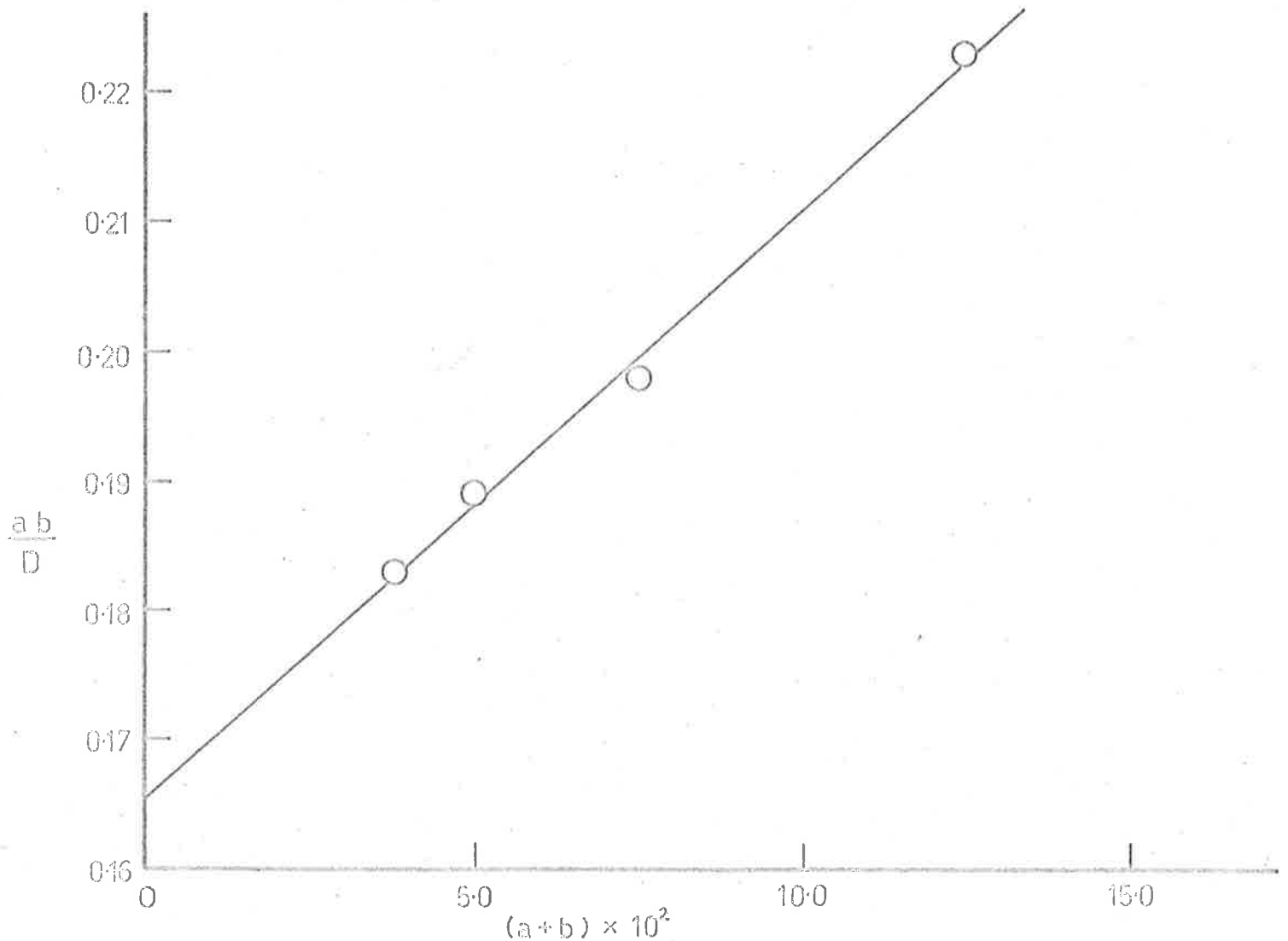

FIG. 26. Plot of $\frac{ab}{D}$ vs $(a+b)$ for the Determination of $\mathcal{E}$ and K.

or less, and were not measured against a reference cell as in normal spectrophotometric measurements, they may be subject to a 5-10% error. This introduces a possible error of $\pm$ 50% to ε, and a similar error to K. It has already been mentioned that the maximum optical density does not correspond to the equilibrium concentration of complex, and although this would not affect ε greatly, it could affect the value of K by an estimated 20-30%. Because of these sources of error, it is thought that ε and K can be reliably quoted only as 11 $\pm$ 6 and 0.55 $\pm$ 0.4 respectively.

Using the value for the extinction coefficient of 11, the maximum concentrations of complex formed in runs K23/1-7 and K26/1-5 have been calculated, then from these were computed the values of the formation constants corresponding to each run. The values are shown in Table 17, and although there appears to be considerable variation in the values of K, they are in fact well within the error limits quoted above.

Table 17

Calculated Values for Formation Constant Using ε = 11

Run No.	K	Run No.	K
K23/1	1.07	K26/1	0.80
K23/2	0.93	K26/2	0.53
K23/3	0.65	K26/3	0.61
K23/4	0.67	K26/4	0.61
K23/5	0.49	K26/5	0.40
K23/6	0.47		
K23/7	0.44		

2.4.d Study at $0^{\circ}C$

The runs K25/1-K25/6 showed that lowering the temperature from $25^{\circ}C$ to $0^{\circ}C$ caused a decrease in the rate of the second step in the complex formation by a factor of about 25, but since measurements of the faster first step could not be made at $25^{\circ}C$ it is not possible to say by what factor this first step is slowed down on lowering the temperature. At $0^{\circ}C$ it is possible to make measurements on the first step, and although subject to considerable errors, estimates of the initial rates and maximum optical densities of the first step only can be given for different concentrations of Fe^{3+} ion and ascorbic acid. These values have been quoted in Table 16. Unfortunately, the optical density changes in runs K30-K32 are so small that errors are probably such as to make the quoted values meaningless. From runs K27-K29 however, it can be seen that both the rate of formation of the complex, and the amount formed are in proportion to the first power of the ferric concentration. Assuming the rate law to be of the form

$$\text{Rate} = k\left[Fe^{3+}\right]\left[H_2A\right]$$

a value of 30 ± 10 litres $\text{moles}^{-1}\text{sec}^{-1}$ can be calculated for k at $0^{\circ}C$.

2.5 Proposed Mechanism of Intermediate Formation

It is clear that two stages are involved in the formation of the intermediate, and since the shape of the spectrum does not alter appreciably from one stage to the next (merely an increase in the optical density), it is proposed that the second step may only involve some type of rearrangement of the ferric-ascorbate complex formed in the first stage. The possibility of the formation of the di-ascorbate complex ($Fe(HA)_2^+$) cannot be completely ignored, although the dependence on ascorbic acid concentration tends to confirm that this is not formed to any appreciable extent.

The optical density corresponding to the end of the first stage is usually 0.5-0.7 times the maximum optical density formed by the end of the second stage regardless of the concentrations of the reactants. If a second complex of the type $Fe(HA)_2^+$ were involved, it would be expected that at high ascorbate concentration the ratio [second complex] : [first complex] would be much larger than at low ascorbate concentrations.

Three possible mechanisms which appear to comply equally well with the available data have been considered and it is not possible to draw any really clear distinction between them. For convenience these are called the "Chelating", "Proton Loss", and "Electron Transfer" mechanisms.

2.5.a The "Chelating" Mechanism

Figure 17 shows that the ascorbate anion may be considered to be a bidentate ligand and the two successive steps in the intermediate formation could be interpreted as the formation of the mono-associated complex followed by the attachment of the other end of the chelate.

$$\text{i.e. } Fe^{3+} + H_2A \rightleftharpoons H^+ + \underset{\substack{\text{mono-associated}\\ \text{complex}}}{Fe\overset{*}{H}A^{2+}}$$

$$Fe\overset{*}{H}A^{2+} \rightleftharpoons \underset{\text{chelated complex}}{FeHA^{2+}}$$

The first step is probably the association between the negatively charged oxygen and the Fe^{3+} ion (Figure 27). This forms fairly rapidly and the consequent distortion of the d orbitals of the metal increases the intensity of the Fe(III) d-d transition. The second step is the association of the second group to form the chelated complex (Figure 27). The d orbitals are distorted even more in this chelated complex and so the extinction coefficient increases.

It is generally thought that the second step in chelation is faster than the first because of the different probabilities of reaction, although there has been very little experimental evidence given for this. In the present case it is difficult to estimate the relative rates of the two steps in the formation of

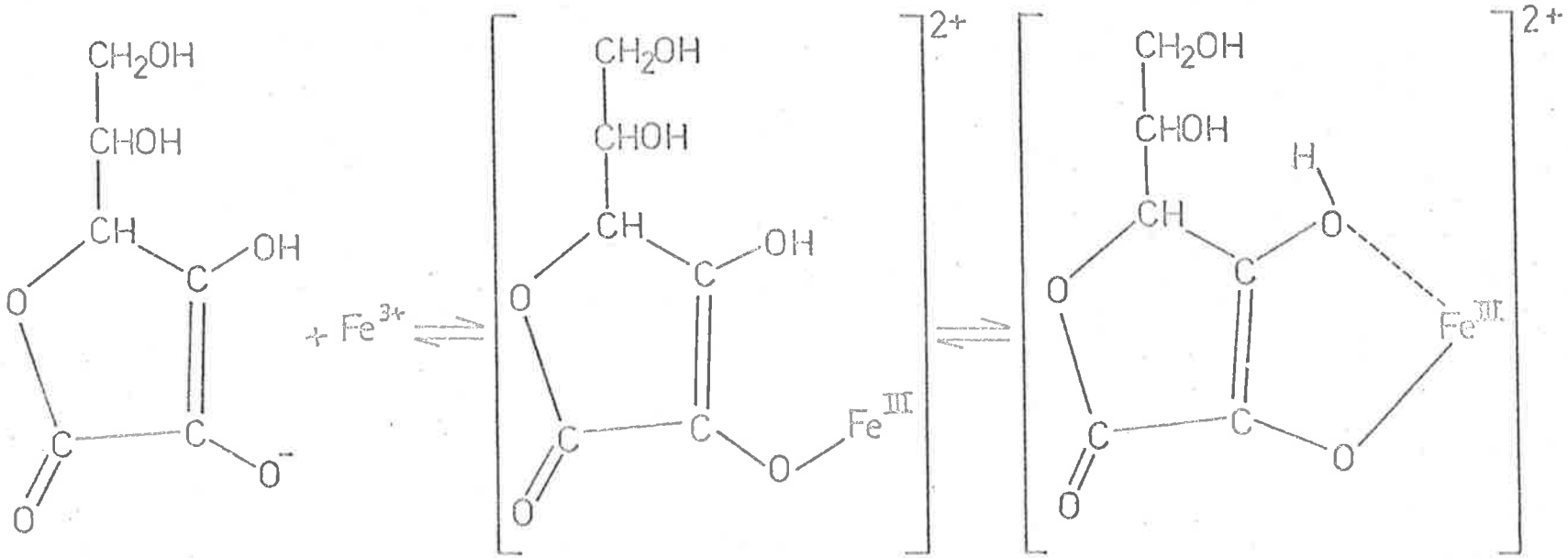

FIG. 27. The Chelating Mechanism

the intermediate because of the way in which the corresponding sections of the optical density versus time curves interact, but it does seem that the second step is considerably slower than the first. This may only be due, however, to the differences in the reactant concentrations for each step, and not to the relative values of the rate constants

i.e. for the first step,

$$\text{Rate} = k_1 [Fe^{3+}] [H_2A]$$

and for the second step

$$\text{Rate} = k_2 [\overset{*}{FeHA}^{2+}]$$

Thus, if the "equilibrium" concentration of the mono-associated complex ($\overset{*}{FeHA}^{2+}$) is small compared with the product $[Fe^{3+}].[H_2A]$, then the rate of the second step will be lower than for the first step, even if k_1 and k_2 are of the same order of magnitude. It is possible then to explain the two step process of complex formation by this mechanism. The value of 0.55 for the formation constant refers to the overall formation of the chelated complex and it is not possible, with the available data, to measure independently the formation constants of the two individual processes. Similarly, the value of the extinction coefficient as calculated in Section 2.4.c refers to the chelated complex, although

this value may be in error due to the equilibrium concentration of the mono-associated complex contributing to some extent to the light absorption, even at the point at which the maximum optical density is reached.

2.5.b The "Proton Loss" Mechanism

This mechanism pictures the first step in the formation of the intermediate as the formation of the chelated complex, the second step being the loss of another proton to yield the FeA^{+} complex (Figure 28)

i.e. $$Fe^{3+} + H_2A \rightleftharpoons H^{+} + \underbrace{FeHA^{2+}}_{\text{chelated complex}}$$

$$FeHA^{2+} \rightleftharpoons FeA^{+} + H^{+}$$

Taqui Khan and Martell[105] have suggested that a proton is released during the dissociation of the complex *following* electron transfer, but there does not seem to be any reason why the proton loss cannot occur *prior* to electron transfer. It is possible that a complete study of the dependence of the rate of both steps on H^{+} concentration *might* show evidence for this process, but with the available data it can only be suggested as a possible mechanism. In general, however, the rates of reactions involving protonation-deprotonation equilibria are very high, and it would therefore be a little surprising for the proposed reaction to be as slow as is observed in the second step

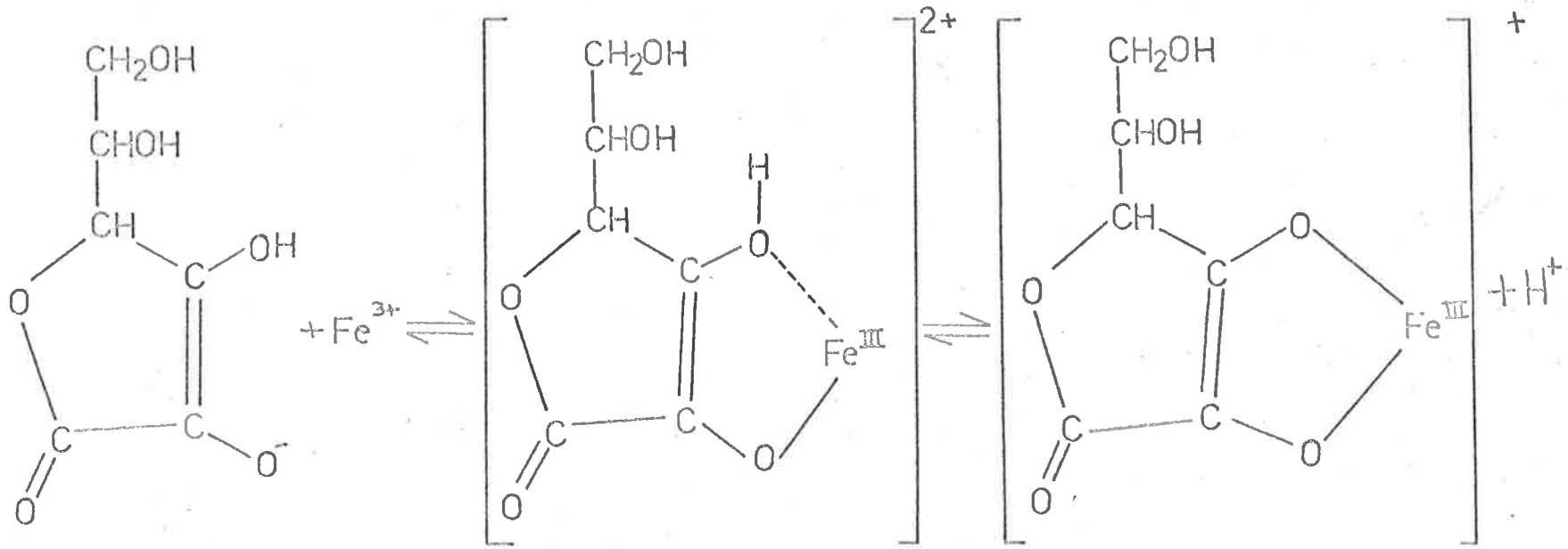

FIG. 28. The "Proton-Loss" Mechanism.

of the formation of the intermediate.

The calculated values of the extinction coefficients and formation constants are not very meaningful, since it is unlikely that step two occurs to completion, and the calculated values therefore contain contributions from both species.

2.5.c The "Electron Transfer" Mechanism

It is assumed in this mechanism, that the second step in the intermediate formation is caused by the transfer of an electron from the chelated ascorbate molecule to the central metal ion (Figure 29)

i.e. $Fe^{3+} + H_2A \rightleftharpoons \underset{\text{chelated complex}}{FeHA^{2+}} + H$

$FeHA^{2+} \rightleftharpoons \underset{\text{reduced-metal complex}}{Fe^{*}HA^{2+}}$

The first step is chelation to form the ferric ascorbate complex, which then undergoes an intramolecular electron transfer process to produce a species which is a complex between a ferrous ion and an ascorbate free radical (Figure 29). It is unlikely that this mechanism is operative since it would be expected that such a complex would be very short-lived, whereas the experimental results show that step three (corresponding in this case to the dissociation of the

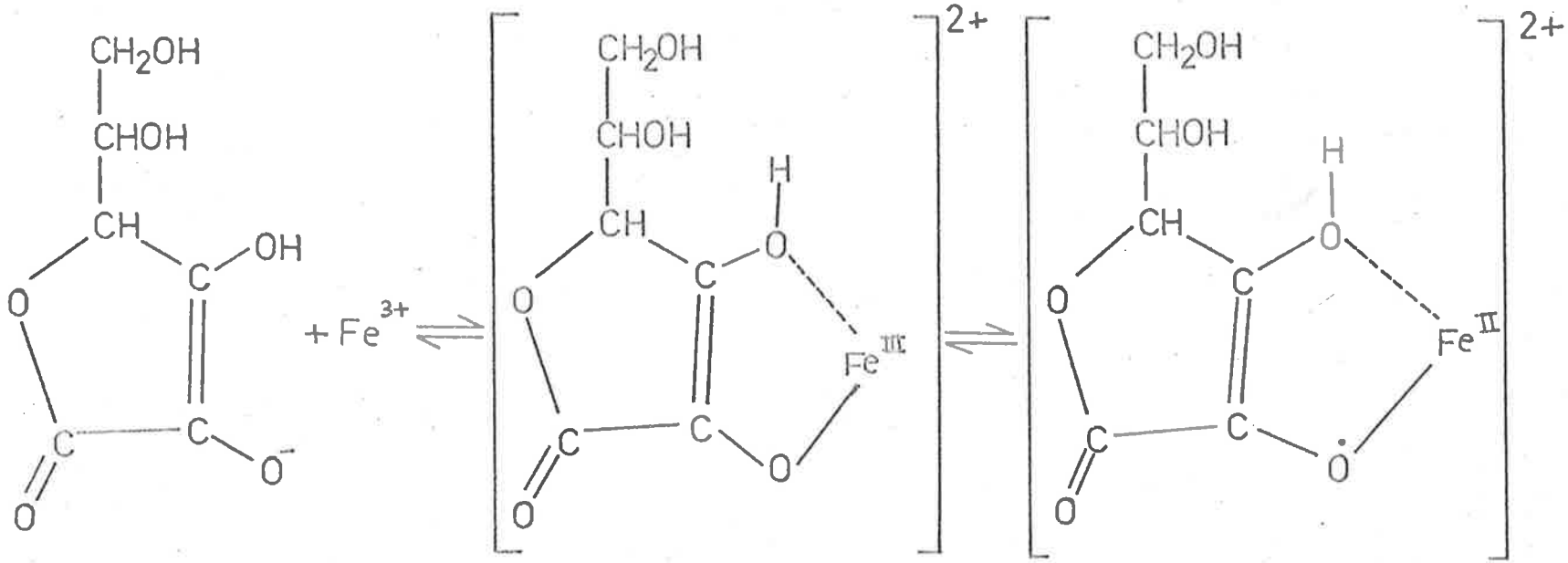

FIG. 29. The "Electron Transfer" Mechanism.

ferrous complex) is relatively slow.

Once again, the calculated values for the extinction coefficients would be a combination of factors from both steps if this were the correct mechanism.

2.6 The Overall Reaction

In the previous section, three possible explanations have been given for the formation of the intermediate, all of which assume that the complex at some stage consists of an association between a ferric ion and the ascorbate anion. The value of the rate constant (k) for the formation of the first step of the complex is of a reasonable magnitude for this type of reaction, and the calculated extinction coefficient and formation constant are in agreement with the general theory of the perturbation of the metal d orbitals so that the d-d transitions become more allowed (see Part 2, Chapter 1).

Of the three mechanisms suggested, it is felt that the chelating mechanism may be the most likely process by which the intermediate is formed.

Following the chelate formation it is proposed that there is an intramolecular electron transfer from ascorbate to metal ion. The reduced-metal complex then dissociates rapidly to produce a Fe^{2+} ion, an H^{+} ion, and a free radical which undergoes further rapid reaction with another Fe^{3+} ion to produce the semiquinone and another Fe^{2+} ion (Figure 30).

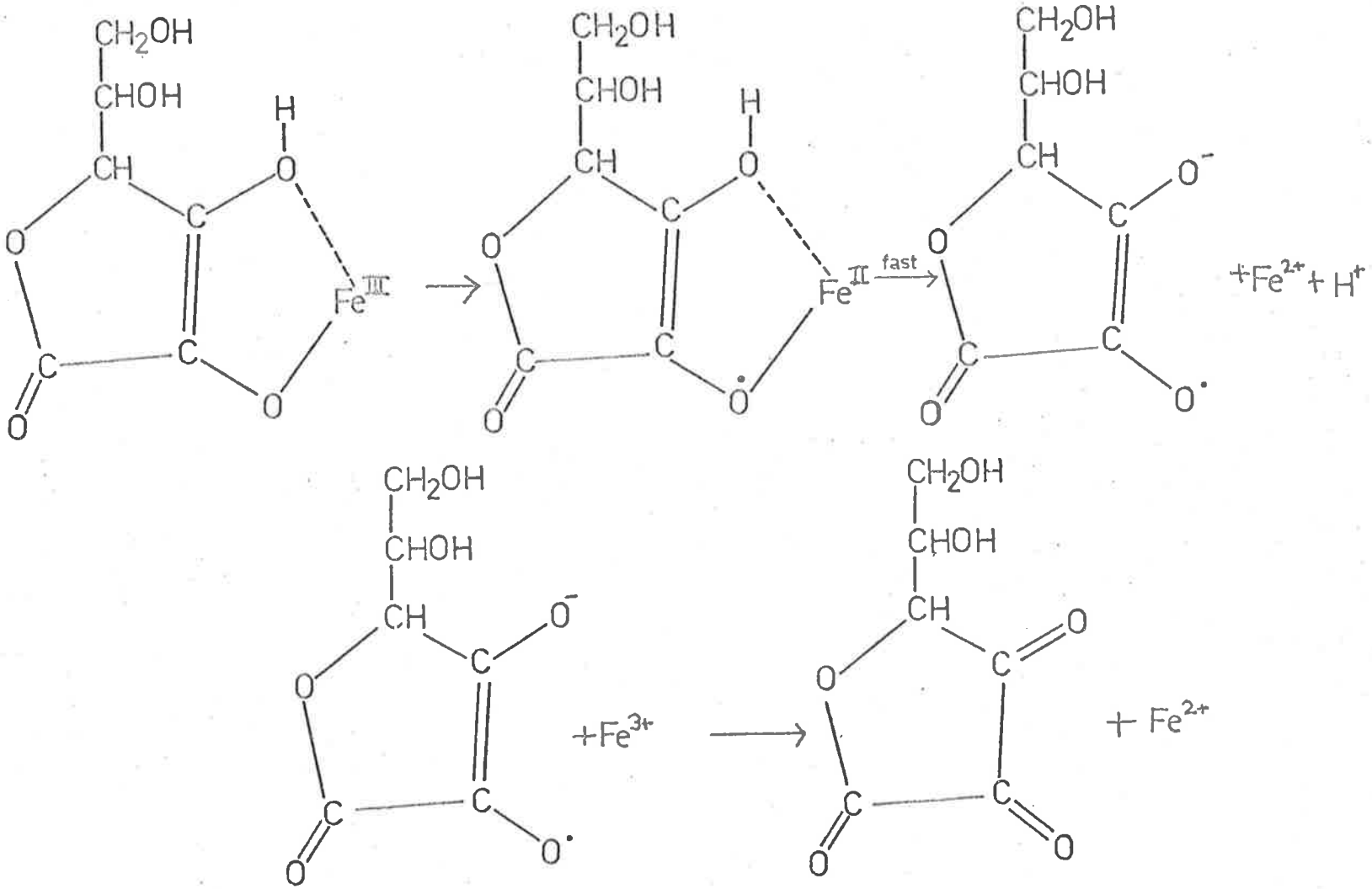

FIG. 30. The Overall Oxidation Reduction Mechanism.

$$Fe^{3+} + H_2A \rightleftharpoons FeHA^{2+} + H^+$$

chelated complex

$$FeHA^{2+} \rightleftharpoons Fe\overset{*}{H}A^{2+}$$

reduced metal complex

$$Fe\overset{*}{H}A^{2+} \longrightarrow Fe^{2+} + H^+ + A^-$$

ascorbate free radical

$$A^- + Fe^{3+} \longrightarrow A + Fe^{2+}$$

semi-quinone

---

i.e. $$2Fe^{3+} + H_2A \rightleftharpoons 2Fe^{2+} + 2H^+ + A$$

That is, for every mole of ascorbic acid oxidised to the semi-quinone, two moles of ferric ion are reduced. This is in agreement with the stoichiometry measured by other workers.[103,104]

There is a subtle difference between this proposal and the redox step suggested in Section 2.5.c. In this case, the rate controlling reaction in step three of the overall reaction (the destruction of the intermediate) is the electron transfer process, which is followed by a rapid dissociation of the reduced-metal complex. In the "Electron Transfer" mechanism, the rate controlling step in the reaction leading to the destruction of the intermediate must be the dissociation of the reduced-metal complex, since the electron transfer is proposed as the second step in the formation of the intermediate.

The proposed mechanism for the overall reaction could also include the "Proton Loss" mechanism for intermediate formation, the

only difference being that the complex would lose the proton before the electron transfer, and the fast dissociation of the reduced intermediate would yield a ferrous ion and the ascorbate free radical as described above.

For the proposed process to occur, it is unnecessary for a transition state containing more than one ferric ion and one ascorbate ion to be formed, but only when the order of the overall oxidation-reduction reaction has been studied (under the present conditions) with respect to both reactants, will it be possible to state the probable form of the transition state.

If the mechanism proposed above is correct, the rate of the overall reaction would be first order in both ferric ion and ascorbic acid, and the chelated ferric ascorbate complex would be the direct precursor of the transition state.

CHAPTER 3

The Oxidation of Iodide Ion by Ferric Ion in Aqueous Solution

3.1 Introduction

It has been known for many years that iodide ion in aqueous solution is oxidised spontaneously by ferric ion according to the stoichiometric equation

$$Fe^{3+} + I^- \longrightarrow Fe^{2+} + \tfrac{1}{2}I_2 \qquad (3.1)$$

The first kinetic measurements on the system were made by Schukarew[109] who found that the reaction was first order with respect to ferric ion and second order with respect to iodide ion. There have been many kinetic studies made on the system since then, but the interpretation of the results has been made difficult by the lack of control over the ionic strength of the reacting solution, and by the presence of other species, particularly chloride, which form complexes with the ferric ion.

In the most recent study, Fudge and Sykes[86] discussed the previous results and reinvestigated the kinetics of the process at constant ionic strength, and with the ferric ion present in its aquo form. The reaction scheme which they propose is

$$Fe^{3+} + I^- \underset{k_2}{\overset{k_1}{\rightleftharpoons}} FeI^{2+} \quad \text{fast} \qquad (3.2)$$

$$FeI^{2+} + I^- \underset{k_4}{\overset{k_3}{\rightleftharpoons}} Fe^{2+} + I_2^- \quad \text{rate determining} \qquad (3.3)$$

$$Fe^{3+} + I_2^- \underset{k_6}{\overset{k_5}{\rightleftharpoons}} Fe^{2+} + I_2 \qquad (3.4)$$

and the rate expression derived from this scheme is

$$-\frac{d[Fe^{3+}]}{dt} = \frac{2k_1k_3}{k_2} \frac{[Fe^{3+}][I^-]^2}{(1 + k_4[Fe^{2+}]/k_5[Fe^{3+}] + k_3[I^-]/k_2)}$$

It had been suggested previously by Wagner[110] that the reduction of the first ferric ion occurred by the process,

$$Fe^{3+} + I^- + I^- \longrightarrow Fe^{2+} + I_2^-$$

but this is unlikely because of the very low probability of a termolecular reaction occurring. The scheme given by equations (3.2)-(3.4) is a much more likely process as it consists of a series of bimolecular reactions between oppositely charged ions. The complex ions $FeCl^{2+}$ and $FeBr^{2+}$ are both well known species and have been studied extensively in aqueous solution so that it is not unreasonable to suggest that the species FeI^{2+} may exist in a solution containing Fe^{3+} and I^- ions. However, as stated by Fudge and Sykes,[86] "Since the stability decreases on passing from the chloride to the bromide, it is reasonable to suppose that the iodide has the properties of a transient intermediate in a rapid reaction".

Part 2 of this thesis is concerned with the detection of such transient intermediates in oxidation-reduction reactions and it was decided to reinvestigate the Fe^{3+}/I^- system spectrophotometrically

with the stopped flow apparatus in an attempt to find definite evidence for the species FeI^{2+}. If FeI^{2+} exhibited a charge transfer spectrum in solution as do the other ferric halide and pseudo-halide complex ions, the absorption maximum would be expected to occur at a wavelength of about 500 mμ and with an extinction coefficient of the order of 10^3-10^4. There might even be a splitting of the spectrum into two bands corresponding to the two possible states ($2P_{1/2}$ and $2P_{3/2}$) of the iodine atom produced by the electronic transition. These predictions have been made by comparing the electron affinity of the iodine atom with the other halogen atoms, and by using the theory of charge transfer spectra discussed in Part 1, Section 1.1.

3.2 Experimental

3.2.a Materials and Analyses

All iodide solutions were prepared from Unilab reagent grade sodium iodide. Stock solutions of relatively high concentrations (0.2 M) were prepared by dissolving accurately weighed quantities of reagent in known volumes of doubly distilled water, and the lower concentration solutions were prepared by accurate dilution of these stock solutions. Since the reagent is hygroscopic, the stock bottle was kept well sealed, and the appropriate samples were quickly removed and weighed before any appreciable amount of water was taken up from the atmosphere. The occasional analysis of the solutions by potentiometric titration with standardised silver nitrate solution[47,48] served as a check on the accuracy of this method of preparing solutions of known concentrations, and showed that the method was reliable to within $\pm$ 1%.

It was found that a neutral solution kept in a well stoppered bottle and out of direct sunlight, was stable for several months, but that in the presence of acid, oxygen, and light, the iodide was readily oxidised to iodine.

For a study of the ferrous dependence of this reaction it was found that highly concentrated ferrous solutions containing a very low concentration ($<0.05\%$) of Fe^{3+} were required (see Section 3.3.c). As it was not possible to obtain ferrous perchlorate ($Fe(ClO_4)_2$) with this low Fe^{3+} contamination commercially, the

$Fe(ClO_4)_2$ had to be prepared in the laboratory. Initially it was prepared by dissolving "pure" B.D.H. iron wire in A.R. perchloric acid, but tests showed that samples prepared in this way contained considerable quantities of chloride ion which is known to interfere with the ferric/iodide reaction[86].

The electrolytic reduction of $Fe(ClO_4)_3$ solutions was then chosen as a convenient means of preparing pure $Fe(ClO_4)_2$. The apparatus used is shown in Figure 31. With current from a 25 volt D.C. power supply, 500 ml of an 0.2 M solution of Fe(III) ion in 0.5 M $HClO_4$ could be reduced in 24 hours. Analysis of the reduced solution for Fe(III) by the formation of the $FeNCS^{2+}$ complex and subsequent measurement of the optical density at 460 mμ[42,57] showed that the Fe(III) concentration remaining in the reduced solution was approximately 3×10^{-6} M. i.e. Only 1.5×10^{-3}% of the total iron.

The current through the cell was usually about 200 mA, and the 0.1 moles of Fe(III) used in a typical preparation would have been reduced in about 12 hours if it had been the only reducible species in solution. As the concentration of Fe(III) fell, the current efficiency fell as some H_3O^+ was also reduced at the cathode. The total hydrogen ion concentration was not altered appreciably because hydrogen ion was able to migrate from the anodic to the cathodic cell.

The Fe^{2+} concentration in these solutions was determined by titration with permanganate,[46] and the hydrogen ion concentration was

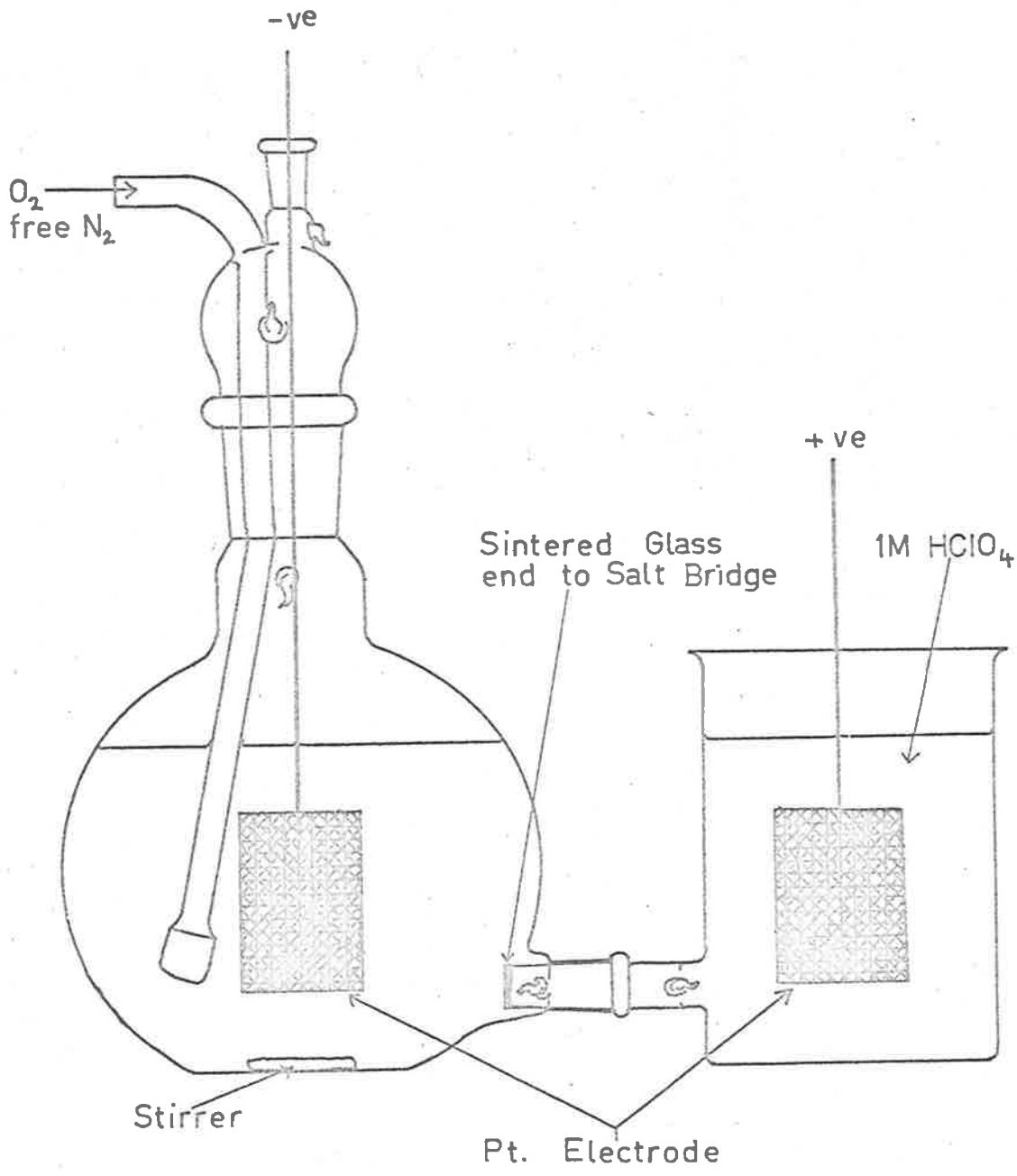

FIG. 31. Apparatus for the Electrolytic Reduction of Ferric Solutions.

determined by titrating the total (Fe^{2+} + H^{+}) with NaOH solution. This method is similar to that used previously in the analysis of Fe^{3+} solutions (see Part 1, Section 2.2.a). Ferrous hydroxide does not coagulate readily and masks the colour change of the indicator, so that the end point had to be detected with a pH meter. Because of the lower K_{sp} (10^{-14}) of $Fe(OH)_2$ compared with $Fe(OH)_3$ (10^{-38}), the end point was taken to be at pH = 10. This corresponds to 10^{-6} M free Fe^{2+} ion in solution at the end point (original concentration $\simeq$ 0.1 M). The errors in this analysis were of the same order as those discussed in Part 1, Section 2.2.a, i.e. Fe^{2+}, $\pm$ 0.1%; H^{+}, $\pm$ 2%.

The electrolytic reduction of Fe^{3+} was adapted for use as a method of analysis of stock Fe^{3+} solutions. Using a smaller, somewhat modified version of the apparatus shown in Figure 31, a 20 ml sample of a 0.1 M Fe^{3+} solution could be quantitatively reduced in 15 minutes, and the total Fe^{2+} concentration was then determined by titration with potassium permanganate.[46] Sulphuric acid (2 N) was used in the anodic cell, in the salt bridge, and as a supporting electrolyte for the sample in the reduction cell. The internal resistance of the cell was therefore quite low, allowing a current of up to 450 ma. to pass so that reduction took place rapidly. An added advantage of the presence of the acid was that the permanganate could be titrated directly into the reaction cell without first having to add acid before titrating.

The sintered glass end to the salt bridge was of very low porosity, and provided the level of liquid in the anodic cell was higher than in the reaction cell, there was only a very slow movement of acid into the solution being analysed, but no Fe^{2+} was lost by a reverse flow of the iron solutions.

The advantage of this method of analysis lies mainly in its simplicity, once the apparatus has been set up. No other reagents are required as in the reduction of Fe(III) by stannous chloride. There was no adverse effect on letting the reduction proceed for too long (that is, after all Fe(III) had been reduced), and it was found that sample analyses agreed within $\pm$ 0.1% with those in which the Fe(III) was reduced with stannous chloride.

The preparation and analyses of other reactant solutions have already been described in a previous section (Part 1, Section 2.2.a).

3.2.b Apparatus

Most kinetic runs were carried out on the stopped-flow apparatus described in Section 2.2.b, but for conditions under which the reaction had a half-life of five minutes or more, the reaction was followed using the SP800 recording spectrophotometer. The rapid mixing device for use with the SP800, shown in Figure 32, enabled equal quantities of each reactant to be mixed accurately and introduced rapidly into the reaction cell, which was a standard 2, 10 or 40 mm spectrophotometer cell; the reaction could be followed

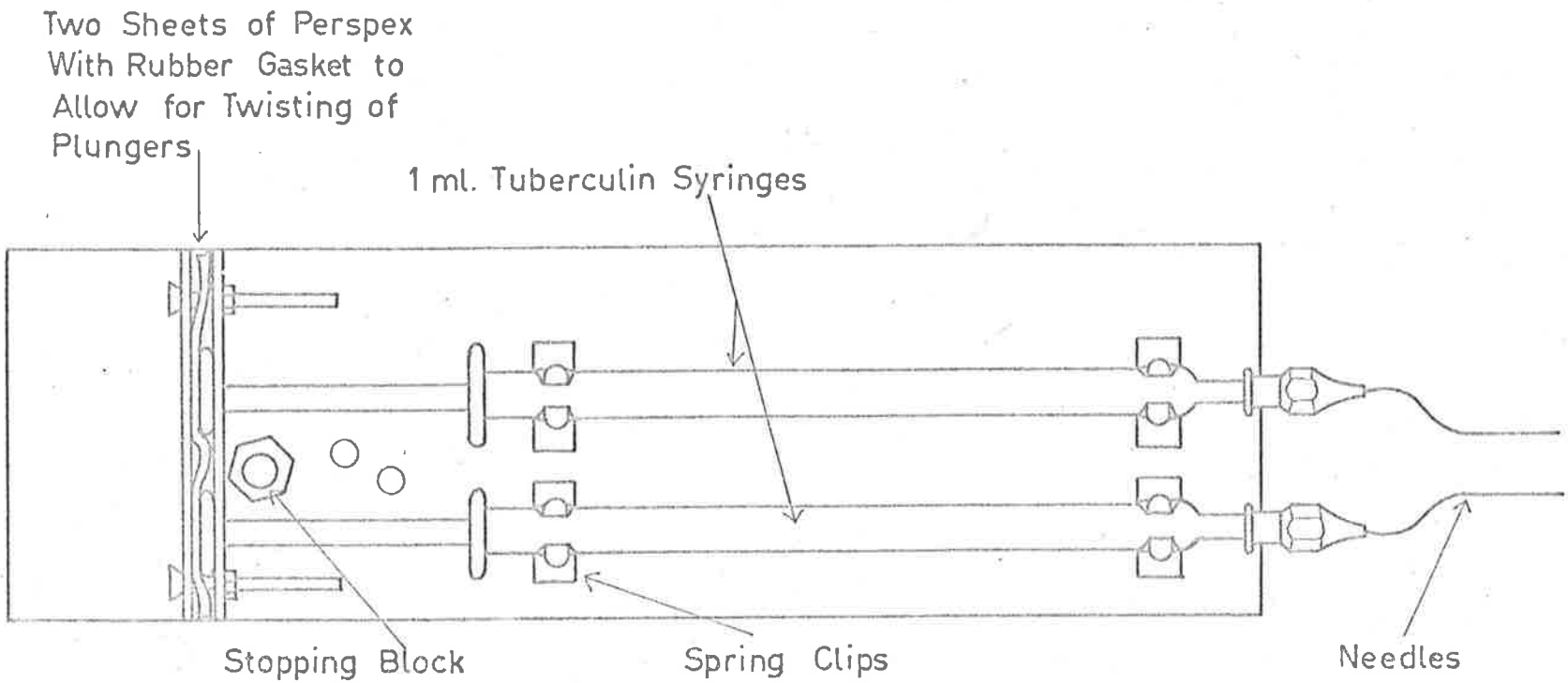

FIG. 32. Rapid Mixing Device for Use With SP800 Spectrophotometer.

from about 3-4 seconds after mixing by injecting the reactants directly into the spectrophotometer cell placed in the cell block.

3.2.c Treatment of Data

The way in which the oscilloscope traces (from runs done on the stopped flow apparatus) were converted to give curves of optical density versus time has been described previously in Section 2.2.d, along with the method for calculating the absorption spectrum of any intermediate which may be formed during reaction. In this system it was often necessary to study the reaction under conditions in which the total optical density change produced in the reduction of the Fe(III), was of the order of 10-100, and because of the logarithmic relationship between the optical density and the output voltage of the photomultiplier tube, only the first few percent of reaction could be followed under these conditions with any degree of precision. The reaction was therefore followed by the method of initial rates.

Even though it corresponded to only a very small percentage of reaction, the change in light absorption of the solution in travelling from the mixing chamber to the observation tube was so large that an accurate extrapolation of the oscilloscope trace as described in Section 2.2.d could not be made. The reference point for the determination of all optical densities was therefore taken as

a point on the trace at a time shortly after the flow had stopped. Since only the rate of change of optical density was needed for the measurement of initial rates, and the absolute values of optical densities were not required, this method was quite valid.

The plot of optical density versus time was linear and it was simple to extrapolate this back to the point of mixing to illustrate that the optical density immediately following mixing was due only to the absorptions of the two reactants, and that no other absorbing species (apart from final products) were formed in the time interval corresponding to the transit of the reaction solution from the mixing chamber to the observation tube.

The rates of reaction were followed by monitoring the change in light absorption due to oxidised iodide species (I_2 and I_3^-) at a wavelength of 370 mμ. The proportion of these two species in solution is governed by the equilibrium

$$I_2 + I^- \overset{K}{\rightleftharpoons} I_3^-$$

and from data to be discussed in Section 3.3.b, it is possible to derive a value for K of 720 under the present experimental conditions. Since the data of Awtrey and Connick[111] shows that at $\lambda = 370$ mμ the extinction coefficient of I_2 is less than 5% of the value for I_3^-, the approximation was made that all of the absorption was due to I_3^-, but under differing iodide concentrations, allowance had to be made for the different ratio of I_3^- / I_2 in calculating the

concentration of iodine in the zero oxidation state. From the equilibrium expression for I_3^- it can be shown that, provided $[I^-] \gg [I_2][I_3^-]$, which is true under all conditions for initial rate measurements,

$$[I_3^-] = \frac{(720[I^-])}{(1 + 720[I^-])} [I^o]_{total}$$

(where $[I^o]_{total}$ = total concentration of iodine in zero oxidation state),

so that at 0.1 M I^- concentration, $[I_3^-] = 0.99\ [I^o]_{total}$, while at $[I^-] = 0.01$ M, $[I_3^-] = 0.88\ [I^o]_{total}$.

In the measurement of the initial rates it was necessary that the calculated rates of optical density change per time be converted to the rate of production of I_3^- using the value for the extinction coefficient for I_3^-, and this in turn converted to the rate of production of $[I^o]_{total}$ using the appropriate factor. During the initial portion of any run, the I^- concentration remained effectively constant, and the one proportionality factor could be used, but a different factor had to be used for each run at different I^- concentrations.

3.3 Results and Discussion

3.3.a Evidence for the Existence of FeI^{2+} as an Intermediate

A probable mechanism for the oxidation-reduction reaction between Fe^{3+} and I^- ions in aqueous solution has already been discussed (Section 3.1). The mechanism suggests the species FeI^{2+} as an intermediate. It was decided to try and find evidence for this (or other) transient species using the same method as described for the ferric/ascorbate reaction (Section 2.3.b).

Measurements were made at wavelengths from 350 mμ to 650 mμ using solutions of a variety of concentrations of Fe^{3+} (10^{-4}-10^{-1} M), I^- (10^{-4}-10^{-1} M) and H^+ (0.01-0.5 M), and at both 0^o and 25^oC, but there was no spectrophotometric evidence for the formation of any transient species during reaction. Since it is known that the addition of Fe^{2+} ion slows down the oxidation-reduction reaction, a few runs were also done in the presence of 0.2 M ferrous in the hope that this might aid the detection of any intermediate by slowing down the rate of production of products.

The only change noticed during the course of the reaction under any of the experimental conditions was a steady increase with time of the optical density at wavelengths below 400 mμ, which was attributed to the I_3^- ion. A comparison is made in Figure 33 of the spectrum of this product (compiled from the stopped-flow measurements) with the spectrum of I_3^- measured on the SP800 spectrophotometer.

As discussed in Chapter 1, the non-detection of an intermediate

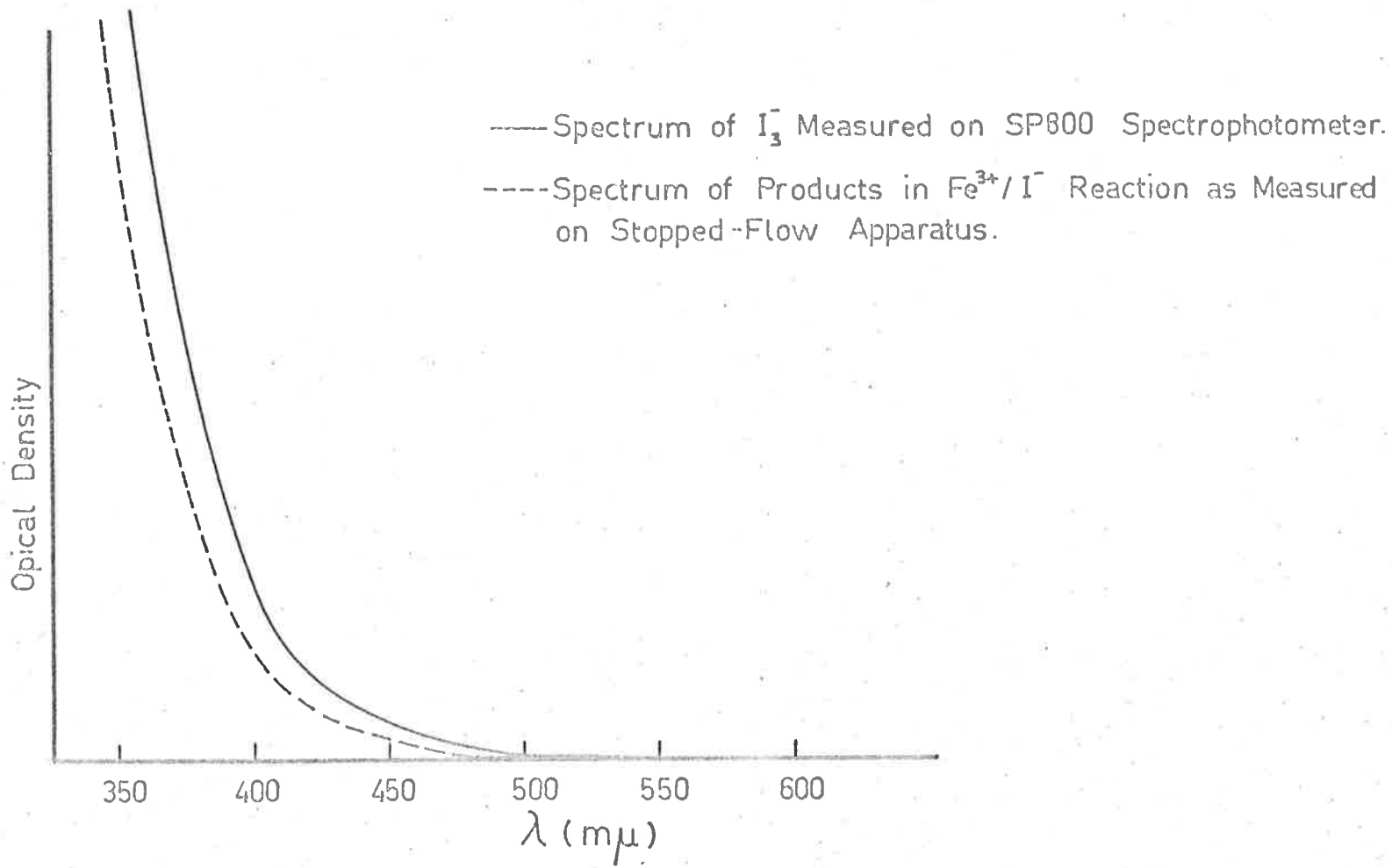

FIG. 33. The Spectrum of I_3^- in Aqueous Solution.

does not rule out the possibility of the transient formation of, for example, the FeI^{2+} species. It could be that the stationary state concentration of FeI^{2+} is so low that it cannot be observed on our stopped-flow apparatus. There are two cases to be considered.

In the first case it is assumed that the concentration of FeI^{2+} is very low because the speed at which it reacts with another I^- ion to produce a Fe^{2+} and an I_2^- ion is much faster than the rate of formation of FeI^{2+} itself.

$$Fe^{3+} + I^- \xrightarrow{k_f} FeI^{2+}$$

$$FeI^{2+} + I^- \xrightarrow{k_r} Fe^{2+} + I_2^-$$

i.e. $k_f \ll k_r$

If this were the case, the rate controlling step would be the formation of the intermediate, and the overall reaction would show a first order dependence on iodide ion. Previous workers[86,112] have found a second order dependence on iodide ion for the rate of product formation, and this is confirmed by the results presented in Section 3.3.c of this thesis. Because of this, the rate controlling step cannot be the formation of the FeI^{2+} species and it is not possible to suggest that the low stationary state concentration of FeI^{2+} arises from k_r being greater than k_f.

On the other hand, a low stationary state concentration could be

due to a rapid rate of dissociation of the complex

$$Fe^{3+} + I^- \underset{k_b}{\overset{k_f}{\rightleftharpoons}} FeI^{2+} \qquad \text{fast equilibrium}$$

$$FeI^{2+} + I^- \xrightarrow{k_r} Fe^{2+} + I_2^-$$

That is, the rate determining step is the reaction between the complex FeI^{2+} and I^- so that the reduction of Fe^{3+} is second order in iodide ion,

$$\text{i.e.} \qquad \text{Rate} = k_r[FeI^{2+}][I^-]$$

$$= k_r \cdot k_f/k_b \; [Fe^{3+}][I^-]^2$$

and the stationary state concentration is controlled by the rates of formation and dissociation of FeI^{2+}. An estimate of the maximum possible formation constant, K ($= k_f/k_b$) can be made from the present experiments.

From the theoretical treatment of charge transfer spectra, (see Part 1) it is certain that if the complex did form, its charge transfer absorption maximum would be in the wavelength range which has been covered. Assuming it to have an extinction coefficient of only 500 $M^{-1}.\,cm^{-1}$ (charge transfer absorptions are generally 2-20 times more intense than this), a concentration of as little as 10^{-5} M FeI^{2+} could be detected by this method since optical density changes down to 0.001 can be detected in the stopped-flow apparatus. Concentrations

of both reactants of up to 10^{-1} M were used, and as no absorption was detected, the concentration of FeI^{2+} must have been less than 10^{-5} M. This corresponds to a maximum value of 10^{-3} for K.

i.e. $[Fe^{3+}] = 10^{-1}$ M; $[I^-] = 10^{-1}$ M; $[FeI^{2+}] = 10^{-5}$ M (maximum)

$$K = \frac{[FeI^{2+}]}{[Fe^{3+}][I^-]} = \frac{10^{-5}}{10^{-1} \cdot 10^{-1}} = 10^{-3}$$

Comparison with similar complexes (e.g. $FeCl^{2+}$, K = 2.89 at $\Gamma = 1.0$;[113] $FeBr^{2+}$, K = 0.61 at $\Gamma = 1.2$[114]) shows that this value is lower than might be expected for the formation of FeI^{2+}.

The value of K of 10^{-3} can be used in conjunction with the measured rate of the oxidation-reduction reaction to estimate the rate constant for the presumed rate determining step

$$FeI^{2+} + I^- \xrightarrow{k_r} Fe^{2+} + I_2^-$$

It has already been shown that

$$\text{Rate} = k_r \cdot k_f/k_b \, [Fe^{3+}] [I^-]^2$$

$$= k_r K \cdot [Fe^{3+}] [I^-]^2$$

i.e. $$k_{obs} = k_r \cdot K$$

Using the value for k_{obs} at 25°C of 16 litres^2 moles^{-2} sec^{-1} (derived experimentally in Section 3.3.c) and substituting $K = 10^{-3}$

in this equation we find that

$$16 = k_r \cdot 10^{-3}$$

$$k_r = 16{,}000 \text{ litres moles}^{-1}\text{sec}^{-1}$$

As this treatment assumes that k_r is rate determining and the FeI^{2+} equilibrium is faster than this, then the rate of attainment of the FeI^{2+} equilibrium must be greater than 16,000 $l.m^{-1}sec^{-1}$. This is very much larger than the corresponding rates for the formation of similar iron complexes, ($FeCl^{2+}$, $k = 9.4\ l.m^{-1}sec^{-1}$ at $\Gamma = 1.0$, 25°;[115] $FeBr^{2+}$, $k = 20\ l.m^{-1}sec^{-1}$ at $\Gamma = 1.7$, 22°C;[116] $FeNCS^{2+}$, $k = 127\ l.m^{-1}sec^{-1}$ at $\Gamma = 0.4$, 25°C[117]), and is unlikely to be a valid estimation of the rate of attainment of the equilibrium. It seems probable therefore that K for the formation of FeI^{2+} <u>is</u> greater than 10^{-3}, but that FeI^{2+} cannot be observed in this reaction because of its removal by the electron transfer reaction.

However, in view of the second order dependence on iodide of the rate of the oxidation-reduction reaction, it is apparent that the transition state <u>must</u> contain two iodide ions.

$$(I^- \ldots Fe^{3+} \ldots I^-)$$

It is suggested therefore that the reaction involves the initial formation of an ion pair ($Fe^{3+} \ldots I^-$) which could be a precursor to the

formation of the species FeI^{2+}, but that the ion pair reacts with another iodide ion to lead to the transition state for the oxidation-reduction reaction, so that the complex FeI^{2+} is not formed.

The rate of formation of ion pairs is known to be fast,[118] as is required by this mechanism. Such an ion pair would not exhibit a charge transfer absorption spectrum, but instead the d orbitals would be perturbed slightly, making the d-d transition more allowed. The extinction coefficient corresponding to this d-d transition would be expected to be much lower than in the case of a charge transfer absorption of a complex, so making the detection of the intermediate by spectrophotometry even more difficult.

3.3.b The Formation Constant and Extinction Coefficient of I_3^-

There have been many studies made on the I_2/I_3^- equilibrium, and the quoted values for the formation constant K[119] of the reaction

$$I_2 + I^- \rightleftharpoons I_3^-$$

at 25°C range from 630 to 780. The most reliable value seems to be $720 \pm 20\ M^{-1}$ and is the figure used in this work. By measuring the optical densities of a series of solutions of known I_2 and I^- concentrations, and using the value of K = 720 to calculate the equilibrium concentration of I_3^-, the value for the extinction coefficient of I_3^- at λ = 370 mμ was found to be $19{,}420 \pm 400\ M^{-1}cm^{-1}$. The error quoted refers only to the precision of the experimental

measurements and does not allow for the possible inaccuracy of K. However, the value for ε at λ = 370 m$\mu$is in reasonable agreement with the value of 20,000 $\pm$ 1,000 extrapolated from the data of Awtrey and Connick.[111]

At this wavelength, the extinction coefficient of I_2 in aqueous solution is only of the order of 1% of the value for I_3^-, and any absorption due to molecular I_2 can be ignored if $[I^-] > [I_2]$ as the high speed at which the I_2/I_3^- equilibrium is achieved ($k \doteq 10^{10}$ litres/moles/sec[120]) ensures that there is very little free I_2 in solution. This is true in the measurement of initial rates, but care must still be taken in calculating the concentration of total iodine from the observed optical densities so that due allowance is made for the percentage of I_2 existing as I_3^-. The method by which this is done has already been described in Section 3.2.c.

3.3.c The Kinetics of the Oxidation-Reduction Reaction

Since no direct evidence was found for the existence of the FeI^{2+} complex as an intermediate in the reduction of ferric ion by iodide ion, the overall kinetics of the reaction were briefly investigated on the stopped-flow apparatus. Previous investigations were conducted at rather high conversions of Fe^{3+} to Fe^{2+}, but the stopped-flow apparatus allowed the initial rates to be measured at higher concentrations of reactants than previously. The course

of reaction was followed by measuring the $[I_3^-]$ produced.

Ferric and Iodide Dependences

The initial rates were measured at 25°C using the concentrations of reagents shown in Table 18. The ionic strength and acid concentration were maintained constant at 1.0 and 0.25M respectively throughout the whole series of runs. It can be seen that the reaction in the absence of Fe^{2+} ion is first order in ferric ion and second order in iodide ion over the complete range studied, the third order rate constant for the reaction being 16.0 ± 1.0 litres^2. moles^{-2}. sec^{-1} at 25°C.

Although it is not possible to make an accurate adjustment to allow for the effect of different ionic strengths on the value of the rate constant because of the high ionic strengths used in this study, it is possible to compare the present value with those of previous workers and to show that all of the results are in reasonable agreement.

Hershey and Bray[112] obtained values at 25°C of 87 and 810 litres^2. moles^{-2}. sec^{-1} at ionic strengths of 0.09 and 0.0 respectively. At an ionic strength of unity the value would be much lower, and could well be of the order 10 litres^2. moles^{-2}. sec^{-1}. From the results of Fudge and Sykes,[86] it is possible to calculate values for k_1 ranging from 9 litres^2. moles^{-2}. sec^{-1} at 20°C and $\Gamma = 0.164$ to about 30 litres^2. moles^{-2}. sec^{-1} at 19°C and $\Gamma = 0.60$. After allowing for

Table 18

The Effect on the Rate of Reaction of Varying Fe^{3+} and I^- Concentrations

$[H^+] = 0.25$ M T = 25°C $\Gamma = 1.0$ $\lambda = 370$ mμ

Run No.	$[Fe^{3+}] \times 10^3$ M.	$[I^-] \times 10^3$ M.	Initial Rate $\times 10^4$ moles/litre/sec	$k_1 = \frac{\text{Rate}}{[Fe^{3+}][I^-]^2}$ (litres^2 moles^{-2} sec^{-1})
J.11	99.00	96.0	137.58	15.1
12	49.45	"	73.19	16.1
13	19.80	"	30.14	16.5
14	9.90	"	15.02	16.4
15	3.95	"	6.09	16.7
16	1.18	"	1.75	16.0
61	99.00	9.6	1.32	14.5
62	49.45	"	0.68	14.9
63	19.80	"	0.30	16.3
64	9.90	"	0.15	15.9
65	3.95	"	0.06	16.2
66	1.18	"	0.02	17.0
21	99.00	86.0	113.15	15.5
31	"	74.4	88.36	16.1
41	"	60.7	60.60	16.6
51	"	43.1	29.78	16.1
26	1.18	86.0	1.36	15.5
36	"	74.4	1.08	16.5
46	"	60.7	0.70	16.1
56	"	43.1	.35	16.0

changes in temperature and ionic strength, it is again probable that these values are in reasonable agreement with that found in the present work.

Ferrous Dependence

A test of the equation used by Fudge and Sykes[86]

$$\text{Rate} = \frac{k_1 [Fe^{3+}] [I^-]^2}{1 + R} \qquad (3.5)$$

was made by carrying out runs at fixed Fe^{3+} and I^- concentrations but at different Fe^{2+} concentrations. The results in Table 19 confirm to a first approximation the dependence of the retardation term on the first power of the Fe^{2+} concentration, but show that there is also some dependence on both Fe^{3+} and I^-.

Since the value of $R/[Fe^{2+}]$ from each set of runs is not directly proportional to the Fe^{3+} and I^- concentrations, but does vary to some extent with these concentrations, it is probable that the retardation term R contains yet another term, which must also be Fe^{2+} dependent in order to maintain the strict first order ferric and second order iodide dependences at low Fe^{2+} concentration which have been discussed above.

Ferric and Iodide Dependences at High Constant Ferrous Concentratio

A series of experiments was performed in which a large amount of

Table 19

Values of the Retardation Term Showing the First Order Dependence on $[Fe^{2+}]$

$[H^+]$ = 0.25 M Γ = 1.0 T = 25°C

Run No.	$[Fe^{3+}]$ x 10^3 M	$[I^-]$ x 10^3 M	$[Fe^{2+}]$ x 10^3 M	Rate x 10^6 (m/l/sec)	R	$\frac{R}{[Fe^{2+}]}$
M.111	99.13	99.77	10.20	14,330	0.104	10.20
M.112	99.14	99.77	20.40	12,770	0.239	11.72
M.115	99.17	99.77	51.00	9,990	0.584	11.45
M.161	1.24	99.77	10.20	21.83	8.07	791
M.162	1.25	"	20.40	12.24	15.30	750
M.163	1.26	"	30.60	8.55	22.52	736
M.164	1.27	"	40.80	7.24	26.99	662
M.165	1.28	"	51.00	6.01	33.02	648
M.611	99.13	9.93	10.20	97.43	0.609	59.7
M.612	99.14	"	20.40	91.45	0.714	35.0
M.615	99.17	"	51.00	41.38	2.790	54.7
M.661	1.24	9.93	10.20	0.053	36.2	3,550
M.662	1.25	"	20.40	0.025	77.0	3,780
M.663	1.26	"	30.60	0.019	101.9	3,330
M.664	1.27	"	40.80	0.017	115.0	2,820
M.665	1.28	"	51.00	0.015	130	2,540

Fe^{2+} ion was added to the reaction mixtures, and the effect of varying the Fe^{3+} and I^- concentrations were observed. The conditions and results are given in Table 20.

Unfortunately very little information about the form of the extra retardation term can beobtained from these results since the dependence of R on both Fe^{3+} and I^- concentrations is not of a simple order. It is probable that the term R consists of several terms, but the existing data is not precise enough to elucidate the problem.

Table 20

Determination of the Dependence of the Retardation Term on Fe^{3+} and I^- Concentrations

$[Fe^{2+}] = 0.0502$ $[H^+] = 0.25$ M $T = 25^oC$ $\Gamma = 1.0$

Run No.	$[Fe^{3+}]$ x 10^3 M	$[I^-]$ x 10^3 M	Rate x 10^6 (moles/litre/sec)	$\frac{R}{[Fe^{2+}]}$
L.11	99.30	96.00	8,825	13.20
L.12	49.80	"	3,737	19.30
L.13	20.00	"	835	50.6
L.14	10.10	"	268	90.8
L.15	4.20	"	589	190
L.16	1.40	"	10.3	382
L.61	99.30	9.80	32.62	73.5
L.62	49.80	"	9.16	148
L.63	20.00	"	1.70	341
L.64	10.10	"	0.604	493
L.65	4.20	"	0.167	754
L.66	1.40	"	0.050	847
L.11	99.30	96.00	8,825	13.2
L.21	99.40	86.00	6,596	15.7
L.31	"	74.50	5,716	10.9
L.41	"	60.65	2,973	19.4
L.56	"	43.25	1,304	25.6
L.61	99.30	9.80	32.6	73.5
L.16	1.40	96.00	10.25	382
L.26	1.55	86.00	8.44	413
L.36	"	74.50	6.74	387
L.46	"	60.65	4.36	397
L.56	"	43.25	2.92	297
L.66	1.40	9.80	0.05	847

3.4 Conclusion

In the light of the experimental results so far discussed in this work, it is possible to do little more than to confirm the results of earlier workers.[86,112] From a purely abstract consideration of the system, it would appear that the mechanism proposed by Fudge and Sykes[86] is quite reasonable.

$$Fe^{3+} + I^- \underset{k_2}{\overset{k_1}{\rightleftharpoons}} FeI^{2+}$$

$$FeI^{2+} + I^- \underset{k_4}{\overset{k_3}{\rightleftharpoons}} Fe^{2+} + I_2^-$$

$$Fe^{3+} + I_2^- \underset{k_6}{\overset{k_5}{\rightleftharpoons}} Fe^{2+} + I_2$$

All of the reactions included are of types known to occur in aqueous solutions. From the discussion in Section 3.3.a it is probable that the first step consists not of the formation of the complex FeI^{2+} as suggested by Fudge and Sykes, but of the formation of an ion pair species between a Fe^{3+} and an I^- ion.

$$Fe^{3+} + I^- \rightleftharpoons (Fe^{3+}....I^-)$$

The reaction between the ion pair and another I^- ion is proposed as the rate determining step and leads to the kinetics of the overall reaction being second order in I^- ion.

$$(Fe^{2+}....I^-) + I^- \rightleftharpoons Fe^{2+} + I_2^-$$

This scheme would seem to imply an "outer-sphere" type of mechanism for the electron transfer.

Whereas the earlier workers had only suggested that I_2^- might form in aqueous solution, recent studies[121,122] have confirmed that the species can form in aqueous solution.

However, although all of the reactions in the scheme appear feasible, the rate expression derived from the reaction scheme,

$$\text{Rate} = \frac{k_1 k_3}{k_2} \left[Fe^{3+}\right]\left[I^-\right]^2 / \left(1 + \frac{k_4 \left[Fe^{2+}\right]}{k_5 \left[Fe^{3+}\right]} + \frac{k_3}{k_2}\left[I^-\right]\right)$$

does not agree with all of the experimental results. Apart from being dependent on the ferrous ion concentration, the nature of the retardation term in the rate expression cannot be explained, but it certainly is not of the form given by the above equation.

In order to explain the overall mechanism it is obviously necessary that a more complete study be undertaken. In particular, it could be that a study of the acid dependence might be helpful. In this work, the presence of the species $FeOH^{2+}$ has been ignored because its concentration is only about 1% of the total Fe^{3+} concentration under the conditions used. However, $FeOH^{2+}$ may play a significant role in the reaction, and this could be best detected by studying the effect of changing the ratio Fe^{3+}/H^+.

Appendix I

Rate Expression Derivations Considering Reactions of the Radical with Water and Bimolecular Combination

$$FeNCS^{2+} \xrightarrow[I_{abs}]{\phi_1} Fe^{2+} + SCN^{\bullet}$$

$$SCN^{\bullet} + SCN^{-} \overset{\text{v.fast}}{\rightleftharpoons} (SCN)_2^{-}$$

$$(SCN)_2^{-} + Fe^{2+} \xrightarrow{k_1} FeNCS^{2+} + SCN^{-}$$

$$(SCN)_2^{-} + FeNCS^{2+} \xrightarrow{k_2} Fe^{2+} + (SCN)_2 + SCN^{-}$$

$$(SCN)_2^{-} + FeOH^{2+} \xrightarrow{k_3} Fe^{2+} + (SCN)_2 + OH^{-}$$

$$(SCN)_2^{-} + Fe^{3+} \xrightarrow{k_4} Fe^{2+} + (SCN)_2$$

$$(SCN)_2^{-} + H_2O \xrightarrow{k_5} X$$

$$2(SCN)_2^{-} \xrightarrow{k_6} (SCN)_2 + 2SCN^{-}$$

$$X_y(SCN)_2 + H_2O \longrightarrow \text{hydrolysis products}$$

a Consider that $k_6 \gg k_5$

$$\frac{\delta[Fe^{2+}]}{\delta t} = \phi_1 I_{abs} - k_1[Fe^{2+}][(SCN)_2^{-}] + k_2[FeNCS^{2+}][(SCN)_2^{-}] + k_3[FeOH^{2+}][(SCN)_2^{-}] + k_4[(SCN)_2^{-}][Fe^{3+}]$$

(contd.)

$$= \phi_1 I_{abs} - \left[(SCN)_2^-\right]\left[k_1\left[Fe^{2+}\right] - k_2\left[FeNCS^{2+}\right] - k_3\left[FeOH^{2+}\right] - k_4\left[Fe^{3+}\right]\right]$$

$$= \phi_1 I_{abs} - \left[(SCN)_2^-\right] \cdot A \qquad (1)$$

where $A = k_1\left[Fe^{2+}\right] - k_2\left[FeNCS^{2+}\right] - k_3\left[FeOH^{2+}\right] - k_4\left[Fe^{2+}\right]$

$$\frac{\delta\left[(SCN)_2^-\right]}{\delta t} = \phi_1 I_{abs} - \left[(SCN)_2^-\right]\left[k_1\left[Fe^{2+}\right] + k_2\left[FeNCS^{2+}\right] + k_3\left[FeOH^{2+}\right] + k_4\left[Fe^{3+}\right] + k_6\left[(SCN)_2^-\right]\right]$$

$$= \phi_1 I_{abs} - \left[(SCN)_2^-\right] \cdot B - k_6\left[(SCN)_2^-\right]^2 \qquad (2)$$

where $B = k_1\left[Fe^{2+}\right] + k_2\left[FeNCS^{2+}\right] + k_3\left[FeOH^{2+}\right] + k_4\left[Fe^{3+}\right]$

Applying the steady state assumption to $(SCN)_2^-$

$$\frac{\delta\left[(SCN)_2^-\right]}{\delta t} = 0,$$

i.e. $k_6\left[(SCN)_2^-\right]^2 + \left[(SCN)_2^-\right] \cdot B - \phi_1 I_{abs} = 0$

$$\therefore \left[(SCN)_2^-\right] = \frac{-B \pm \sqrt{B^2 + 4k_6\phi_1 I_{abs}}}{2k_6}$$

Substituting in (1)

$$\frac{\delta\left[Fe^{2+}\right]}{\delta t} = \phi_1 I_{abs} + A\left[\frac{B \pm \sqrt{B^2 + 4k_6\phi_1 I_{abs}}}{2k_6}\right] \qquad (3)$$

i.e. $$\phi_{Fe^{2+}} = \phi_1 + \frac{A}{I_{abs}}\left[\frac{B \pm \sqrt{B^2 + 4k_6\phi_1 I_{abs}}}{2k_6}\right] \qquad (4)$$

b Consider that $k_5 \gg k_6$

$$\frac{\delta[Fe^{2+}]}{\delta t} = \phi_1 I_{abs} - [(SCN)_2^-]\left[k_1[Fe^{2+}] - k_2[FeNCS^{2+}] - k_3[FeOH^{2+}] - k_4[Fe^{3+}]\right] \quad (5)$$

$$\frac{\delta[(SCN)_2^-]}{\delta t} = \phi_1 I_{abs} - [(SCN)_2^-]\left[k_1[Fe^{2+}] + k_2[FeNCS^{2+}] + k_3[FeOH^{2+}] + k_4[Fe^{3+}] + k_5\right] \quad (6)$$

$\therefore$ Using the steady-state approximation

$$[(SCN)_2^-] = \frac{\phi_1 I_{abs}}{k_1[Fe^{2+}] + k_2[FeNCS^{2+}] + k_3[FeOH^{2+}] + k_4[Fe^{3+}] + k_5}$$

$$\therefore \frac{\delta[Fe^{2+}]}{\delta t} =$$

$$\phi_1 I_{abs}\left[1 - \frac{k_1[Fe^{2+}] - k_2[FeNCS^{2+}] - k_3[FeOH^{2+}] - k_4[Fe^{3+}]}{k_1[Fe^{2+}] + k_2[FeNCS^{2+}] + k_3[FeOH^{2+}] + k_4[Fe^{3+}] + k_5}\right] \quad (7)$$

$$\phi_{Fe^{2+}} = \phi_1\left[\frac{2k_2[FeNCS^{2+}] + 2k_3[FeOH^{2+}] + 2k_4[Fe^{3+}] + k_5}{k_1[Fe^{2+}] + k_2[FeNCS^{2+}] + k_3[FeOH^{2+}] + k_4[Fe^{3+}] + k_5}\right] \quad (8)$$

Appendix II

Derivation of Rate Law Considering Destruction of the Radical by an Acid Dependent Hydrolysis Reaction

i.e. In the reaction scheme presented in Appendix I, the reaction

$$(SCN)_2^- + H_2O \longrightarrow X \qquad (9)$$

is to be replaced by

$$(SCN)_2^- + H_3O^+ \xrightarrow{k_5} X \qquad (10)$$

and the bimolecular recombination step

$$2(SCN)_2^- \longrightarrow (SCN)_2 + 2SCN^-$$

is to be ignored.

The derivation is then the same as in Appendix I,b, with the exception of the term $k_5[(SCN)_2^-]$ which is replaced by $k_5[H^+][(SCN)_2^-]$ since the acid concentration is much less than the water concentration, and reaction (10) is second order, whereas reaction (9) is a pseudo-first order.

The expressions derived using this scheme are:

$$\frac{\delta[Fe^{2+}]}{\delta t} = \phi_1 I_{abs}\left[1 - \frac{k_1[Fe^{2+}] - k_2[FeNCS^{2+}] - k_3[FeOH^{2+}] - k_4[Fe^{3+}]}{k_1[Fe^{2+}] + k_2[FeNCS^{2+}] + k_3[FeOH^{2+}] + k_4[Fe^{3+}] + k_5[H^+]}\right] \qquad (11)$$

and

$$\phi_{Fe^{2+}} = \phi_1 \left[\frac{2k_2 [FeNCS^{2+}] + 2k_3 [FeOH^{2+}] + 2k_4 [Fe^{3+}] + k_5 [H^+]}{k_1 [Fe^{2+}] + k_2 [FeNCS^{2+}] + k_3 [FeOH^{2+}] + k_4 [Fe^{3+}] + k_5 [H^+]} \right]$$

(12)

Appendix III

(a) Values of Optical Densities ($\times 10^2$) at Different Time Intervals for the Compilation of the Spectrum of the Intermediate in the Ferric/Ascorbic Acid Reaction

$[Fe^{3+}] = 2.5 \times 10^{-2}$ M; $[H_2A] = 5 \times 10^{-2}$ M; $[H^+] = 0.2$ M; T = 25°C.

Run	Time (secs) 0.00	0.20	0.40	0.60	0.80
LDA380	1.02	1.05	0.95	0.85	0.72
LDA390	0.68	0.78	0.71	0.62	0.55
LDA400	0.49	0.60	0.54	0.41	0.00
LDA410	0.43	0.52	0.47	0.42	0.36
LDA420	0.26	0.42	0.39	0.36	0.32
LDA430	0.24	0.38	0.37	0.33	0.30
LDA450	0.15	0.35	0.37	0.36	0.33
LDA460	0.17	0.37	0.39	0.38	0.34
LDA470	0.18	0.41	0.44	0.42	0.38
LDA480	0.23	0.46	0.49	0.47	0.43
LDA490	0.23	0.48	0.51	0.48	0.43
LDA500	0.23	0.49	0.53	0.49	0.45
LDA510	0.31	0.55	0.58	0.55	0.50
LDA520	0.28	0.57	0.62	0.59	0.54
LDA530	0.29	0.58	0.63	0.60	0.55
LDA540	0.32	0.60	0.65	0.60	0.55
LDA550	0.27	0.60	0.65	0.60	0.55
LDA560	0.30	0.62	0.67	0.63	0.57
LDA570	0.31	0.62	0.68	0.64	0.58
LDA580	0.32	0.60	0.64	0.60	0.55
LDA590	0.32	0.63	0.68	0.63	0.55
LDA600	0.27	0.56	0.62	0.58	0.52

(contd.)

Appendix III(a) (contd.)

Run	Time (secs)	0.00	0.20	0.40	0.60	0.80
LDA610		0.26	0.53	0.58	0.55	0.51
LDA620		0.28	0.55	0.59	0.56	0.51
LDA630		0.29	0.51	0.55	0.53	0.48
LDA640		0.23	0.48	0.53	0.50	0.46
LDA650		0.23	0.46	0.49	0.46	0.42

Appendix III

(b) Optical Densities (x 10^2) from the Reaction Traces for the Ferric/Ascorbate System (Concentrations, temperature etc., are listed in the text.)

Run	T (m.sec.)	Time (m.secs.) 0xT	1xT	2xT	3xT	4xT	5xT	6xT	7xT	8xT	9xT	10xT	O.D. max.
K15/1	100	5.07	4.37	3.85	3.28	2.92	2.56	2.26	1.96	1.76			
K15/2	100	5.01	4.37	3.80	3.33	2.87	2.51	2.21	2.01	1.76			
K15/3	100	4.93	4.23	3.76	3.24	2.83	2.47	2.11	1.91	1.66			
K16/1	100	4.97	4.24	3.70	3.22	2.87	2.56	2.30	2.09	1.88			
K16/2	100	4.93	4.10	3.60	3.15	2.79	2.48	2.22	2.00	1.83			
K16/3	100	5.22	4.32	3.75	3.34	2.92	2.65	2.38	2.15	1.93			
K17/1	100	4.57	3.86	3.40	2.99	2.71	2.39	2.19	1.95	1.75			
K17/2	100	4.56	3.97	3.48	3.08	2.72	2.46	2.24	2.03	1.85			
K18/1	100	4.53	3.68	3.38	3.05	2.80	2.55	2.35	2.18	2.06			
K18/2	100	4.47	3.66	3.34	3.03	2.77	2.55	2.33	2.20	2.03			
K18/3	100	4.75	3.92	3.59	3.32	3.00	2.73	2.56	2.38	2.20			
K19/1	10	0.24	0.27	0.28	0.31	0.33	0.35	0.37	0.39	0.41	0.42	0.44	0.63
K20/1	10	0.17	0.18	0.18	0.19	0.20	0.20	0.21	0.21	0.22	0.23	0.23	0.33
K21/1	10	0.11	0.11	0.11	0.12	0.12	0.12	0.12	0.13	0.13	0.13	0.14	0.17
K22/1	10	0.54	0.59	0.64	0.70	0.75	0.81	0.85	0.89	0.92	0.95	0.98	1.12
K23/1	4	4.78	5.33	5.78	6.24	6.65	6.96	7.12	7.28	7.38	7.44	7.49	7.49
K23/2	4	4.19	4.58	4.98	5.33	5.63	5.83	6.09	6.29	6.39	6.50	6.55	6.60
K23/3	10	2.07	2.46	2.82	3.15	3.39	3.58	3.73	3.82	3.87	3.92	3.95	3.95

Appendix III (b) (contd.)

Run	T (m.sec.)	Time (m.secs.) 0xT	1xT	2xT	3xT	4xT	5xT	6xT	7xT	8xT	9xT	10xT	O.D. max.
K23/4	10	1.16	1.25	1.32	1.40	1.47	1.54	1.60	1.66	1.71	1.75	1.79	2.04
K23/5	20	0.70	0.81	0.90	0.96	1.01	1.06	1.10	1.14	1.16	1.18	1.20	1.25
K23/6	20	0.50	0.54	0.59	0.63	0.67	0.71	0.73	0.76	0.78	0.80	0.81	0.90
K23/7	20	0.28	0.29	0.31	0.32	0.34	0.35	0.36	0.37	0.38	0.38	0.39	0.41
K25/1	4	4.73	5.28	5.78	6.19	6.55	6.76	6.96	7.07	7.17	7.23	7.23	7.23
K25/2	50	1.67	2.70	3.41	3.99	4.48	4.83	5.08	5.28	5.48	5.58	5.68	5.73
K25/3	10	0.18	1.40	1.81	2.00	2.09	2.18	2.28	2.37	2.46	2.61	2.70	5.63
K25/4	5	0.13	0.67	1.22	1.58	1.81	1.90	1.95	2.00	2.04	2.09	2.14	3.70
K25/5	2	0.00	0.63	0.94	1.17	1.35	1.49	1.58	1.67	1.77	1.81	1.90	2.75
K25/6	1	0.45	0.60	0.76	0.92	1.08	1.19	1.31	1.42	1.54	1.63	1.72	2.39
K26/1	10	4.39	5.08	5.68	6.24	6.76	7.07	7.28	7.49	7.65	7.75	7.81	7.81
K26/2	10	3.32	3.95	4.53	5.03	5.43	5.73	5.93	6.14	6.24	6.29	6.24	6.29
K26/3	10	2.00	2.56	2.94	3.32	3.66	3.90	4.04	4.19	4.24	4.29	4.34	4.39
K26/4	10	1.58	1.90	2.21	2.44	2.61	2.75	2.84	2.91	2.96	2.98	3.01	3.03
K26/5	10	0.70	0.90	0.98	1.03	1.07	1.12	1.16	1.18	1.19	1.20	1.19	1.20
K27	2	0.00	0.14	0.27	0.36	0.43	0.49	0.55	0.58	0.61	0.64	0.66	0.78
K28	2	0.00	0.40	0.72	0.98	1.18	1.35	1.49	1.62	1.72	1.79	1.84	1.99
K29	1	0.00	0.40	0.76	1.08	1.35	1.67	1.95	2.23	2.42	2.65	2.80	3.70
K30	2	0.00	0.12	0.20	0.26	0.33	0.39	0.45	0.49	0.53	0.56	0.58	0.66
K31	2	0.00	0.03	0.05	0.08	0.09	0.11	0.13	0.14	0.16	0.17	0.18	0.22
K32	2	0.00	0.02	0.04	0.06	0.07	0.09	0.10	0.11	0.12	0.13	0.14	0.20

References

1. Orgel, L.E., "Introduction to Transition Metal Chemistry", Methuen (1960).
2. Dunn, T.M., "Modern Coordination Chemistry" edited by J. Lewis and R.G. Wilkins (1960).
3. Jørgensen, C.K., "Absorption Spectra and Chemical Bonding in Complexes", Addison Wesley (1962).
4. Mulliken, R.S., J.A.C.S. 72, 600 (1950); 74, 811 (1952); J. Phys. Chem. 56, 801 (1952).
5. Frank, J., Kuhn, H. and Rollefson, G., Z. Physik. 43, 155 (1927).
6. Rabinowitch, E., Rev. of Modern Physics, 14, 112 (1942).
7. Murrel, J.N., Quart. Revs. 15, 191 (1961).
8. Orgel, L.E., Quart. Revs. 8, 422 (1954).
9. Dainton, F.S., The Chemical Society, Special Publications No. 1, (1954), p. 18.
10. Airey, P.L. and Dainton, F.S., Proc. Roy. Soc. A291, 340 (1966).
11. Dainton, F.S., "Fast Reactions and Primary Processes in Chemical Kinetics", Proceedings of 5th Nobel Symposium 1967, p. 185.
12. Dainton, F.S., J. Chem. Soc. 1952, 1533.
13. Balzanni, V., Carassiti, V. and Scandola, F., Gazz. Chim. Ital. 96, 1213 (1966).
14. Sleight, T.P. and Hare, C.R., Inorg. Nucl. Chem. Letters, 4, 165 (1968).

15. Balzani, V., Moggi, L. and Carassiti, V., Ber. der Bunsengesellschaft für Phys. Chemie, 72, 288 (1968).

16. Kenney, D.J., Clinckemaillie, G.G. and Michaels, C.L., J. Phys. Chem. 72, 410 (1968).

17. Jaselkis, B. and Edwards, J.C., Anal. Chem. 32, 381 (1960).

18. Adamson, A.W., Waltz, W.L., Zinato, E., Watts, D.W., Fleischauer, P.D. and Lindholm, R.D., Chem. Rev. 68, 541 (1968).

19. Wegner, E.E. and Adamson, A.W., J.A.C.S. 88, 394 (1966).

20. Adamson, A.W., J. Phys. Chem. 71, 798 (1967).

21. Balzani, V. and Carassiti, V., J. Phys. Chem. 72, 383 (1968).

22. Spees, S.T. and Adamson, A.W., Inorg. Chem. 1, 531 (1962).

23. Adamson, A.W. and Sporer, A.H., J.A.C.S., 80, 3865 (1958).

24. Stirling, G.C., Ph.D. Thesis, Melbourne, 1967.

25. Endicott, J.F. and Hoffman, M.Z., J.A.C.S. 87, 3348 (1965).

26. Parker, C.A. and Hatchard, C.G., J. Phys. Chem. 63, 22 (1959).

27. Malati, M.A. and Rophael, M.W., J. Inorg. Nucl. Chem. 28, 915 (1966).

28. Porter, G.B., Doering, J.G.W. and Karanka, S., J.A.C.S., 84, 4027 (1962).

29. Martin, T.W., Rummel, R.E. and Gross, R.C., J.A.C.S. 86, 2595 (1964).

30. Adamson, A.W., Disc. Far. Soc. 29, 163 (1960).

31. Noyes, R.M., J.A.C.S. 77, 2042 (1955).

32. Noyes, R.M. Z. Electrochem. 64, 153 (1960).

33. Noyes, R.M. and Meadows, L.F., J.A.C.S. 82, 1872 (1960).

34. Uri, N., Chem. Reviews, 50, 375 (1952).

35. Evans, M.G. and Uri, N, Nature, 164, 404 (1949).

36. Evans, M.G., Santappa, M. and Uri, N., J. Poly. Sci. 7, 243 (1951).

37. Bates, H.G.C., Evans, M.G. and Uri, N., Nature, 166, 869 (1950).

38. Baxendale, J.H. and Magee, J., Trans. Far. Soc. 51, 205 (1955).

39. Dainton, F.S. and Tordoff, M., Trans. Far. Soc. 53, 666 (1957).

40. Dainton, F.S. and James, D.G.L., Trans. Far. Soc. 54, 649 (1958).

41. Adamson, M.G., Dainton, F.S. and Baulch, D.L., Trans. Far. Soc. 58, 1388 (1962).

42. Peters, C.A., McMasters, M.M. and French, C.L., Ind. Eng. Chem. (Anal.) 11, 502 (1939).

43. Betts, R.H. and Dainton, F.S., J.A.C.S. 75, 5721 (1953).

44. Hart, E.J., J.A.C.S. 73, 68 (1951).

45. Vogel, A.I., "Quantitative Inorganic Analysis" 3rd ed. p. 238.

46. Vogel, A.I., "Quantitative Inorganic Analysis" 3rd ed. p. 287.

47. Vogel, A.I., "Quantitative Inorganic Analysis" 3rd ed. p. 569.

48. Vogel, A.I., "Quantitative Inorganic Analysis" 3rd ed. p. 933.

49. Hatchard, C.G. and Parker, C.A., Proc. Roy. Soc. A, 235, 518 (1956

50. Laurence, G.S., Trans. Far. Soc. 52, 236 (1956).

51. Milburn, R.M., J.A.C.S. 79, 537 (1957).

52. Gaugin, R., J. Chim. Phys. 42, 138 (1945); C.A. 40, 3968 (1946).

53. Lecher, H., Wittwer, M. and Speer, W., Ber 56B, 1104 (1923); C.A. 17, 3164 (1923).

54. Wilson, I.R. and Harris, G.M., J.A.C.S. 82, 4515 (1960).

55. Wilson, I.R. and Harris, G.M., J.A.C.S. 83, 286 (1961).

56. Smith, R.H. and Wilson, I.R., Aust. J. Chem. 19, 1357 and 1365 (1966).

57. Lister, M.W. and Rivington, D.E., Can. J. Chem. 33, 1572 (1955).

58. Dufflo-Plissonier, Ph.D. Thesis, University of Paris, 1965.

59. Boag, J.W., Adams, G.E., Michael, B.D. and Currant, J., "Pulse Radiolysis - Proceedings of the International Symposium Manchester, April 1965", p. 128.

60. Baxendale, J.H. and Stott, D.A., Chem. Comm. 699 (1967).

61. Baxendale, J.H., Bevan, P.L. and Stott, D.A., Trans. Far. Soc. 64, 2389 (1968).

62. Sutton, H.C., Adams, G.E., Boag, J.W. and Michael, B.D., Ref. 59, page 61.

63. Cercek, B., Ebert, M., Gilbert, C.W. and Swallow, A.J., Ref. 59, p. 83.

64. Grossweiner, L.I. and Matheson, M.S., J. Phys. Chem. 61, 1089 (1957).

65. Dogliotti, L. and Hayon, E., J. Phys. Chem. 72, 1800 (1968).

66. Anbar, M. and Neta, P., Int. Jour. of App. Rad. and Isotopes, 18, 493 (1967).

67. Ellis, K.J. and Laurence, G.S., Trans. Far. Soc. 63, 91 (1967).

68. Oster, G. and Mizutane, Y., J. Pol. Sci. 22, 173 (1956).

69. Horne, R.A., J. Inorg. Nucl. Chem. 25, 1139 (1963).

70. Milburn, R.M. and Vosburgh, W.C., J.A.C.S. 77, 1352 (1955).

71. Page, F.M., Advances in Chemistry Series, 36, 68 (1962).

72. Boag, J.W., Adams, G.E. and Michael, B.D., Proc. Chem. Soc. Dec. 1964, 411.

73. Boag, J.W., Adams, G.E. and Michael, B.D., Trans. Far. Soc. 61, 1417 (1965).

74. Halpern, J., Quart. Rev. 15, 207 (1961).

75. Stranks, D.R., "Modern Coordination Chemistry", Lewis and Wilkins (1960).

76. Zwickel, A.M. and Taube, H., Disc. Far. Soc. 29, 42 (1960).

77. Ogard, A.E. and Taube, H., J.A.C.S. 80, 1084 (1958).

78. Page, F.M., Trans. Far. Soc. 49, 635 (1953).

79. Page, F.M., Trans. Far. Soc. 50, 120 (1954).

80. Patnaik, D., Nanda, C. and Bakshi, K., J. Ind. Chem. Soc. 34, 643 (1957).

81. Bildea, I. and Niac, G., Proceedings of the 9th Int. Conference on Coordination Chemistry, St. Moritz (1966).

82. Page, F.M.,Trans. Far. Soc. 56, 398 (1960).

83. Duke, F.R., J.A.C.S. 69, 2885 (1947).

84. Wells, C.F. and Mays, D., J. Chem. Soc. 577 (1968).

85. Howlett, K.E. and Sarsfield, S., J. Chem. Soc. 683 (1968).

86. Fudge, A.J. and Sykes, K.W., J. Chem. Soc. 119 (1952).

87. Sengupta, K.K., J. Ind. Chem. Soc. 42, 725 (1965) and reference therein.

88. Mehrotra, R.N. and Ghosh, S., Z. Phys. Chemie, 230, 231 (1965) and references therein.

89. McAuley, A. and Brubaker, C.H., J. Chem. Soc. 960 (1966).

90. McAuley, A. and Hill, J., J. Chem. Soc. (A) 1169 (1968).

91. Guilbault, G.G. and McCurdy, W.H., J. Phys. Chem. 67, 283 (1963).

92. Mehrotra, R.N. and Ghosh, S., Z. Phys. Chemie, 231, 91 (1966).

93. McAuley, A., Hill, J. and Pickering, W.F., Chem. Comm. 573 (1967).

94. McAuley, A. and Hill, J., J. Chem. Soc. (A) 156 (1968).

95. McAuley, A. and Pickering, W.F., J. Chem. Soc. (A) 1173 (1968).

96. Henry, P.M., J.A.C.S. 88, 1597 (1966).

97. Kochi, J.K., Science, 155, 415 (1967).

98. Koenig, R.A., Schiefelbusch, T.L., Johnson, C.R., Ind. and Eng. Chem. (Anal.), 15, 181 (1943).

99. Erdey, L. and Bodor, E., Ind. and Eng. Chem. (Anal.), 24, 418 (1952).

100. Onishi, I. and Tadashi, H., Bull. Chem. Soc. Japan, 37, 1314 (1964

101. Weissberger, A. and LuValle, J.E., J.A.C.S. 66, 700 (1944).

102. Nord, V., Acta Chem. Scand. 9, 442 (1955).

103. Grinstead, R.G., J.A.C.S. 82, 3464 (1960).

104. Taqui Khan, M.M. and Martell, A.E., J.A.C.S. 89, 4176 (1967).

105. Taqui Khan, M.M. and Martell, A.E., J.A.C.S. 89, 7104 (1967).

106. Taqui Khan, M.M. and Martell, A.E., J.A.C.S. 90, 3386 (1968).

107. Sturtevant, J.M., "Rapid Mixing and Sampling Techniques in Biochemistry", Academic Press Inc., New York, 1964, p. 89.

108. Tregloan, P.A., Ph.D. Thesis, University of Adelaide, 1969.

108A. Tregloan, P.A., and Lawrence, G.S., J. Sci. Inst., 43, 865 (1965).

109. Schukarew, A., Z. Phys. Chemie, 38, 353 (1901).

110. Wagner, C., Z. Phys. Chemie, 113, 269 (1924).

111. Awtrey, A.D. and Connick, R.E., J.A.C.S. 73, 1842 (1951).

112. Hershey, A.V. and Bray, W.C., J.A.C.S. 58, 1760 (1936).

113. Wood, M.J.M., Gallagher, P.K. and King, E.L., Inorg. Chem. 1, 55 (1962).

114. Lister, M.W. and Rivington, D.E., Can. J. Chem. 33, 1603 (1955).

115. Connick, R.E. and Coppel, C.P., J.A.C.S. 81, 6389 (1959).

116. Matthies, P. and Wendt, H., Z. Phys. Chemie (Frankfurt), 30, 137 (1961).

117. Below, J.F., Connick, R.E. and Coppel, C.P., J.A.C.S. 80, 2961 (1958).

118. De Maeyer, L. and Kustin, K., Ann. Rev. of Phys. Chem. 14, 1 (1963).

119. "Stability Constants", The Chemical Society Special Publication No. 17 (1964).

120. Eigen, M. and Kustin, K., J.A.C.S. 84, 1355 (1962).

121. Edgecombe, F.H.C. and Norrish, R.G.W., Proc. Roy. Soc. A253, 154 (1959).

122. Langmuir, M. and Hayon, E., J. Phys. Chem. 71, 3808 (1967).